

Molecular Mechanisms Governing the Differential Regulation of Tandemly Replicated Visual Opsin Genes

A Dissertation

Presented in Partial Fulfillment of the Requirements for the
Degree of Doctor of Philosophy

with a

Major in Microbiology, Molecular Biology and Biochemistry

in the

College of Graduate Studies

University of Idaho

by

Robert D. Mackin

Major Professor: Deborah Stenkamp, Ph.D.

Committee Members: Allan Caplan, Ph.D.; Peter Fuerst, Ph.D.; Adam Jones, Ph.D.

Department Administrator: James Nagler, Ph.D.

August 2020

Authorization to Submit Dissertation

This dissertation of Robert D. Mackin, submitted for the degree of Doctor of Philosophy with a Major in Microbiology, Molecular Biology and Biochemistry and titled "Molecular Mechanisms Governing the Differential Regulation of Tandemly Replicated Visual Opsin Genes," has been reviewed in final form. Permission, as indicated by the signatures and dates below, is now granted to submit final copies to the College of Graduate Studies for approval.

Major Professor: _____ Date: _____
Deborah Stenkamp, Ph.D.

Committee Members: _____ Date: _____
Allan Caplan, Ph.D.

_____ Date: _____
Peter Fuerst, Ph.D.

_____ Date: _____
Adam Jones, Ph.D.

Department Administrator: _____ Date: _____
James Nagler, Ph.D.

Abstract

Our sense of sight is the primary way humans interface with our surroundings. A significant portion of the human brain is devoted to detecting and processing visual stimuli. Vision is made possible by a specialized structure of the central nervous system called the retina located at the back of the eye. Color vision is made possible by specialized cells called cone photoreceptors in the outer most layer of the retina. Humans have three subtypes of cones red, green, and blue. The subtype is determined by the expression of opsin proteins that are sensitive to specific wavelengths of light. These are short wavelength sensitive (SWS; blue), medium wavelength sensitive (MWS; green), and long wavelength sensitive (LWS; red). Enormous efforts have been made in deciphering how these cone subtypes are determined. Understanding of the regulatory processes involved in the determination of cone subtypes will provide the knowledge required to identify factors that can disrupt normal development of the visual system and will provide insight into the creation of novel therapeutics designed to treat a multitude of visual disorders that specifically involve cone photoreceptors.

This body of work begins with an overview of retinal development, structure, and function. Next, I present my published work that has identified the nuclear signaling molecule thyroid hormone (TH) as an endogenous regulator of an interesting set of visual opsin genes in zebrafish called tandemly replicated opsin genes. Tandemly replicated genes are the result of one or more duplication events that results in two or more functionally related genes that are found next to each other in the genome and may be regulated by the same upstream regulatory regions. These include the tandemly duplicated *lws1/lws2* array and the tandemly quadruplicated *rh2* array. Chapter 3 describes unpublished work in which I identify regions of the *lws* locus that are required for regulation by TH including two potential response elements that are critical for the differential regulation of *lws1* vs *lws2* in response to TH. Next I present astonishing findings that detail the involvement of TH in the differential regulation of the tandemly duplicated *LWS/MWS* visual opsin array found on the X chromosome in humans. I also present preliminary findings in zebrafish that identify specific nuclear signaling receptors that contribute to the differential regulatory mechanism governing expression of the tandemly replicated visual opsin arrays. This body of work significantly expands upon our understanding of how cone subtypes are determined and the components of the regulatory mechanisms involved in making this determination.

Acknowledgements

First and fore-most I would like to acknowledge my committee members Allan Caplan, Peter Fuerst, and Adam Jones. I would especially like to thank Ruth Frey for more than I have space to list as well as the other Stenkamp lab members. I would also like to thank the department chair James Nagler as well as Gina Tingley and Kristi Accola for the administrative help they provided. I would like to thank our collaborators Dr. Shoji Kawamura and the Kawamura lab for the *lws* reporter transgenics and constructs, and Dr. Valeria Canto-Soler and the Canto-Soler lab for the human 3D retina cups, and Diana Mitchell for technical assistance, editing assistance, and project planning. I thank Dr. Jens Tiefenbach for the gift of the T3 “Ligand Trap” transgenic line, Dr. Rachel Wong for the *trβ2:tdTomato* transgenic line, Dr. David Parichy for the *Tg(tg:nVenus-2a-nfsB)^{wp.r18}* transgenic line and the *trab* mutant line, Dr. Joe Corbo for the *trβ* mutant line, Dr. Ralph Nelson for the *trβ2* mutant line, Dr. Chi Sun and Carlos Galicia for generating the *rxrya* mutant line, Dr. Elwood Linney for the *RARE:YFP* transgenic line, and Dr. Thomas Euler for providing the WinDRP program. I am grateful to Ms. Ann Norton and Dr. Onesmo Balemba of the UI Optical Imaging Core, to Jaclyn Huffman and Kiah Stewart of the UI Laboratory Animal Research Facility. NIH Grant S10 OD0108044 (DLS) funded the purchase of the Nikon/Andor spinning disk confocal microscope and camera. This work was supported by NIH R01 EY012146 (DLS), NIH R01 EY012146-16S1 (DLS, AAF), The Malcolm and Carol Renfrew Faculty Fellowship (DLS), NSF REU Site 146096 (CG), project support funds available through the University of Idaho (UI) Institute for Bioinformatics and Evolutionary Studies (NIH P30 GM103324) and Idaho INBRE (NIH P20 GM103408), and the Japan Society for the Promotion of Science 18H04005 (SK). Travel grants were provided by The Knights Templar Eye Foundation, University of Idaho GPSA, and Idaho INBRE.

Dedication

I dedicate this work to all who have bettered themselves in the face of adversity. To those who have lived a nightmare but still dream of a better life. To those who have fought for the entirety of their lives to make something of themselves. To those who grew up without mentors or role models that forged a future based upon their own ideals. To those that have chosen to not accept the cards that life has dealt them, but to force their own manifest destiny despite what the world has ordained them to be. I dedicate this work to my wife who has believed in me and encouraged me to succeed even when I didn't believe in myself or trust in my future. I dedicate this work to my daughter, my inspiration, my reason for being, the one who will carry on and continue to show the world what we are made of. To those who endeavor to advance our knowledge of the natural world to make the paradise we all know is possible a reality for those that come after.

Table of Contents

Authorization to Submit Dissertation	ii
Abstract	iii
Acknowledgements	iv
Dedication	v
Table of Contents	vi
List of Tables	viii
List of Figures	ix
Chapter 1: Introduction to Vision: Retinal Development, Structure and Function	1
Chapter 2: Endocrine Regulation of Multi-Chromatic Color Vision	11
Abstract	11
Introduction	11
Methods and Materials	14
Results	19
Discussion	29
Literature Cited.....	33
Chapter 3: Cis-Regulatory Sequences Required for Differential Regulation of Long Wavelength Sensitive Visual Opsins by Thyroid Hormone	52
Abstract	52
Introduction	52
Methods and Materials	55
Results	57
Discussion	60
Literature Cited.....	62
Chapter 4: Nuclear Signaling Molecule Regulation of Visual Opsin Expression in Human iPSC Derived 3D Retinal Organoids	72
Abstract	72

Introduction	72
Methods and Materials	75
Results	75
Discussion	78
Literature Cited.....	80
Chapter 5: Future Directions	88
Discussion	88
Literature Cited.....	90

List of Tables

Table S2.1. Quantitative PCR indicates T4 increases abundance of *cyp27c1* transcript in juvenile zebrafish.

Table S2.3. Primer pairs used for qPCR.

Table S3.1. Primers for modification of the reporter constructs

Table S4.1. Primers used in qPCR for human transcripts in retina cups

List of Figures

Figure 2.1. Quantitative PCR and in situ hybridization for *lws* transcript abundance reveals robust differential regulation after thyroid hormone (T3) treatment from 2-4dpf.

Figure 2.2. *Lws* reporter transgenic indicates a switch from *lws2* to *lws1* in response to thyroid hormone (T3).

Figure 2.3. Live imaging of 5dpf *lws:PAC(H)* *lws* reporter transgenic confirms a switch from *lws2* to *lws1* in individual cones in response to thyroid hormone (T3).

Figure 2.4. Thyroid hormone “Ligand Trap” reporter transgenic and *thyroid receptor β 2* reporter transgenic indicate accumulation of thyroid hormone (T3) in *lws+* (TR β 2+) cones after T3 treatment.

Figure 2.5. Thyroid hormone (TH) loss of function by thyroid ablation suppresses *lws1* expression at time of native onset of expression.

Figure 2.6. Plasticity of *lws* differential expression by thyroid hormone (T4) in normal and athyroid juveniles.

Figure 2.7. Quantitative PCR and in situ hybridization for *rh2-1* and *rh2-2* gene expression reveals differential regulation after thyroid hormone (T3) treatment from 2-4dpf.

Figure 2.8. Plasticity of *rh2* differential expression by thyroid hormone (T4) in normal and athyroid juveniles.

Figure S2.1. Local pattern analysis (two-dimensional nearest-neighbor distance; NND) of LWS cones in *lws:PAC(H)* embryos exposed to 100 nM thyroid hormone (T3): T3-induced GFP+ (*lws1+*) cones do not disrupt the LWS cone mosaic.

Figure S2.2. Thyroid hormone (T3) treatment time-course reveals kinetics of changes in *lws* regulation in larvae.

Figure S2.3. Response element analysis of the *lws* and *rh2* proximal upstream regulatory regions.

Figure S2.4. Plasticity of *sws1/sws2* opsins and *six7* transcript abundance by thyroid hormone (T4) in control, T4 treated, and athyroid juveniles.

Figure 3.1. The element required for upregulation of *lws1* in response to TH (T3) resides in the 2.6kb region upstream from *lws1* but the element required for the downregulation of *lws2* in response to T3 is not in the 1.8kb region upstream from *lws2*.

Figure 3.2. The 1.3kb region upstream from *lws1* that includes the LAR and 0.6kb immediately upstream from *lws1* is sufficient for normal *lws* expression at 4 days, the upregulation of *lws1* in response to T3 but not the downregulation of *lws2* in response to T3.

Figure 3.3. The 2.6kb-0.6kb region upstream is not sufficient for normal expression of the *lws* array at 4dpf or the upregulation of *lws1* in response to T3. The numbers of *lws2* positive cones increased in response to T3 instead of decreased with the intact locus.

Figure 3.4. The ppTRE1 element is required for suppression of *lws1* at 4dpf, expression of *lws2* at 4dpf, and upregulation of *lws1* in response to T3.

Figure 3.5. The ppTRE2 element is required for *lws1* suppression at 4dpf, the upregulation of *lws1* in response to T3, and the downregulation of *lws2* in response to T3.

Figure 3.6. The *lws* locus contains more than one element that contributes to proper endogenous regulation and response to T3.

Figure 4.1. Quantitative PCR for *OPNILW* and *OPNIMW* transcript abundance reveals a decrease in abundance for both transcripts in the retinoic acid (RA) treated retina cups (RCs) and an increase in abundance for both transcripts in the thyroid hormone treated RCs at 90 days.

Figure 4.2. Quantitative PCR for *OPNILW*, *OPNIMW*, *OPNISW*, *OPN2RHO* transcript abundance reveals a switch in regulation of *OPNIMW* by T3 and new roles for RA and T3 suppressing *OPN2RHO* transcription in treated RCs at 120 days.

Figure 4.3. Quantitative PCR for *OPNILW*, *OPNIMW*, *OPNISW*, *OPN2RHO* transcript abundance reveals differential regulation of *OPNILW* vs *OPNIMW* by T3 in RCs at 150 days as well as new roles for RA in promoting *OPNISW* transcription.

Figure 4.4. Quantitative PCR for *OPNILW*, *OPNIMW*, *OPNISW*, *OPN2RHO* transcript abundance reveals continued differential regulation of *OPNILW* vs *OPNIMW* by T3 in RCs at 180 days as well as a switch from suppression of *OPN2RHO* at 150 days to promotion by RA at 180 days.

Supplementary Figure S4.1. Primer alignments for *OPN1LW* and *OPN1MW*

Fig. 5.1. Inducible CRISPR-Cas9 mediated disruption of thyroid hormone receptor TR β .

Fig 5.2. The *rh2* thyroid hormone response is still maintained in the absence of TR β 2.

Fig 5.3. Downregulation of *lws2* and *rh2-1* in response to TH is dependent on TR α B.

Fig 5.4. Downregulation of *lws2* and *rh2-1* in response to TH is dependent on RXR γ a.

Chapter 1: Introduction to Vision: Retinal Development, Structure and Function

The sensory nervous system is the interface between us and the world around us. We experience our surroundings through stimuli that are detected and transduced into nervous signals by the various sensory systems that in turn transmit the information to the brain for processing. Vision is the primary sensory system that humans use to perceive our environment. The light sensitive tissue of the neural retina located at the back of the eye is the main source for detecting visual information. The retina is divided into the outer nuclear layer (ONL) containing the photoreceptors (PR) followed by the outer plexiform layer which consists of synapses between the photoreceptors and cells of the inner nuclear layer (INL) ¹. Cell types of the INL include bipolar neurons, amacrine cells, and horizontal cells ¹. These inner nuclear neurons form synapses in the inner plexiform layer with retinal ganglion cells of the retinal ganglion cell layer (GCL) ¹.

Photons of light travel through the lens of the eye and are first detected by the photoreceptors. Photoreceptors are a highly specialized cell that can be anatomically divided into a synaptic body which forms a synapse with INL neurons, a cell body that contains the organelles, an inner segment that houses mostly mitochondria, and the outer segment which is made of modified cilia that form stacks of membranous disks filled with photopigments ². Photopigments are a protein moiety composed of a chromophore (either the A1 form 11-*cis* retinal or the A2 form 11-*cis* dehydroretinal) and a light sensitive opsin protein ³. Visual opsin proteins are like other G protein coupled receptors in that they contain seven transmembrane loops ⁴. The chromophore is connected to the opsin through a Schiff base at a lysine residue in loop seven ⁵. Absorption of a photon causes the isomerization of 11-*cis* retinal to all-*trans* retinal ⁵. This leads to a conformational change that activates the G-protein transducin ⁶. The stimuli are transduced into a nervous signal that is transmitted to the interneurons of the INL before being relayed to the retinal ganglion cells of the GCL. The axons of these ganglion cells make up the optic tract and optic nerve which carries the nerve impulse from the eye to the visual processing areas of the brain.

The retina is structured and organized in such a way to optimally extract, differentiate and encode the complex nature of visual information. Each of the cell types that make up this visual circuit contain multiple different subtypes that form a neural network which allows for the detection and encoding of visual information such as motion, luminance contrast, and color contrast. Throughout the development of the retina an array of gene regulatory networks are employed to

orchestrate the proliferation, differentiation, and fate of retinal progenitor cells (RPCs) destined to become the more than 60 different cell types of the mature retina ¹. It is beyond the scope of this review to cover the full suite of regulatory networks involved in the development and organization of these various cell types. There is a vast amount of knowledge solely pertaining to the regulatory networks involved in the determination of the rod and cone subtypes of the photoreceptor cells (reviewed here ^{7, 8, 9}). The primary focus of this review will be on the development of cones and the regulatory processes that determine their identity and fate. The elucidation of these regulatory networks and the identification of their critical components is of vital importance to our pursuit of understanding how the visual system develops and to further the advancement of novel therapies for the treatment of visual disorders.

Photoreceptors are classified as either rods or cones based on their morphology and the type of light sensitive opsin protein expressed. Rod photoreceptors have a rod like morphology and express the rhodopsin protein. The function of rods is to detect luminance contrast. They are highly sensitive to light and are used in low light conditions. Cone photoreceptors have a cone like morphology and express one of four phylogenetic types of cone opsin ¹⁰. Cones are required for daylight vision, high acuity vision, and color contrast.

The types of cones are determined by the spectral sensitivity of the opsin protein expressed. These include: SWS1 (short wavelength-sensitive type 1, UV), SWS2 (short wavelength sensitive type 2, blue), RH2 (medium wavelength sensitive, green), and MWS/LWS (medium to long wavelength sensitive, green/red) ¹⁰. The types of cones can vary significantly from one organism to the next. Zebrafish have a total of eight different cone types including SWS1 (UV), SWS2 (blue), RH2-1/2/3/4 (green), and LWS1/LWS2 (red) ^{11 12}. Mice only have two types including S (UV) and M (green) ¹³. Humans have three S (blue), M (green), and L (red) ¹⁴. Some organisms such as humans and mice have a rod dominant retina in which the number of rods significantly outnumber the number of cones. Others like zebrafish have a cone dominant retina. The total number of and the ratio between rods and cones as well as the spatio-temporal patterns of expression differ between organisms based upon the visual requirements of the environments that they live in.

Investigation into the factors that determine photoreceptor differentiation, fate, and identity as well as the spatio-temporal dynamics of these decisions is an intensely focused on area of research. The factors involved in the regulatory networks that determine these outcomes can be both intrinsic and extrinsic signals. In zebrafish, Gdf6a a ligand of the BMP family is required for SWS2 opsin expression ¹⁵ and works in concert with the T box transcription factor Tbx2b to promote SWS1/UV cone development ^{16 17}. Tbx2b null zebrafish have an increased number of rods ¹⁷. Also, in zebrafish

the retinoic acid receptor RAR α is involved in the cone to rod fate¹⁸. The leucine containing transcription factor, NRL, has been demonstrated to be a key regulator of rod fate and rod gene transcription². Mice lacking NRL or the orphan nuclear receptor ROR β do not develop rods and have an increased number of S cones¹⁹. Another orphan nuclear receptor, NR2E3, is required for rod gene expression and suppression of cone specific genes²⁰. NR2E3 mutants have decreased rod gene expression, defective rods, and an increased abundance of S opsin²¹. The retinoid X receptor RXR γ is involved with the thyroid hormone receptor TR β 2 in mice to suppress S opsin²². Knockout of RXR γ results in S opsin expression in all cones. TR β 2 is required for proper M opsin expression but not cone development in mice^{22, 23}. Knockout of TR β 2 results in S opsin expression in all cones²³. TR β 2 is required for LWS cone differentiation in zebrafish²⁴⁻²⁶. Zebrafish lacking TR β 2 results in a complete absence of LWS cones²⁴. TR β is required for L and M opsin expression in humans. A case study of an individual with a mutation in TR β resulted in S cone monochromacy²⁷. In addition, knockout of TR β in human iPSC derived 3D retinal organoids resulted in complete suppression of L and M opsin expression²⁸.

Extrinsic factors that regulate the spatio-temporal patterns of cone fate and identity have been co-opted by evolution to create a plethora of different photoreceptor expression patterns amongst different taxonomic groups. The most highly investigated of these are retinoic acid (RA) and thyroid hormone (TH). Thyroid hormone is synthesized in the thyroid gland mainly in the stable tetraiodothyronine (T4) form. T4 is transported throughout the body via the circulatory system where it is peripherally converted to the activated triiodothyronine (T3) form by the deiodinase Dio2²⁹. Activated TH ligand binds to one of the thyroid hormone receptors (TRs) which translocates to the nucleus to enable interaction between the liganded receptor and *cis*-regulatory elements in the genome³⁰. Liganded receptors once bound to the response element form a complex with transcriptional activators to promote gene transcription. T3 can be converted to the deactivated form reverse triiodothyronine (rT3) by the deiodinase Dio3²⁹. Unliganded TH receptors have been demonstrated to bind response elements, form a complex with transcriptional deactivators, and suppress gene transcription³¹. Retinoic acid is synthesized by the enzyme aldehyde dehydrogenase (ADH). It is degraded by a member of the cytochrome p450 family of enzymes Cyp26. RA is a nuclear hormone signaling molecule that binds the retinoic acid receptors (RARs) or retinoid X receptors (RXRs) that in turn interact with *cis*-regulatory response elements in the genome to affect transcription. TRs, RARs, and RXRs can all homodimerize or heterodimerize together²³. The genomic response elements they interact with are usually composed of a hexameric halfsite having the sequence AGGTCA or small variations of the classical sequence³². The halfsites can be a direct

repeat, an inverted repeat, or an everted repeat³³. The number of base pairs between the halfsites determines which receptor dimers can bind and whether transcription is promoted or suppressed³³.

This dynamic scheme of enzyme mediated activation and deactivation of RA and TH in addition to the multiple receptor subtypes and possible hetero and homo dimerization combinations along with variations of cis regulatory elements in the genome create an elaborate network of possible signaling paradigms that enables the fine tuning of transcription for a host of genes in multiple cellular subtypes. In the mouse retina the enzymes that activate TH or RA (Dio2 and ADH respectively) are expressed in higher amounts in dorsal retina^{34 35}. This creates a gradient of TH and RA that is highest at the source of activation in the dorsal retina. The promotion of M opsin expression and the suppression of S opsin correlates to the gradients of TH and RA³⁴. The concentration of RA in the mouse retina is manipulated further by the expression of a different variant of ADH in ventral retina as well as Cyp26 in central retina³⁶ which results in the formation of localized gradients. In some animals that heavily rely on vision there is an area of the retina referred to as the High Acuity Area (HAA)³⁷. It was demonstrated in chick that localized regulation of RA contributes to the establishment of a HAA by suppressing the expression of rods. It was also demonstrated that the patterning of RA signaling component expression is likely involved in the formation of the human HAA called the fovea³⁷. The human fovea is required for high acuity vision that we utilize in visually demanding tasks like driving and reading. The fovea is exclusively composed of densely packed L and M opsin expressing cones³⁸. It has been demonstrated that TH is involved in the regulation of both L and M opsin^{27 28} making TH signaling another possible regulatory component in establishing the fovea. The manipulation of these signaling pathways offers enticing possibilities for the differentiation of proper cone number and types in human retinal cultures for cell transplant strategies as well as the development of therapies and treatments for visual disorders involving photoreceptors.

The regulation of opsin gene transcription has been an extensively studied area of retinal development. A branch of this research that has not gained much attention involves the regulation of opsin genes that are located next to each other in the genome and are the result of a tandem replication. The human L and M opsin genes are arranged in a tail to head manner on the X chromosome, and are expressed in separate cone populations³⁹. Fish are the only other vertebrate taxonomic group besides primates known to contain tandemly-replicated opsin genes⁴⁰. In zebrafish, the *lws* gene locus (orthologous to human *LWS/MWS*) has undergone a tandem replication (independent of the *L/M* replication event in humans) resulting in a second member (*lws2*) encoding an opsin with a shorter wavelength-shifted sensitivity¹². In addition to the tandemly-duplicated *lws*

opsins, the *rh2* cone opsin array in zebrafish has been tandemly-quadruplicated¹². These properties make the zebrafish an excellent model to study the regulation of tandemly replicated opsin genes. Recently it was reported that when zebrafish were treated with RA the expression of *lws1* was increased and the expression of *lws2* was decreased when compared to controls⁴¹. However, when RA signaling was disrupted the expected decrease in *lws1* was observed but *lws2* was either downregulated as well or not significantly changed depending on the method used to disrupt RA signaling⁴¹. This suggests that there are other components involved in regulating the *lws* locus.

In this dissertation I demonstrate that in addition to RA signaling, TH is an endogenous regulator of not only the *lws* gene locus but also the *rh2* locus. Chapter 2 describes our initial findings that TH is an endogenous regulator of LWS and RH2 opsin expression. Gain of function studies in which exogenous T3 or T4 were administered caused an increase of expression of *lws1* and *rh2-2* and a decrease in *lws2* and *rh2-1*. This was true in both larval and juvenile zebrafish for all transcripts except for *rh2-2*. We then employed a loss of function strategy involving the selective ablation of the thyroid gland to initiate hypothyroid conditions which resulted in a decrease in *lws1* and *rh2-2* and an increase in *lws2* expression but no change in *rh2-1* in juveniles. These changes could be rescued by the administration of TH except for *rh2-2*. We also demonstrated that the pattern of the cone mosaic was not disrupted and through *in vivo* imaging of transgenic *lws* reporter fish we recorded *lws2* positive cones switching to *lws1* in response to TH treatment. These findings are concrete evidence that TH is indeed an endogenous regulator of tandemly replicated opsin genes in zebrafish.

Chapter 3 is an investigation of the *cis*-regulatory sequences involved in the expression of *lws1* and *lws2* and the elements required for the response to TH treatment. We employed a promoter manipulation strategy consisting of transient expression of various constructs that contain deletions in the upstream regulatory region of the *lws* locus driving the expression of reporters for *lws1* and *lws2* expression. We found that the 0.6kb region between the LWS activating region (LAR) and the transcriptional start site of *lws1* is all that is necessary for the expression of *lws2*, the normal onset of *lws1*, and the change in expression due to TH treatment. We also found that two potential response elements residing in this 0.6kb region are required for the suppression of *lws1*, the upregulation of *lws1* in response to TH, and the expression of *lws2*. These elements correspond to predicted thyroid response elements and can also be found in the upstream region of the human L/M locus.

In chapter 4 we demonstrate that both TH and RA are involved in opsin regulation in 3D retinal organoids, referred to as Retina Cups (RC) derived from human induced pluripotent stem cells (iPSC). RCs treated with T3 from 63 days to 90 days show increased L and M opsin transcript. RCs treated with RA have decreased expression of both. This remains the case for RCs treated with RA

until 120 days, 150 days, and 180 days. RCs treated with T3 have increased expression of L opsin at the same time points. M opsin is unchanged compared to controls at 120 days but is significantly decreased at the later timepoints. These results demonstrate that RA suppresses the human L and M opsin at the concentration used for these durations of treatment. T3 on the other hand promotes both M and L opsin up until 120 days where M opsin expression is not changed compared to controls but is decreased at later timepoints. These findings are an incredible contribution to the understanding of the mechanisms that are involved in the regulation of the human L and M opsin genes.

Chapter 5 describes “Future Directions” and presents preliminary evidence regarding which receptors are involved in the response to TH treatment in zebrafish. When TR α B and RXR γ a mutant zebrafish were treated with TH there was still the expected increase in *lws1* and *rh2-2* transcript but not a decrease in *lws2* or *rh2-1* transcript. TR β knockout fish do not express *lws1* or *lws2* and are completely lacking in LWS cones. However, the changes in *rh2-1* and *rh2-2* expression in response to TH treatment were still normal. These results serve to illuminate the complexity of the mechanisms involved. TR β knockout results in the loss of LWS cones. This makes investigating the involvement of TR β in the response to TH treatment a difficult prospect. Strategies to overcome this dilemma are discussed in greater detail. These initial findings demonstrate that TR β is not required for the changes in transcription for the *rh2* locus. Also, the fact that changes in response to TH for *lws2* and *rh2-1* do not occur in TR α B and RXR γ a mutants but the response to TH is observed for *lws1* and *rh2-2* highlights another level of complexity in this mechanism governing transcription of these tandemly replicated opsin genes.

A more complete understanding of the gene regulatory landscape that determines cone fate and identity is emerging. Identification of the molecular mechanisms governing these processes is of great interest for the entire field of vision research. The potential impacts are vast and profound. According to the Center of Disease Control in the US there are 3.4 million people over the age of 40 that are either legally blind or are visually impaired. The World Health Organization has said that globally there are at least 2.2 billion people that have a vision impairment. Whether it is the study of development or disease, the ecological and environmental factors that influence development and disease, or the pursuit of novel therapeutics and treatments the knowledge gleaned from this study will help to propel the progress of many scientific endeavors.

Literature Cited

- 1 Masland, R. H. The neuronal organization of the retina. *Neuron* **76**, 266-280, doi:10.1016/j.neuron.2012.10.002 (2012).
- 2 Swaroop, A., Kim, D. & Forrest, D. Transcriptional regulation of photoreceptor development and homeostasis in the mammalian retina. *Nature Reviews Neuroscience* **11**, 563-576, doi:10.1038/nrn2880 (2010).
- 3 Wald, G. THE PORPHYROPSIN VISUAL SYSTEM. *The Journal of general physiology* **22**, 775-794 (1939).
- 4 Shichida, Y. & Imai, H. Visual pigment: G-protein-coupled receptor for light signals. *Cell Mol Life Sci* **54**, 1299-1315, doi:10.1007/s000180050256 (1998).
- 5 Shichida, Y. & Matsuyama, T. Evolution of opsins and phototransduction. *Philos Trans R Soc Lond B Biol Sci* **364**, 2881-2895, doi:10.1098/rstb.2009.0051 (2009).
- 6 Morizumi, T., Imai, H. & Shichida, Y. Two-step mechanism of interaction of rhodopsin intermediates with the C-terminal region of the transducin alpha-subunit. *J Biochem* **134**, 259-267, doi:10.1093/jb/mvg139 (2003).
- 7 Stenkamp, D. L. Development of the Vertebrate Eye and Retina. *Prog Mol Biol Transl Sci* **134**, 397-414, doi:10.1016/bs.pmbts.2015.06.006 (2015).
- 8 Cepko, C. L. The Determination of Rod and Cone Photoreceptor Fate. *Annu Rev Vis Sci* **1**, 211-234, doi:10.1146/annurev-vision-090814-121657 (2015).
- 9 Brzezinski, J. A. & Reh, T. A. Photoreceptor cell fate specification in vertebrates. *Development* **142**, 3263-3273, doi:10.1242/dev.127043 (2015).
- 10 Yokoyama, S. Molecular evolution of vertebrate visual pigments. *Progress in Retinal and Eye Research* **19**, 385-419, doi:[https://doi.org/10.1016/S1350-9462\(00\)00002-1](https://doi.org/10.1016/S1350-9462(00)00002-1) (2000).
- 11 Raymond, P. A., Barthel, L. K., Rounsifer, M. E., Sullivan, S. A. & Knight, J. K. Expression of rod and cone visual pigments in goldfish and zebrafish: A rhodopsin-like gene is expressed in cones. *Neuron* **10**, 1161-1174, doi:[https://doi.org/10.1016/0896-6273\(93\)90064-X](https://doi.org/10.1016/0896-6273(93)90064-X) (1993).
- 12 Chinen, A., Hamaoka, T., Yamada, Y. & Kawamura, S. Gene duplication and spectral diversification of cone visual pigments of zebrafish. *Genetics* **163**, 663-675 (2003).
- 13 Applebury, M. L. *et al.* The Murine Cone Photoreceptor: A Single Cone Type Expresses Both S and M Opsins with Retinal Spatial Patterning. *Neuron* **27**, 513-523, doi:[https://doi.org/10.1016/S0896-6273\(00\)00062-3](https://doi.org/10.1016/S0896-6273(00)00062-3) (2000).
- 14 Nathans, J., Thomas, D. & Hogness, D. S. Molecular genetics of human color vision: the genes encoding blue, green, and red pigments. *Science* **232**, 193-202 (1986).

- 15 Duval, M. G., Oel, A. P. & Allison, W. T. *gdf6a* is required for cone photoreceptor subtype differentiation and for the actions of *tbx2b* in determining rod versus cone photoreceptor fate. *PLoS One* **9**, e92991, doi:10.1371/journal.pone.0092991 (2014).
- 16 Raymond, P. A. *et al.* Patterning the cone mosaic array in zebrafish retina requires specification of ultraviolet-sensitive cones. *PLoS One* **9**, e85325, doi:10.1371/journal.pone.0085325 (2014).
- 17 Alvarez-Delfin, K. *et al.* *Tbx2b* is required for ultraviolet photoreceptor cell specification during zebrafish retinal development. *Proceedings of the National Academy of Sciences* **106**, 2023-2028, doi:10.1073/pnas.0809439106 (2009).
- 18 Stevens, C. B., Cameron, D. A. & Stenkamp, D. L. Plasticity of photoreceptor-generating retinal progenitors revealed by prolonged retinoic acid exposure. *BMC Dev Biol* **11**, 51, doi:10.1186/1471-213X-11-51 (2011).
- 19 Mears, A. J. *et al.* *Nrl* is required for rod photoreceptor development. *Nature genetics* **29**, 447-452, doi:10.1038/ng774 (2001).
- 20 Webber, A. L. *et al.* Dual role of *Nr2e3* in photoreceptor development and maintenance. *Experimental Eye Research* **87**, 35-48, doi:<https://doi.org/10.1016/j.exer.2008.04.006> (2008).
- 21 Corbo, J. C. & Cepko, C. L. A hybrid photoreceptor expressing both rod and cone genes in a mouse model of enhanced S-cone syndrome. *PLoS Genet* **1**, e11, doi:10.1371/journal.pgen.0010011 (2005).
- 22 Ng, L. *et al.* A thyroid hormone receptor that is required for the development of green cone photoreceptors. *Nature genetics* **27**, 94-98, doi:10.1038/83829 (2001).
- 23 Roberts, M. R., Hendrickson, A., McGuire, C. R. & Reh, T. A. Retinoid X receptor (γ) is necessary to establish the S-opsin gradient in cone photoreceptors of the developing mouse retina. *Invest Ophthalmol Vis Sci* **46**, 2897-2904, doi:10.1167/iovs.05-0093 (2005).
- 24 Suzuki, S. C. *et al.* Cone photoreceptor types in zebrafish are generated by symmetric terminal divisions of dedicated precursors. *Proc Natl Acad Sci U S A* **110**, 15109-15114, doi:10.1073/pnas.1303551110 (2013).
- 25 Volkov, L. I. *et al.* Thyroid hormone receptors mediate two distinct mechanisms of long-wavelength vision. *Proc Natl Acad Sci U S A* **117**, 15262-15269, doi:10.1073/pnas.1920086117 (2020).
- 26 Deveau, C. *et al.* Thyroid hormone receptor beta mutations alter photoreceptor development and function in *Danio rerio* (zebrafish). *PLoS Genet* **16**, e1008869, doi:10.1371/journal.pgen.1008869 (2020).
- 27 Liu, Y., Fu, L., Chen, D. G. & Deeb, S. S. Identification of novel retinal target genes of thyroid hormone in the human WERI cells by expression microarray analysis. *Vision Res* **47**, 2314-2326, doi:10.1016/j.visres.2007.04.023 (2007).

- 28 Eldred, K. C. *et al.* Thyroid hormone signaling specifies cone subtypes in human retinal organoids. *Science* **362**, doi:10.1126/science.aau6348 (2018).
- 29 Bianco, A. C. & Larsen, P. R. Cellular and Structural Biology of the Deiodinases. *Thyroid* **15**, 777-786, doi:10.1089/thy.2005.15.777 (2005).
- 30 Brent, G. A. Mechanisms of thyroid hormone action. *J Clin Invest* **122**, 3035-3043, doi:10.1172/JCI60047 (2012).
- 31 Shibusawa, N., Hollenberg, A. N. & Wondisford, F. E. Thyroid hormone receptor DNA binding is required for both positive and negative gene regulation. *J Biol Chem* **278**, 732-738, doi:10.1074/jbc.M207264200 (2003).
- 32 Wu, Y., Xu, B. & Koenig, R. J. Thyroid hormone response element sequence and the recruitment of retinoid X receptors for thyroid hormone responsiveness. *J Biol Chem* **276**, 3929-3936, doi:10.1074/jbc.M006743200 (2001).
- 33 Paquette, M. A., Atlas, E., Wade, M. G. & Yauk, C. L. Thyroid hormone response element half-site organization and its effect on thyroid hormone mediated transcription. *PLoS One* **9**, e101155, doi:10.1371/journal.pone.0101155 (2014).
- 34 Roberts, M. R., Srinivas, M., Forrest, D., Morreale de Escobar, G. & Reh, T. A. Making the gradient: Thyroid hormone regulates cone opsin expression in the developing mouse retina. *Proceedings of the National Academy of Sciences of the United States of America* **103**, 6218-6223, doi:10.1073/pnas.0509981103 (2006).
- 35 McCaffery, P., Posch, K. C., Napoli, J. L., Gudas, L. & Dräger, U. C. Changing Patterns of the Retinoic Acid System in the Developing Retina. *Developmental Biology* **158**, 390-399, doi:<https://doi.org/10.1006/dbio.1993.1197> (1993).
- 36 Sakai, Y., Luo, T., McCaffery, P., Hamada, H. & Drager, U. C. CYP26A1 and CYP26C1 cooperate in degrading retinoic acid within the equatorial retina during later eye development. *Dev Biol* **276**, 143-157, doi:10.1016/j.ydbio.2004.08.032 (2004).
- 37 da Silva, S. & Cepko, C. L. Fgf8 Expression and Degradation of Retinoic Acid Are Required for Patterning a High-Acuity Area in the Retina. *Dev Cell* **42**, 68-81 e66, doi:10.1016/j.devcel.2017.05.024 (2017).
- 38 Xiao, M. & Hendrickson, A. Spatial and temporal expression of short, long/medium, or both opsins in human fetal cones. *Journal of Comparative Neurology* **425**, 545-559, doi:10.1002/1096-9861(20001002)425:4<545::Aid-cne6>3.0.Co;2-3 (2000).
- 39 Vollrath, D., Nathans, J. & Davis, R. Tandem array of human visual pigment genes at Xq28. *Science* **240**, 1669-1672, doi:10.1126/science.2837827 (1988).
- 40 Hofmann, C. M. & Carleton, K. L. Gene duplication and differential gene expression play an important role in the diversification of visual pigments in fish. *Integr Comp Biol* **49**, 630-643, doi:10.1093/icb/icp079 (2009).

- 41 Mitchell, D. M. *et al.* Retinoic Acid Signaling Regulates Differential Expression of the Tandemly-Duplicated Long Wavelength-Sensitive Cone Opsin Genes in Zebrafish. *PLoS Genet* **11**, e1005483, doi:10.1371/journal.pgen.1005483 (2015).

Chapter 2: Endocrine Regulation of Multi-Chromatic Color Vision

Abstract

Vertebrate color vision requires spectrally-selective opsin-based pigments, expressed in distinct cone photoreceptor populations. In primates and in fish, spectrally divergent opsin genes may reside in head-to-tail tandem arrays. Mechanisms underlying differential expression from such arrays have not been fully elucidated. Regulation of human red (*LWS*) vs. green (*MWS*) opsins is considered a stochastic event, whereby upstream enhancers associate randomly with promoters of the proximal or distal gene, and one of these associations becomes permanent. We demonstrate that, distinct from this stochastic model, the endocrine signal thyroid hormone (TH) regulates differential expression of the orthologous zebrafish *lws1/lws2* array, and of the tandemly-quadruplicated *rh2-1/rh2-2/rh2-3/rh2-4* array. TH treatment caused dramatic, dose-dependent increases in abundance of *lws1*, the proximal member of the *lws* array, and reduced *lws2*. Fluorescent *lws* reporters permitted direct visualization of individual cones switching expression from *lws2* to *lws1*. Athyroidism increased *lws2* and reduced *lws1*, except within a small ventral domain of *lws1* that was likely sustained by retinoic acid signaling. Changes in *lws* abundance and distribution in athyroid zebrafish were rescued by TH, demonstrating plasticity of cone phenotype in response to this signal. TH manipulations also regulated the *rh2* array, with athyroidism reducing abundance of distal members. Interestingly, the opsins encoded by the proximal *lws* gene and distal *rh2* genes are sensitive to longer wavelengths than other members of their respective arrays; therefore endogenous TH acts upon each opsin array to shift overall spectral sensitivity toward longer wavelengths, underlying coordinated changes in visual system function during development and growth.

Introduction

Cone photoreceptors of the vertebrate retina mediate daylight vision and are critical for high acuity vision and color discrimination. Cone types are determined by the opsin protein expressed. Vertebrate cone opsins are classified into four phylogenetic types: SWS1 (short wavelength-sensitive type 1, UV-blue), SWS2 (short wavelength-sensitive type 2, blue), RH2 (medium wavelength-sensitive, green), and M/LWS (medium to long wavelength-sensitive, red)¹. Humans have three cone

types: LWS (red), MWS (green), and SWS1 (blue)². The *LWS* and *MWS* opsin genes are arranged in a tail to head manner on the X chromosome, and are expressed in separate cone populations³. The choice of *LWS* or *MWS* expression is thought to be a stochastic event. In the current model, an upstream locus control region (LCR) preferentially associates with either the *LWS* or *MWS* promoter⁴. This association then becomes permanent, resulting in mutually exclusive expression of only one of the opsin genes from the array⁴. However, this stochastic model does not explain the relative distribution of LWS vs. MWS cones as a function of retinal eccentricity, with LWS:MWS ratios higher in peripheral than in central retina⁵. This gradient suggests the potential for additional, trans-regulatory mechanisms.

Fish are the only other vertebrate taxonomic group besides primates known to contain tandemly-replicated opsin genes⁶. In zebrafish, the *lws1* gene (orthologous to human *LWS*) has undergone a tandem replication (independent of the *LWS/MWS* replication event in humans) resulting in a second member (*lws2*) encoding an opsin with a shorter wavelength-shifted sensitivity⁷. The zebrafish *lws* locus contains an upstream regulatory region termed the LWS Activating Region (LAR) that is required for proper expression of either member of the array⁸. The adult zebrafish displays an *lws1/lws2* gradient similar to the LWS/MWS gradient in humans⁵, with a *lws1:lws2* ratio lower in the central retina compared to the periphery⁹. During zebrafish retinal development, *lws1* expression is absent in the early larval retina; onset of its expression occurs in ventral retina at approximately six days post fertilization (6dpf)⁹. The expression domain of *lws1* then expands into nasal/dorsal retina in juveniles and remains in the periphery throughout the remainder of fish growth⁹. These dynamic spatiotemporal expression patterns, and changes in *lws1/lws2* ratio seen during development, further indicate that regulation of these tandemly-replicated opsin genes goes beyond a stochastic mechanism. Indeed, we recently demonstrated that the paracrine signal retinoic acid (RA) is involved in differentially regulating *lws1* vs *lws2*¹⁰. Exogenous RA treatment of embryos during photoreceptor differentiation resulted in increased *lws1* and a decrease in *lws2*. Conversely, *lws1* was decreased when RA signaling was reduced. However, *lws2* expression was either decreased or unaffected by

reduced RA signaling, suggesting other factors are likely involved in the endogenous regulation of *lws2*. This was the first reported evidence of a trans-acting mechanism involved in differentially regulating tandemly-replicated opsin genes, providing evidence of regulation beyond a stochastic mechanism.

In addition to the tandemly-duplicated *lws* opsins, the *rh2* cone opsin array in zebrafish has been tandemly-quadruplicated⁷. The *rh2* array has an upstream LCR required for the expression of any of the four opsin genes¹¹. In contrast with the *lws* array, the *rh2* gene encoding the longest wavelength-sensitive opsin (*rh2-4*) is most distally positioned, while that encoding the shortest wavelength-sensitive opsin (*rh2-1*) is most proximally positioned on the array. The *rh2-1* expression domain, like the *lws2* domain, is widespread throughout the larval retina, then recedes in the periphery and is isolated to central retina in juveniles and adults⁹. *rh2-2* expression is also widespread throughout the larval retina, recedes from central retina in juveniles, but is restored in the central retina of adults⁹. Expression of both *rh2-3* and *rh2-4* remains low and restricted to peripheral regions throughout life. In summary, expression of the shorter wavelength-sensitive members of both the *lws* and *rh2* arrays occurs before the longer wavelength-sensitive members, and in adult retina the shorter wavelength-sensitive members are expressed in central/dorsal retina while longer wavelength-sensitive members are expressed in ventral/peripheral areas⁹. The mechanisms governing these dynamic changes in expression patterns throughout development and growth have not been fully elucidated, but the establishment of the adult patterns is known to involve cis-elements in upstream and intergenic regions and the relative proximal-to-distal position of each member of the array¹².

The endocrine signal thyroid hormone (TH) plays a pivotal role in the development of the retina, specifically in cone differentiation^{13,14,15,16,17 18}. TH is synthesized in the thyroid as tetra-iodothyronine (thyroxine; T₄). T₄ enters the circulatory system where in the periphery it is converted into tri-iodothyronine (T₃) by the cellular enzyme deiodinase 2 (Dio2)¹⁹. T₃ binds to nuclear TH receptors to regulate gene expression. In addition to TH homodimers, TH receptors can heterodimerize with retinoid X receptors (RXRs) to influence gene expression²⁰. Considering our

previous work¹⁰, accompanied by the known involvement of TH in regulating opsin expression in other organisms^{21,22,23}, we hypothesized that TH may also be involved in the differential regulation of the tandemly-duplicated *lws* opsin genes in zebrafish. We performed gain of function studies involving a TH (T3) treatment regimen 2-4dpf, a time of *lws2* expression but prior to the normal onset of expression of *lws1*⁹. Utilizing reverse transcription quantitative PCR, *in situ* hybridization, and transgenic zebrafish reporting *lws1* and *lws2* expression⁸, we identified TH as a potent regulator of differential expression of tandemly-replicated opsins in zebrafish, including both the *lws* and *rh2* opsin arrays. Loss of function and T3 localization studies provided further evidence of TH's endogenous role in this regulatory mechanism. Furthermore, we demonstrated that expression of tandemly-replicated opsin genes remains plastic and can be influenced by TH exposure in both normal and athyroid juvenile zebrafish.

Methods and Materials

Animals

Zebrafish were maintained in monitored aquatic housing units on recirculating system water at 28.5°C. Embryos were collected according to⁴⁹, with light onset considered to be zero hours postfertilization (hpf) and embryonic age timed accordingly thereafter, with 24hpf considered 1 day postfertilization (dpf), 48hpf considered 2dpf, etc. Embryos used for whole mount analyses were kept transparent by incubating them in system water containing 0.003% phenylthiourea (PTU) to inhibit melanin synthesis. All experiments using animals were approved by the University of Idaho's Animal Care and Use Committee. Wild-type embryos were of an in-house outbred strain originally obtained from Scientific Hatcheries (now Aquatica Tropicals, Plant City, FL) and are referred to as "wildtype". In the transgenic line *Tg (LWS1/GFP-LWS2/RFP-PAC(H)) #430*, the "transgene" consists of a PAC clone in which the first exons of *lws1* and *lws2* were replaced with GFP and RFP, respectively, each followed by a polyadenylation sequence⁸. The spatiotemporal expression patterns of GFP and RFP replicate endogenous patterns of *lws1* and *lws2*. We refer to this line as *lws:PAC(H)*. The transgenic

zebrafish line “Ligand Trap-Thyroid Receptor β ” (LT-TR β) was a generous gift from Jens Tiefenbach at InDanio Bioscience Inc., Toronto, Ontario, Canada. In the ligand trap (LT) system, a Lex-DNA-binding domain (DBD) human nuclear receptor ligand-binding domain (LBD) fusion protein is used to signal the presence of ligand in vivo. Binding of the fusion protein to a Lex-dependent GFP reporter results in GFP expression in the presence of endogenous or added ligands and cofactors. The LT-TR β line also has an element called LOOP. This element contains the Col1 binding sites for LEXDBD followed by a LEX-DBD-GAL activation domain (AD). Therefore, an activated TR β will lead to reporter GFP expression but also to GAL AD expression which will increase GFP expression²⁷. The transgenic line *Tg(tg:nVenus-2a-nfsB)wp.rt8* was a generous gift from David Parichy at the University of Virginia. The transgene consists of the thyroglobulin start site driving expression of nuclear Venus linked to the 2A viral peptide and nitroreductase encoded by *nfsB*²⁹. The transgenic zebrafish line RGnY was generously provided by Elwood Linney. The transgene consists of three copies of retinoic acid response elements (RAREs) derived from the mouse RAR β gene, a zebrafish basal promoter, a Topaz YFP sequence, an SV40 polyadenylation signal, and a small t intron. The endogenous expression patterns of YFP in these fish are consistent with known areas undergoing RA signaling and YFP reporter expression increases in response to exogenous RA^{32,50}. We refer to this line as *RARE:YFP*.

T3/T4 and metronidazole treatments and heat shock

Stock solutions of T3 and metronidazole were prepared in dimethylsulfoxide (DMSO; Sigma) and stored in the dark at -20°C. Prior to treatment, embryos/larvae were manually dechorionated, and then 1000X stock solution was added to the water to result in the final concentrations indicated in Results (DMSO was at a final concentration of 0.1%). T3 was used as the experimental treatment for embryos/larvae, because T3 treatment was shown to result in T3 accumulation within the eyes of embryonic zebrafish to a greater extent than did a T4 treatment²⁷. T3-treated larvae did not appear grossly different from controls, except for a lack of pigmentation. The appearance of athyroid

juveniles was similar to that reported by McMenamin et al.²⁹. T4 stock solutions were prepared in NaOH and stored in the dark at -20°C. Juveniles were maintained in 250ml beakers in system water. 1000X stock T4 solution was added to the water to result in the final concentrations indicated in Results (NaOH was at a final concentration of 0.01%). T4 was used as the experimental treatment for juveniles, because T4 must travel to target tissues via the circulation at this stage, and to be consistent with other studies of TH treatment in post-larval fish^{29,33,44}. T4 treatments had no noticeable effect on the general appearance of juveniles. For treatments lasting longer than one day, solutions were refreshed every 24 hrs. Heat shocks (to induce expression of “Ligand Trap”) were performed at 2 or 3dpf by transferring embryos to 37°C for 30 min.

Quantitative reverse transcriptase polymerase chain reaction analysis

Total RNA from each treatment group of pooled (5-6) whole larvae or in the case of juveniles, total RNA from the two eyes of each fish from each condition was extracted using the Machery-Nagel kit, and was used to synthesize cDNA template using the High Capacity cDNA Reverse Transcription kit with random primers (Applied Biosystems, Inc. [ABI], Foster City, CA). Gene-specific primer pairs are listed in Supplemental Table 3. Amplification to measure abundance of specific transcripts was performed on a model 7900HT Fast Real-Time PCR System using SYBR-Green PCR Master Mix (ABI). Relative quantitation of gene expression using the ddCT method (Applied Biosystems-Guide to Performing Relative Quantitation of Gene Expression Using Real-Time Quantitative PCR) between control and experimental treatments was determined using the 18s ribosomal RNA and *β-actin* as the endogenous references. Graphing and statistics were performed using Excel. p-values were calculated using a Wilcoxon Mann-Whitney U test, or the Kruskal- Wallis Test with a Conover post- hoc test further adjusted by the Benjamini-Hochberg False Discovery Rate method.

Histological processing and in situ hybridization

Fixation and preparation of embryos for tissue sectioning and in situ hybridization were performed as previously described^{50,51}. For in situ experiments, cRNA probes were generated by in vitro reverse transcription of cDNAs. Digoxigenin- (dig-) UTPs were incorporated into probes for detection with anti-dig antibodies conjugated to alkaline phosphatase and visualized with NBT-BCIP substrate. Images were captured using a Leica DM2500 compound microscope with a Leica DFC700T camera system. *in situs* were viewed and photographed using Nomarski (differential interference contrast) optics and brightfield optics.

Confocal photography and quantification: *lws:PAC(H)* embryos

lws:PAC(H) embryos were maintained in system water with PTU starting at 24 hpf. At 2 or 3dpf, embryos were treated with T3 or DMSO through 3 or 4dpf, and then fixed in 4% paraformaldehyde in phosphate-buffered (pH=7.0) 5% sucrose solution for 1 hour, washed once in phosphate-buffered sucrose solution for 30 minutes followed by three washes in phosphate buffered saline (PBS). Following fixation and washing, embryos were incubated in PBS at 4°C in the dark for no longer than 24 hours. Immediately prior to imaging, whole eyes were removed from fixed embryos, the sclera teased away by microdissection, and eyes were then coverslipped in glycerol. Imaging was performed with a 20X dry or 40X water-immersion lens using a Nikon Andor spinning disk confocal microscope equipped with a Zyla sCMOS camera running Nikon Elements software. A z-series covering the entire globe of the eye was obtained with 3-micron step sizes. FIJI (ImageJ) was used to flatten z stacks via max projection and adjust brightness/contrast. Images from samples where GFP signal was not resolvable in all planes (due to the developing RPE and/or iridophores in residual sclera) were excluded from analysis.

Confocal photography: juvenile zebrafish retinal whole mounts

One-month old juvenile zebrafish were anaesthetized and decapitated. Heads were fixed in 4% paraformaldehyde/sucrose solution as described above for 30 minutes. After 30 minutes, heads

were removed and corneas punctured with a dissecting pin, then returned to the fixation solution for another 30 minutes. The lens was removed followed by the whole retina. The retina was flattened and mounted in glycerol and coverslipped. Imaging was performed at 20X magnification using a Nikon Andor spinning disk confocal microscope equipped with a Zyla sCMOS camera running Nikon Elements software. The stitching feature was used to capture the whole retina. A z-series covering the entire retina was obtained with 3 micron step sizes. FIJI (ImageJ) was used to flatten z stacks via max projection and adjust brightness/contrast.

Confocal microscopy: live imaging

5dpf *lws:PAC(H)* larvae were immersed in 100nM T3 at 8am. Before imaging, larvae were immobilized in a 2% agarose pad in a 35mm glass bottom dish and overlaid with 28°C system water containing 100nM T3 and 0.02% MS-222 solution. Imaging was performed with a 40X water-immersion lens using a Nikon Andor spinning disk confocal microscope equipped with a Zyla sCMOS camera running Nikon Elements software. Timecourse began at 4pm and lasted for 9 hours total. Images were captured at 30 min intervals. A 3-micron step z-series covering the area of interest was converted into volume view using the Nikon Elements software. The Director feature in Nikon Elements software was used to create the time-lapse movie.

Supplementary Methods:

Thyroid hormone (T3) treatment timecourse

WT or *lws:PAC(H)* larvae were treated with DMSO or 100nM T3 from 2-3, 2-4, or 3-4dpf. Larvae were collected for RNA isolation and qPCR or fixed and imaged by confocal microscopy using the same methods for the larval T3 treatments above.

Pattern analysis

Z-stacks of whole mounted eyes of DMSO or T3 treated *lws:PAC(H)* embryos at 20X magnification were flattened in FIJI using max projection. Rectangular regions showing minimal

curvature were selected from these images. LWS cones were manually identified, and regions were analyzed using WinDRP software (downloaded from the Euler Lab) to calculate the Nearest Neighbor Distance (NND) and Regularity Index (RI) of the LWS cone mosaic^{59,60}. Patterns were compared to 1000 randomly-distributed simulated patterns of the same number of cones using a Kruskal-Wallis test.

Response element analysis

FASTA sequences including the proximal upstream regulatory regions for the *lws* (*opn1lw1* ENSDARG00000044862, *opn1lw2* ENSDARG00000044861) and *rh2* (*opn1mw1* ENSDARG00000097008, *opn1mw2* ENSDARG00000044280, *opn1mw3* ENSDARG00000044279, *opn1mw4* ENSDARG0000000638) opsin genes were analyzed using MatInspector⁶¹ and PROMO^{62,63} software for putative response elements for TRs, RXRs, and RARs. These programs use consensus sequences for transcription factor binding sites from databases such as Transfac (TRANSCRIPTION FACTOR database) to predict potential binding sites.

Results

Thyroid hormone treatment alters relative expression levels and patterns of *lws* opsin transcripts.

To test our hypothesis that TH signaling regulates the differential expression of tandemly-replicated opsin genes, we augmented levels of TH in wild-type zebrafish embryos/larvae by immersion in 4, 20, or 100nM T3 from 2-4dpf and determined the effects on *lws1* vs. *lws2* expression in comparison to a control (0.1% DMSO) treatment. Quantitative PCR revealed that T3 treatment resulted in a strong dose-dependent increase in *lws1* transcript abundance (Fig. 2.1A), with up to a 1000-fold increase compared to control at the highest T3 concentration (Fig. 2.1A). Abundance of *lws2* did not change due to 4nM or 20nM T3 treatment but decreased as much as 30-fold with the highest concentration (Fig. 2.1B). T3 was much more effective than retinoids, since retinoids increased *lws1* three-fold and decreased *lws2* two-to-five-fold¹⁰. We then employed *in situ* hybridization using transcript-specific probes for both members of the *lws* array. *lws1* was not detected in cryosectioned, control retinas at 4dpf, consistent with previous reports indicating that the

normal onset of expression of *lws1* is approximately 6dpf⁹. In T3 treated larvae, expression of *lws1* in the outer nuclear layer (ONL, containing photoreceptors) was detected at 4dpf, and included dramatic expansion of the expression domain (Fig. 2.1C). Expression of *lws1* appeared most concentrated in the ventral retina and expanded dorsally with increasing T3. *lws2* expression in controls was widespread throughout the retina, consistent with previous reports⁹, but diminished with increasing amounts of T3 (Fig. 2.1D). Ventral retina became progressively *lws2*-depleted by 4nM and by 20nM T3, while a more complex pattern of remnant *lws2* expression resulted from 100 nM T3 (Fig. 2.1D). These findings demonstrate a robust effect of exogenous TH on relative levels of *lws1* vs. *lws2* transcript, together with substantial changes of their expression domains.

Global patterns of *lws1* and *lws2* in the developing retina are altered due to thyroid hormone treatment.

To better visualize the spatial distribution of *lws1/lws2* expression in the developing retina, as well as any cones coexpressing both opsins, we utilized a transgenic line *Tg(LWS1/GFP-LWS2/RFP-PAC(H)) #430*⁸, which we refer to as *lws:PAC(H)*. This line reports *lws1* expression with GFP and *lws2* with RFP, and faithfully reports the native expression patterns of the two opsins⁸, albeit with a slight delay in *lws2* (RFP) expression in comparison with native transcript¹⁰. *lws:PAC(H)* embryos were treated with T3 or DMSO (control) from 2-4dpf. RFP+ (*lws2*) cones were detected in cryosections from control embryos throughout most of the retina (Fig. 2.2A). GFP+ (*lws1*+) cones were not detected in controls at 4dpf (Fig. 2.2A). In contrast, in T3 treated embryos, GFP+ cones were detected in ventral retina (Fig. 2.2B), which matches the location of later, endogenous onset of *lws1* expression⁹. With increasing concentrations of T3, the distribution of GFP+ cells expanded into central and dorsal retina (Fig. 2.2C, D).

When we examined whole retinas, RFP+ (*lws2*+) cones were detected in control embryos throughout most of the retina, but little to no RFP was present in the dorsal/temporal region. Again, GFP+ (*lws1*+) cones were not detected in control embryos at 4dpf (Fig. 2.2E). Corroborating our

results from cryosections, in 4nM T3 treated embryos, GFP+ cones were detected in ventral retina (Fig. 2.2F). With increasing concentrations of T3, the distribution of GFP+ cones expanded nasally and dorsally (Fig. 2.2G, H). Areas displaying increased numbers of GFP+ cones included a ventral patch and a dorsal/nasal area largely isolated to the periphery. T3 caused dose-dependent increases in the number of GFP+ cones (Fig. 2.2I), and in the number of co-labeled cones (Fig. 2.2K). These co-labeled cones simultaneously expressed both reporters, suggesting that these cones were switching expression from *lws2* to *lws1*. The numbers of RFP+ (*lws2*+) cones were significantly reduced with the highest concentration of T3 (Fig. 2.2J). These results, together with evidence from qPCR and *in situ* hybridization, suggest that the dramatic increase in *lws1* is at the expense of *lws2* expression in individual LWS cones. Alternatively, or in addition, co-expressing cells could be explained by transcription of *lws1* from one allele while *lws2* is transcribed from the other.

Exogenous thyroid hormone triggers opsin switching in individual cones.

We used two complementary strategies to determine whether individual LWS cones engage in “opsin switching” in response to T3: live confocal imaging, and two-dimensional (2D) pattern analysis of the LWS cone mosaic²⁴, both using the *lws:PAC(H)* transgenic zebrafish. To directly observe LWS cones switching opsin expression in real time, we treated *lws:PAC(H)* larvae with 100nM T3, and imaged ventral retina for 9 hrs at 40X magnification starting 8 hours after the T3 treatment began. Time-lapse video revealed that some RFP+ cones began to express GFP, showing domains of co-expression that then expanded within each cone, followed by a switch to primarily GFP expression, with some remaining co-expression (Fig. 2.3 and SI Video S1). These results strongly support a switch from *lws2* to *lws1* in individual LWS cones in response to the T3 treatment.

The rationale for 2D pattern analysis is that, if an *lws2*-to-*lws1* switch (RFP to GFP) takes place within individual cones, vs. recruiting other cone types to express *lws1* (GFP), then T3 treatment should result in no disruption of the spatial arrangement of LWS cones labeled by either or both reporters¹⁰. Average nearest neighbor distances (NNDs) (SI Appendix, SI Methods) were similar

for RFP+ cones in untreated larvae in comparison with the entire population of labeled cones (GFP+ and RFP+) in treated larvae, suggesting that the GFP+ cones did not disrupt the pattern of LWS cones (SI Appendix, Fig. S2.1). However, the combined GFP+ and RFP+ average NND was greater than that of the GFP+ cones, consistent with the GFP+ cones comprising a fraction of a total LWS cone population (SI Appendix, Fig. S2.1E). Calculating the regularity index (RI: mean NND/s.d., adjusted for object density)^{24,25} as a measure of pattern regularity (SI Appendix, Fig. S2.1F), and comparing each selected region with 1000 random simulations having the same number of objects (SI Appendix, Fig. S2.1G) revealed no differences among groups for both the RI, and the $RI_{\text{sample}}/RI_{\text{random}}$, suggesting that the presence of GFP+ cones in T3-treated samples did not disrupt the regular cone mosaic (SI Appendix, Fig. S2.1F,G).

A time-course treatment with thyroid hormone reveals kinetics of changes in *lws* expression.

Lws expression was analyzed in larvae after different durations of 100nM T3 treatment (SI Appendix, SI Methods). After 12 hours of treatment (ht) beginning at 2dpf, abundance of *lws1* and *lws2* transcripts were unchanged (SI Appendix, Fig. S2.2A, B). By 24ht, the magnitude of *lws1* increase was 85-fold higher compared to controls (SI Appendix, Fig. S2.2A), while in contrast *lws2* levels were unchanged (SI Appendix, Fig. S2.2B), suggesting complex temporal kinetics. The changes in transcript abundance were most pronounced when embryos were treated from 2-4dpf (SI Appendix, Fig. S2.2A,B; see also Fig. 2.1A).

In similar time-course experiments using the *lws:PAC(H)* transgenics, a few GFP+ (*lws1*+) cones were detected after 12ht (treatment beginning at 2dpf) in the ventral retina (SI Appendix, Fig. S2.2C), and at 24ht GFP+ cones increased in number and retinas displayed dorsal expansion of regions containing GFP+ cones (SI Appendix, Fig. S2.2D). GFP+ cones were not detected at 4dpf (Fig. 2.2A). At 24ht RFP+ (*lws2*+) cones were initially detected along with co-labeled cones in the ventral retina of T3 treated embryos (SI Appendix, Fig. S2.2D). By 48ht the RFP+ cones were

detected throughout the retina, as well as GFP+ and co-labeled cones in the ventral retina and dorsal/nasal area in T3 treated embryos (SI Appendix, Fig. S2.2E).

T3 accumulates in LWS cones upon exogenous treatment.

We wished to determine whether LWS cones accumulate T3 in embryos/larvae exposed to exogenous T3, consistent with a potentially cell-autonomous mechanism. LWS cones express *thyroid hormone receptor $\beta 2$* (*tr $\beta 2$*)²⁶. We utilized a transgenic line that reports *tr $\beta 2$* with tdTomato to label all LWS cones²⁶, and crossed it to a “ligand trap” transgenic that reports the intracellular presence of T3 with GFP^{27,28}. Embryos from this cross were treated with 100nM T3 starting at 2dpf. In non-treated embryos, the ligand trap did not detect endogenous levels of T3²⁷. With 100nM T3, GFP+ cells reporting T3 accumulation were observed in multiple retinal layers, including many in the ONL, at both 3 and 4dpf (Fig. 2.4 A,B). Many, but not all, of the GFP+ cells (T3-accumulating) of the ONL co-expressed the *trB2* reporter, and numerous, but not all, of the tdTomato+ (LWS cones) co-expressed GFP (Fig. 2.4 insets). The fraction of LWS cones accumulating T3 appeared consistent with the fraction of LWS cones that switch from *lws2* to *lws1* expression (Fig. 2.2H), leaving open the potential for a cell-autonomous mechanism. The spatial distribution of GFP+ (T3 accumulating) cones did not appear to change from 3-4dpf (Fig. 2.4 A,B).

Ablation of the thyroid gland suppresses the onset of endogenous *lws1* expression.

To evaluate endogenous roles for TH in *lws* regulation, we utilized a transgenic line *Tg(tg:nVenus-2a-nfnB)^{wp.rt8}* in which the thyroid gland is ablated upon metronidazole treatment²⁹. To minimize the levels of circulating TH and to attenuate its synthesis, we experimentally ablated the thyroid in *Tg(tg:nVenus-2a-nfnB)^{wp.rt8}* fish at 2dpf, when the zebrafish thyroid becomes active³⁰. Athyroidism was confirmed by the absence of the Venus YFP reporter-expressing thyroglobulin cells following metronidazole treatment (Fig. 2.5A, B). When measured by qPCR, *lws1* transcript was detected in control larvae at 6dpf. *Lws1* was suppressed in athyroid larvae, consistent with an

endogenous role for TH in controlling *lws1* expression (Fig. 2.5C). However, *lws2* levels were not different in athyroid larvae compared to controls (Fig. 2.5D) at this timepoint.

Crossing *lws:PAC(H)* with *Tg(tg:nVenus-2a-nfnB)^{wp.r18}* allowed visualization of *lws* expression via fluorescent reporters in 6dpf larvae with an active thyroid compared to athyroid larvae. In controls, a small number of GFP+ (*lws1+*) cones were detected in the ventral retina at 6dpf (Fig. 2.5E). In contrast, in athyroid larvae, GFP+ cones were not detected (Fig. 2.5F). Collectively, these results support an endogenous role for embryonically-derived TH in inducing *lws1* expression in LWS cones at the time of normal onset of *lws1* expression.

***Lws* differential expression remains plastic to the effects of TH signaling through juvenile growth.**

We next investigated longer lasting effects of athyroidism on *lws* opsin expression and the plasticity of *lws* expression in response to exogenous TH in growing juvenile zebrafish (Fig 6A). From 26-31dpf, the *lws1* expression domain expands to cover much of ventral and nasal retina⁹. Exogenous T4 (gain-of-function; GOF) over this time did not alter levels of *lws1* transcript, compared to controls (Fig. 2.6B); however, *lws2* was reduced by 30-fold (Fig. 2.6C), indicating that in juvenile zebrafish, LWS cones are plastic to the effects of TH signaling. Following thyroid ablation of *Tg(tg:nVenus-2a-nfnB)^{wp.r18}* embryos at 2dpf, half of the group was immersed in 386 nM T4 from 26-31dpf [as in³¹] (Fig. 2.6A). In athyroid juveniles (loss-of-function; LOF), *lws1* levels were reduced by 15.6-fold and *lws2* was increased by 1.87-fold compared to controls (Fig. 2.6 B, C), supporting roles for endogenous thyroid signaling in both promoting *lws1* expression and reducing *lws2* expression. In athyroid juveniles rescued with T4 (Rescue), abundance of *lws1* transcript was increased by 22-fold, compared with athyroid juveniles (Fig. 2.6B), and *lws2* was reduced 90-fold (Fig. 2.6C), indicating that T4 rescued the effects of athyroidism. Collectively these results demonstrate that *lws1* vs. *lws2* expression can be differentially regulated post-embryonically, and that LWS cones remain plastic to the effects of TH, even in the case of prolonged athyroidism.

Performing the same experiments in the *lws:PAC(H)* transgenics crossed with *Tg(tg:nVenus-2a-nfnB)^{wp.r18}* provided valuable insight into retinal topographic changes in expression of *lws1* vs. *lws2*. In control juveniles, GFP+ (*lws1*+) cones were detected in ventral, nasal, and dorsal retina, and RFP+ (*lws2*+) cones were predominantly observed in central retina, consistent with known patterns of expression of endogenous transcript at this age^{9,10}(Fig. 2.6D). In T4-treated juveniles (GOF), GFP+ cones were detected throughout the peripheral retina, with numerous GFP+ cones in central retina also expressing RFP (Fig. 2.6E, I). In athyroid juveniles (LOF), GFP+ cones were restricted to a ventral sector of the retina, with no nasal or dorsal expansion (Fig. 2.6F). We previously reported a ventral region of juvenile retina in which RA signaling matches a region of *lws1* expression¹⁰. Whole mounted retinas derived from juvenile (age-matched) *RARE:YFP* transgenic fish in which YFP expression is driven by four consecutive retinoic acid response elements (RAREs)³², more precisely revealed this RA signaling domain (Fig. 2.6H). This domain spatially correlates to the restricted domain of *lws1* expression in the athyroid juvenile retinas, suggesting that in the absence of TH, RA signaling in ventral retina is sufficient to promote *lws1* at the expense of *lws2*. In athyroid juveniles rescued with T4 (Rescue), GFP+ cones were detected throughout the peripheral retina, and numerous GFP+ cones in central retina also expressed RFP (Fig. 2.6G). Collectively these results suggest that *lws1* expression in the ventral retina is sustained by RA signaling in athyroid juveniles, but the nasal/dorsal expansion of the *lws1* expression domain requires TH signaling, and can be rescued by T4. These results also provided further evidence that *lws1* vs. *lws2* expression remains plastic and is amenable to TH signaling at least into the juvenile stage of zebrafish growth. We previously reported the presence of predicted consensus RAREs on the *lws* locus¹⁰. We re-analyzed the zebrafish *lws* locus for putative response elements for both thyroid hormone (TRE) and retinoic acid/retinoid X receptors (RARE/RXRE) (SI Appendix, SI Methods), and identified several of these elements upstream from the coding sequence of both genes (SI Appendix, Fig. S2.3A), suggesting the possibility of direct regulatory mechanisms involving both RA and TH.

Differential expression of *rh2-1*, *rh2-2*, and *rh2-3* opsins upon T3 treatment.

The tandemly-quadruplicated *rh2* medium wavelength-sensitive (*opn1mw*) opsin gene locus contains *rh2-1*, *rh2-2*, *rh2-3*, and *rh2-4* genes. To test the hypothesis that TH also regulates differential expression from this array, we performed dose-response T3 studies in larvae, and determined the effects on all four *rh2* transcripts in comparison to a control (0.1%DMSO) treatment. During normal development, at 3dpf, *rh2-1* is expressed in ventral, dorsal, and nasal retina, while *rh2-2* is not detected⁹. Quantitative PCR revealed that the levels of these two *rh2* transcripts were affected in T3 treated (from 2-4dpf) larvae. Abundance of *rh2-1* was not changed due to 4nM T3 treatment but was decreased 2-fold by the higher doses (Fig. 2.7A). Levels of *rh2-2* were increased by 8.9-fold, 6.7-fold, and 7-fold by 4, 20, and 100nM T3, respectively (Fig. 2.7B). Interestingly, in nearly all control (0.1% DMSO) samples, *rh2-3* and *rh2-4* transcripts were not detectable, or unreliably detectable (SI Appendix, Table S1). However, in larvae treated with 100nM T3, *rh2-3* transcript was detectable in all samples, while *rh2-4* was detectable only in three of the six biological replicates (SI Appendix, Table S1). These results collectively suggest that components of the zebrafish *rh2* opsin gene array can be regulated by exogenous T3 in larval zebrafish.

We then employed *in situ* hybridization using gene specific probes for all four members of the *rh2* locus. *rh2-1* expression in controls was widespread throughout the retina, consistent with previous reports⁹, but was diminished with increasing amounts of T3 (Fig. 2.7C). Ventral and dorsal retina was depleted of *rh2-1* by 4nM T3 and little to no *rh2-1* transcript was detected with 20 and 100nM T3, except for a small patch remaining in the central retina (Fig. 2.7C). *rh2-2* was not detected in controls, but was expressed in T3-treated larvae, with larger expression domains resulting from higher doses (Fig. 2.7D). Control sections showed no *in situ* hybridization signal for either *rh2-3* or *rh2-4* (SI Appendix, Fig. S2.4), indicating that transcript levels were below detectable range. We were also unable to detect either of these transcripts in sections of T3-treated larvae (SI Appendix, Fig. S4). It is possible that the levels of *rh2-3* detectable by qPCR (SI Appendix, Table S2.1) cannot be visualized by *in situ* hybridization, or that the sections used for this analysis did not contain the

likely rare *rh2-3+* cone. These outcomes for TH regulation of the *rh2* array are particularly striking because T3 promotes the most proximal gene of the *lws* array (*lws1*), but more distal genes of the *rh2* array (*rh2-2*, *rh2-3*) in larvae, suggesting that, while the general function of TH is conserved, the precise molecular mechanism may be distinct.

***Rh2* differential expression remains plastic to the effects of TH signaling through juvenile growth.**

We next investigated longer lasting effects of athyroidism on *rh2* opsin expression and the plasticity of *rh2* expression in juvenile zebrafish, using the experimental design shown in Fig. 2.6A. In juveniles treated with T4 (GOF), *rh2-1* transcript levels were reduced by 93-fold (Fig. 2.8A), and abundance of *rh2-3* was increased by 1.8-fold (Fig. 2.8C). Levels of *rh2-2* and *rh2-4* were unchanged in comparison with controls (Fig. 2.8B,D). In athyroid juveniles (LOF), *rh2-1* levels were not different (Fig. 2.8A), while levels of *rh2-2*, *rh2-3*, and *rh2-4* transcripts were reduced by 5.3-fold, 9.8-fold, and 2.2-fold, respectively, compared to controls (Fig. 2.8B-D). In athyroid juveniles treated with T4 (Rescue), *rh2-1* was decreased 477-fold, *rh2-2* was not changed, while abundance of *rh2-3* and *rh2-4* transcripts was increased 11-fold and 7-fold respectively (rescued), compared to athyroid juveniles (Fig. 2.8B-D). To summarize, TH GOF drastically decreased *rh2-1* but not *rh2-2* and *rh2-4*, while *rh2-3* was increased. Surprisingly, TH LOF did not alter *rh2-1* levels, but *rh2-2*, *rh2-3* and *rh2-4* were all decreased, consistent with an endogenous role for TH signaling in regulating the distal members of the *rh2* array during juvenile zebrafish growth. Collectively these results demonstrate that *rh2* opsin expression can be differentially regulated post-embryonically, indicating that RH2 cones also remain plastic to the effects of TH. Further, the effects of TH appear to be dependent upon life history stage. For example, *rh2-2* was increased by T3 in larvae (Fig. 2.7B, D), but was unchanged by T4 in juveniles (Fig. 2.8B). We analyzed the *rh2* locus for putative TREs and RARE/RXREs (SI Appendix, SI Methods). Several of these elements were identified in the upstream regulatory regions of all four *rh2* genes (SI Appendix, Fig. S2.3B).

Additional color vision-associated transcripts are plastic to the effects of thyroid hormone.

We next examined expression of the two remaining cone opsin transcripts in response to GOF and LOF of TH signaling, using the experimental design shown in Fig. 2. 6A. In juveniles treated with T4 (GOF), *sws1* (*UV opsin*) transcript abundance was reduced by 2-fold, compared to controls (SI Appendix, Fig. S2.5A), and *sws2* (*blue opsin*) was reduced by 2.6-fold (SI Appendix, Fig. S2.5B), suggesting that exogenous TH can regulate all cone opsin genes in the zebrafish, regardless of whether they are tandemly-replicated. However, in athyroid juveniles (LOF), *sws1* and *sws2* levels were not different compared to controls (SI Appendix, Fig. S2.5A,B), findings which are not consistent with endogenous functions for TH signaling in regulation of these genes in juvenile zebrafish.

Exogenous TH promotes the expression of the *cyp27c1* gene in adult zebrafish, within the retinal pigmented epithelium³³. *cyp27c1* encodes an enzyme that catalyzes the conversion of the A1 type chromophore (11-*cis* retinal) to an A2 type chromophore (11-*cis* didehydroretinal)³³. This change in chromophore causes a red shift in spectral sensitivity of the associated visual pigment³⁴. We confirmed that TH also upregulates *cyp27c1* in juvenile zebrafish. In two of four biological replicates analyzed, *cyp27c1* transcript was not detected in controls, but was in the other two (SI Appendix, Table S2). In all replicates treated with T4, *cyp27c1* was detected, and at lower cycle thresholds (CTs) than the corresponding controls (where this comparison was possible; SI Appendix, Table S2), indicating that T4 increased *cyp27c1* transcript levels in the eyes of juvenile zebrafish. Recently it was reported that the transcription factor Six7 is required for rh2 opsin expression in zebrafish^{35,36}, and we reasoned that Six7 may be involved in the regulation of rh2 genes in response to TH signaling. In juveniles treated with T4 (GOF), levels of *six7* transcript were slightly reduced, by 1.73-fold compared to controls (SI Appendix, Fig. S2.5C). Regulation of *six7* therefore could be downstream of TH signaling, suggesting an indirect mechanism for regulation of the rh2 array by TH. However, in athyroid juveniles (LOF), *six7* was unchanged, compared to controls (SI Appendix, Fig.

S2.5C), suggesting that endogenous TH signaling is not necessary to promote expression of six7, and supporting independent roles for this transcription factor and TH in the regulation of the rh2 opsin genes.

Discussion

Regulation of differential expression of tandemly-replicated opsin genes has been of high interest for decades^{3,4,7}, as these replications provided the raw genetic material for the evolution of trichromatic color vision in primates, and diversification of visually-mediated behaviors in primates^{37,38} and fish^{6,7}. However, in order for replicated opsin genes to contribute to multichromatic color vision, the replicates must be both spectrally divergent and expressed in distinct cone populations⁶. Our previous study revealed that a trans-acting paracrine signal, RA, regulates differential expression of the tandemly-duplicated *lws* array in zebrafish¹⁰. In the present study we demonstrate that *i*) the endocrine signal, TH is a relatively more potent regulator of the *lws* array, *ii*) TH can also regulate expression from the tandemly-quadruplicated *rh2* array, and *iii*) TH is an endogenous regulator of both arrays, likely causing individual cones to switch opsins and change their peak spectral sensitivities as the zebrafish grows. We also reveal striking plasticity of LWS and RH2 cones to differentially express members of the tandem arrays in response to TH manipulations during juvenile growth.

TH has been demonstrated to regulate photoreceptor differentiation, cone survival, and expression of specific opsin genes, in retinal cell cultures and *in vivo*. For example, addition of T3 to cultured embryonic rat retinal cells¹⁶, or to fetal human retinal cells¹⁷, promotes progenitor cell survival and differentiation into cones. In addition, an extensive body of work from many investigators has illuminated roles for TH in mammalian systems in promoting expression of the middle or long wavelength-sensitive cone opsin (MWS/LWS) at the expense of the SWS opsin. Mice treated with T3 show reduced SWS opsin and increased MWS opsin, disrupting the endogenous

dorsal-ventral gradient of MWS to SWS¹⁵. Correspondingly, pharmacological suppression of serum TH in adult mice and rats results in increased SWS opsin and reduced MWS opsin, and the normal pattern of opsin expression and distribution can be restored in athyroid mice by TH treatment³⁹. Recently Eldred and colleagues reported that retinal organoids differentiated from human induced pluripotent stem cells also respond to T3, by increasing expression of MWS/LWS opsin while reducing expression of SWS opsin, and this mirrors an endogenous temporal regulatory pattern of human opsin expression^{23,40}. In teleost fish, the majority of studies have focused upon roles for TH in regulation of the Sws opsins, Sws1 (UV opsin) and Sws2 (blue opsin). In salmonids, TH signaling accelerates opsin expression during photoreceptor differentiation and induces a switch from *sws1* to *sws2* expression in differentiated cones¹⁸. Similarly, TH treatment of rainbow trout reduces expression of *sws1*⁴¹. We add to this body of knowledge an additional and novel endogenous function for TH, in regulating differential expression of opsin genes residing upon tandemly-replicated arrays, and acting as a mechanism for the spatiotemporal control of their expression. We speculate that TH was evolutionarily co-opted for this function as tandemly-replicated opsin genes became subfunctionalized, diverging in peak spectral sensitivities of the encoded opsin proteins. Although spatiotemporal gradients of TH signaling have not been demonstrated in zebrafish, several other vertebrates show pronounced dorsal-ventral gradients of T3 or its deiodinase regulatory enzymes (mouse¹⁵; *Xenopus*⁴²; chick¹³). Specifically in the chick, TH signaling components, including the TH receptors TR α and TR β , as well as the deiodinases Dio2 and Dio3, are expressed in the developing retina in three sequential, spatially stereotyped waves that coincide with neurogenesis, cell differentiation, and loss of progenitors¹³.

We observed that in athyroid juveniles, *lws1* expression was still detected in ventral retina (Fig. 2.6F), a region that coincides with an RA signaling domain in age matched *RARE:YFP* transgenic fish (Fig. 2.6H). The expansion of the *lws1* expression domain is therefore dependent upon TH signaling, but RA signaling is likely sufficient for inducing and maintaining the ventral expression domain. Putative TREs/RAREs/RXREs are predicted in the regulatory regions upstream

of the *lws* genes (Fig. S2.4A), consistent with this interpretation. Predicted TREs and RAREs are located within the essential regulatory region LAR (Fig. S2.4A), which functions as an enhancer of either *lws* gene but does not contain elements necessary for determining spatiotemporally accurate expression⁸. The LAR is hypothesized to interact with sequences that are predicted to reside in other regions of the *lws* locus in order to determine cell specific expression⁸. The putative TREs/RAREs/RXREs residing in these regions outside of the LAR may facilitate this interaction. In contrast, the LCR of the *rh2* locus does contain the necessary elements to determine cell specific and spatially accurate expression of the *rh2* genes in adult zebrafish¹¹. It has been demonstrated that expression from the *rh2* opsin gene array in adult zebrafish is dependent on relative distance of the gene to the *rh2* LCR for the first three members, while *rh2-4* is insensitive to the distance effect¹². In addition, the proximal upstream regions of *rh2-1*, *rh2-2*, and *rh2-4*, but not *rh2-3* are sufficient for specifying their respective expression domains in the retina¹². The putative TREs/RAREs/RXREs predicted in the upstream regulatory regions of all four members of the *rh2* array (Fig. S2.4B) may participate in these regulatory interactions. It is interesting that the role of TH signaling appears distinctive in larvae vs. juvenile zebrafish. These life history-dependent differences may indicate that the *rh2* array, or some of its member genes, may be dependent upon factors other than TH. During the first month of zebrafish growth the *rh2* expression patterns, particularly that of *rh2-2*, undergo extensive and dynamic changes in their respective spatial domains⁹. Analysis of the spatial changes in expression in response to changes in TH signaling, as well as dissection of the regulatory regions of the *rh2* and *lws* loci, together with TH manipulations, will help to reveal the elements necessary and sufficient for the response to TH.

The present work, and many previous, seminal studies, contribute to the current model for vertebrate cone determination, in which a series of transcription factors expressed in photoreceptor progenitors and precursors, including TR β 2, determines cone phenotype and importantly the type of opsin expressed⁴³. However, in case of the choice of opsin from a tandemly-replicated array, the most recent model in the field has considered this choice a stochastic process leading to permanent

expression of a specific opsin⁴. Evidence supporting this model is limited, in part due to reliance upon model organisms, such as the mouse, that do not have tandemly-replicated opsins in their genomes. The zebrafish, with two tandemly-replicated opsin arrays, has provided the means to test alternative hypotheses for their regulation. Together with our prior demonstration that the paracrine signal, RA, acts as an endogenous regulator of differential expression from the zebrafish *lws* array¹⁰, the present study provides evidence that tandemly-replicated opsin arrays are regulated by the endocrine signal, TH, and that the choice of opsin from each array is not always a permanent choice, but remains plastic to TH signaling during organism development and growth.

The responses of the zebrafish *lws* and *rh2* arrays to TH gain- and loss-of-function are complex. In larvae treated with a relatively low dose of T3, the *lws1* transcript was increased in abundance but *lws2* was not changed. The *rh2-1* transcript was unchanged, but abundance of *rh2-2* transcript was increased. With higher concentrations of T3, *lws1* and *rh2-2* expression continues to be increased while *lws2* and *rh2-1* expression is decreased. This suggests that the expression from each array becomes biased towards the longer wavelength-sensitive opsins of the array by TH. TH in larvae promotes *lws1* over *lws2* [*Lws1* λ_{\max} = 558nm, *Lws2* λ_{\max} = 548nm⁷], and *rh2-2* and *rh2-3* over *rh2-1* [*Rh2-3* λ_{\max} = 488nm, *Rh2-4* λ_{\max} = 505nm, *Rh2-1* λ_{\max} = 467nm, *Rh2-2* λ_{\max} = 476nm⁷]. Loss-of-function in juveniles correspondingly suppresses *lws1*, *rh2-2*, *rh2-3*, and *rh2-4*. Together with the generally suppressive effects of TH on the *sws* opsin genes in zebrafish (present study), as well as in salmonids^{18,41}, and mammals^{15,39}, a conserved role for TH appears to be to promote visual changes that favor sensitivity to longer wavelengths of the electromagnetic spectrum. This shift in sensitivity may be further enhanced by a TH-mediated conversion of the A1 chromophore to A2^{31,44} by the enzyme *Cyp27c1*, which is promoted by TH³³ (and present study). The chromatic organization of the larval zebrafish retina matches the chromatic features of the natural environment and the behavioral requirements for feeding and avoiding predation⁴⁵. As zebrafish grow through the juvenile stage, feeding strategies change⁴⁶ in a TH-dependent manner⁴⁷, body pigmentation patterns of conspecifics change in a TH-dependent manner²⁹, shoaling behavior begins⁴⁸, mobility and use of the expanse of

the water column increases⁴⁸, and new predators emerge⁴⁸. It is likely that the TH-mediated shifts in color vision over an animal's lifespan are important in adapting to such changing visual demands in coordination with other anatomical and physiological changes.

Literature Cited

- 1 Yokoyama, S. Molecular evolution of vertebrate visual pigments. *Progress in Retinal and Eye Research* **19**, 385-419, doi:[https://doi.org/10.1016/S1350-9462\(00\)00002-1](https://doi.org/10.1016/S1350-9462(00)00002-1) (2000).
- 2 Nathans, J., Thomas, D. & Hogness, D. S. Molecular genetics of human color vision: the genes encoding blue, green, and red pigments. *Science* **232**, 193-202 (1986).
- 3 Vollrath, D., Nathans, J. & Davis, R. Tandem array of human visual pigment genes at Xq28. *Science* **240**, 1669-1672, doi:10.1126/science.2837827 (1988).
- 4 Wang, Y. *et al.* Mutually exclusive expression of human red and green visual pigment-reporter transgenes occurs at high frequency in murine cone photoreceptors. *Proceedings of the National Academy of Sciences of the United States of America* **96**, 5251-5256 (1999).
- 5 Kuchenbecker, J. A., Sahay, M., Tait, D. M., Neitz, M. & Neitz, J. Topography of the long- to middle-wavelength sensitive cone ratio in the human retina assessed with a wide-field color multifocal electroretinogram. *Vis Neurosci* **25**, 301-306, doi:10.1017/S0952523808080474 (2008).
- 6 Hofmann, C. M. & Carleton, K. L. Gene duplication and differential gene expression play an important role in the diversification of visual pigments in fish. *Integr Comp Biol* **49**, 630-643, doi:10.1093/icb/icp079 (2009).
- 7 Chinen, A., Hamaoka, T., Yamada, Y. & Kawamura, S. Gene duplication and spectral diversification of cone visual pigments of zebrafish. *Genetics* **163**, 663-675 (2003).
- 8 Tsujimura, T., Hosoya, T. & Kawamura, S. A single enhancer regulating the differential expression of duplicated red-sensitive opsin genes in zebrafish. *PLoS Genet* **6**, e1001245, doi:10.1371/journal.pgen.1001245 (2010).
- 9 Takechi, M. & Kawamura, S. Temporal and spatial changes in the expression pattern of multiple red and green subtype opsin genes during zebrafish development. *J Exp Biol* **208**, 1337-1345, doi:10.1242/jeb.01532 (2005).
- 10 Mitchell, D. M. *et al.* Retinoic Acid Signaling Regulates Differential Expression of the Tandemly-Duplicated Long Wavelength-Sensitive Cone Opsin Genes in Zebrafish. *PLoS Genet* **11**, e1005483, doi:10.1371/journal.pgen.1005483 (2015).
- 11 Tsujimura, T., Chinen, A. & Kawamura, S. Identification of a locus control region for quadruplicated green-sensitive opsin genes in zebrafish. *Proceedings of the National*

- Academy of Sciences of the United States of America* **104**, 12813-12818, doi:10.1073/pnas.0704061104 (2007).
- 12 Tsujimura, T., Masuda, R., Ashino, R. & Kawamura, S. Spatially differentiated expression of quadruplicated green-sensitive RH2 opsin genes in zebrafish is determined by proximal regulatory regions and gene order to the locus control region. *BMC Genet* **16**, 130, doi:10.1186/s12863-015-0288-7 (2015).
 - 13 Trimarchi, J. M., Harpavat, S., Billings, N. A. & Cepko, C. L. Thyroid hormone components are expressed in three sequential waves during development of the chick retina. *BMC Dev Biol* **8**, 101, doi:10.1186/1471-213X-8-101 (2008).
 - 14 Houbrechts, A. M. *et al.* Deiodinase knockdown affects zebrafish eye development at the level of gene expression, morphology and function. *Mol Cell Endocrinol* **424**, 81-93, doi:10.1016/j.mce.2016.01.018 (2016).
 - 15 Roberts, M. R., Srinivas, M., Forrest, D., Morreale de Escobar, G. & Reh, T. A. Making the gradient: Thyroid hormone regulates cone opsin expression in the developing mouse retina. *Proceedings of the National Academy of Sciences of the United States of America* **103**, 6218-6223, doi:10.1073/pnas.0509981103 (2006).
 - 16 Kelley, M. W., Turner, J. K. & Reh, T. A. Ligands of steroid/thyroid receptors induce cone photoreceptors in vertebrate retina. *Development* **121**, 3777-3785 (1995).
 - 17 Kelley, M. W., Turner, J. K. & Reh, T. A. Regulation of proliferation and photoreceptor differentiation in fetal human retinal cell cultures. *Invest Ophthalmol Vis Sci* **36**, 1280-1289 (1995).
 - 18 Gan, K. J. & Novales Flamarique, I. Thyroid hormone accelerates opsin expression during early photoreceptor differentiation and induces opsin switching in differentiated TRalpha-expressing cones of the salmonid retina. *Dev Dyn* **239**, 2700-2713, doi:10.1002/dvdy.22392 (2010).
 - 19 Bianco, A. C. & Larsen, P. R. Cellular and Structural Biology of the Deiodinases. *Thyroid* **15**, 777-786, doi:10.1089/thy.2005.15.777 (2005).
 - 20 Roberts, M. R., Hendrickson, A., McGuire, C. R. & Reh, T. A. Retinoid X receptor (gamma) is necessary to establish the S-opsin gradient in cone photoreceptors of the developing mouse retina. *Invest Ophthalmol Vis Sci* **46**, 2897-2904, doi:10.1167/iovs.05-0093 (2005).
 - 21 Ng, L. *et al.* A thyroid hormone receptor that is required for the development of green cone photoreceptors. *Nature genetics* **27**, 94-98, doi:10.1038/83829 (2001).
 - 22 Fei, Y. & Hughes, T. E. Transgenic expression of the jellyfish green fluorescent protein in the cone photoreceptors of the mouse. *Visual Neuroscience* **18**, 615-623, doi:undefined (2001).
 - 23 Eldred, K. C. *et al.* Thyroid hormone signaling specifies cone subtypes in human retinal organoids. *Science* **362**, doi:10.1126/science.aau6348 (2018).

- 24 Cook, J. E. Spatial properties of retinal mosaics: an empirical evaluation of some existing measures. *Vis Neurosci* **13**, 15-30 (1996).
- 25 Rodieck, R. W. The density recovery profile: A method for the analysis of points in the plane applicable to retinal studies. *Visual Neuroscience* **6**, 95-111, doi:10.1017/S095252380001049X (1991).
- 26 Suzuki, S. C. *et al.* Cone photoreceptor types in zebrafish are generated by symmetric terminal divisions of dedicated precursors. *Proc Natl Acad Sci U S A* **110**, 15109-15114, doi:10.1073/pnas.1303551110 (2013).
- 27 Tiefenbach, J. *et al.* A live zebrafish-based screening system for human nuclear receptor ligand and cofactor discovery. *PLoS one* **5**, e9797, doi:10.1371/journal.pone.0009797 (2010).
- 28 Tiefenbach, J. *et al.* Idebenone and coenzyme Q(10) are novel PPAR α / γ ligands, with potential for treatment of fatty liver diseases. *Disease models & mechanisms* **11**, doi:10.1242/dmm.034801 (2018).
- 29 McMenamin, S. K. *et al.* Thyroid hormone-dependent adult pigment cell lineage and pattern in zebrafish. *Science* **345**, 1358-1361, doi:10.1126/science.1256251 (2014).
- 30 Chang, J. *et al.* Changes in thyroid hormone levels during zebrafish development. *Zoolog Sci* **29**, 181-184, doi:10.2108/zsj.29.181 (2012).
- 31 Suliman, T. & Novales Flamarique, I. Visual pigments and opsin expression in the juveniles of three species of fish (rainbow trout, zebrafish, and killifish) following prolonged exposure to thyroid hormone or retinoic acid. *J Comp Neurol* **522**, 98-117, doi:10.1002/cne.23391 (2014).
- 32 Perz-Edwards, A., Hardison, N. L. & Linney, E. Retinoic acid-mediated gene expression in transgenic reporter zebrafish. *Dev Biol* **229**, 89-101, doi:10.1006/dbio.2000.9979 (2001).
- 33 Enright, J. M. *et al.* Cyp27c1 red-shifts the spectral sensitivity of photoreceptors by converting vitamin A(1) into A(2). *Current biology : CB* **25**, 3048-3057, doi:10.1016/j.cub.2015.10.018 (2015).
- 34 Wald, G. THE PORPHYROPSIN VISUAL SYSTEM. *The Journal of general physiology* **22**, 775-794 (1939).
- 35 Ogawa, Y., Shiraki, T., Kojima, D. & Fukada, Y. Homeobox transcription factor Six7 governs expression of green opsin genes in zebrafish. *Proc Biol Sci* **282**, 20150659, doi:10.1098/rspb.2015.0659 (2015).
- 36 Sotolongo-Lopez, M., Alvarez-Delfin, K., Saade, C. J., Vera, D. L. & Fadool, J. M. Genetic Dissection of Dual Roles for the Transcription Factor six7 in Photoreceptor Development and Patterning in Zebrafish. *PLoS genetics* **12**, e1005968, doi:10.1371/journal.pgen.1005968 (2016).

- 37 Lucas, P. W., Darvell, B. W., Lee, P. K. D., Yuen, T. D. B. & Choong, M. F. Colour Cues for Leaf Food Selection by Long-Tailed Macaques (*Macaca fascicularis*) with a New Suggestion for the Evolution of Trichromatic Colour Vision. *Folia Primatologica* **69**, 139-154, doi:10.1159/000021576 (1998).
- 38 Matsumoto, Y. *et al.* Evolutionary renovation of L/M opsin polymorphism confers a fruit discrimination advantage to ateline New World monkeys. *Mol Ecol* **23**, 1799-1812, doi:10.1111/mec.12703 (2014).
- 39 Glaschke, A. *et al.* Thyroid hormone controls cone opsin expression in the retina of adult rodents. *J Neurosci* **31**, 4844-4851, doi:10.1523/JNEUROSCI.6181-10.2011 (2011).
- 40 O'Brien, K. M., Schulte, D. & Hendrickson, A. E. Expression of photoreceptor-associated molecules during human fetal eye development. *Molecular vision* **9**, 401-409 (2003).
- 41 Raine, J. C. & Hawryshyn, C. W. Changes in thyroid hormone reception precede SWS1 opsin downregulation in trout retina. *Journal of Experimental Biology* **212**, 2781-2788, doi:10.1242/jeb.030866 (2009).
- 42 Marsh-Armstrong, N., Huang, H., Remo, B. F., Liu, T. T. & Brown, D. D. Asymmetric growth and development of the *Xenopus laevis* retina during metamorphosis is controlled by type III deiodinase. *Neuron* **24**, 871-878 (1999).
- 43 Forrest, D. & Swaroop, A. Minireview: The Role of Nuclear Receptors in Photoreceptor Differentiation and Disease. *Molecular Endocrinology* **26**, 905-915, doi:10.1210/me.2012-1010 (2012).
- 44 Allison, W. T., Haimberger, T. J., Hawryshyn, C. W. & Temple, S. E. Visual pigment composition in zebrafish: Evidence for a rhodopsin–porphyropsin interchange system. *Visual Neuroscience* **21**, 945-952, doi:10.1017/S0952523804216145 (2004).
- 45 Zimmermann, M. J. Y. *et al.* Zebrafish Differentially Process Color across Visual Space to Match Natural Scenes. *Curr Biol* **28**, 2018-2032 e2015, doi:10.1016/j.cub.2018.04.075 (2018).
- 46 Westphal, R. E. & O'Malley, D. M. Fusion of locomotor maneuvers, and improving sensory capabilities, give rise to the flexible homing strikes of juvenile zebrafish. *Front Neural Circuits* **7**, 108, doi:10.3389/fncir.2013.00108 (2013).
- 47 McMenamin, S., Carter, C. & Cooper, W. J. Thyroid Hormone Stimulates the Onset of Adult Feeding Kinematics in Zebrafish. *Zebrafish* **14**, 517-525, doi:10.1089/zeb.2017.1453 (2017).
- 48 Engeszer, R. E., Patterson, L. B., Rao, A. A. & Parichy, D. M. Zebrafish in the wild: a review of natural history and new notes from the field. *Zebrafish* **4**, 21-40, doi:10.1089/zeb.2006.9997 (2007).
- 49 Westerfield, M. *The Zebrafish Book. A Guide for The Laboratory Use of Zebrafish (Danio rerio)*. Vol. 385 (2000).

- 50 Stevens, C. B., Cameron, D. A. & Stenkamp, D. L. Plasticity of photoreceptor-generating retinal progenitors revealed by prolonged retinoic acid exposure. *BMC Dev Biol* **11**, 51, doi:10.1186/1471-213X-11-51 (2011).
- 51 Stenkamp, D. L., Frey, R. A., Mallory, D. E. & Shupe, E. E. Embryonic retinal gene expression in sonic-you mutant zebrafish. *Dev Dyn* **225**, 344-350, doi:10.1002/dvdy.10165 (2002).

Figures

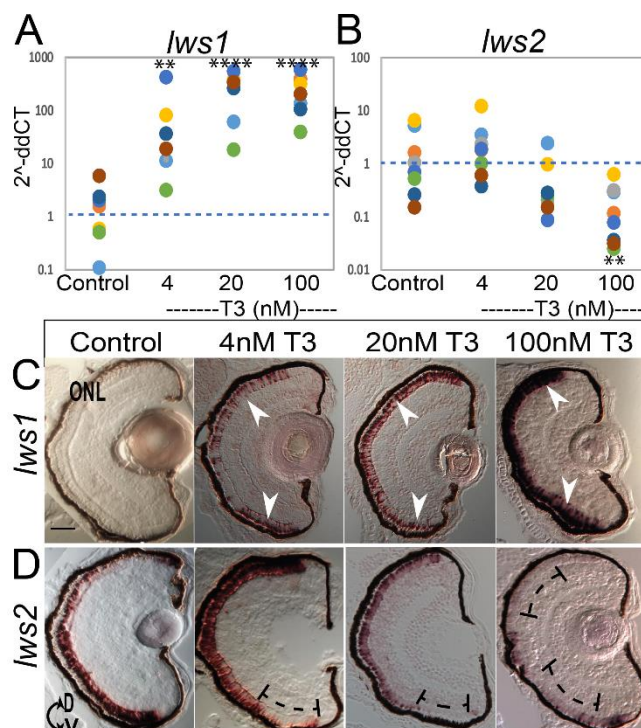


Figure 2.1. Quantitative PCR and in situ hybridization for *lws* transcript abundance reveals robust differential regulation after thyroid hormone (T3) treatment from 2-4dpf. (A,B). Scatter plots indicate fold change ($2^{-\Delta\Delta CT}$) abundance of the indicated transcripts. Colors of dots correspond to separate experiments. Each dot represents one biological sample (pooled RNA from ~ five larvae). For each condition $n = 8$ (A). *lws1* abundance in DMSO control, increased by 4nM T3 $p=0.001502$, increased by 20nM T3 $p=0.000003$, increased by 100nM T3 $p=0.000002$. (B). *lws2* abundance in control, was unchanged by both 4nM T3 and 20nM T3 $p=0.288195$ and $p=0.073120$ but decreased by 100nM T3 $p=0.004823$. p -values were calculated by comparing the $\Delta\Delta CT$ values for treated vs control from each experiment using the Kruskal- Wallis Test and the Conover post- hoc test further adjusted by the Benjamini-Hochberg False Discovery Rate method. Statistical notation: ** $p<0.01$, **** $p<0.0001$. (C, D). In situ hybridization of cryosectioned eyes using gene specific probes for *lws1* (C) and *lws2* (D) from larvae treated 2-4dpf with DMSO (control) or T3. Arrows in C indicate induced and expanded expression domain of *lws1* due to T3 treatment; brackets in D indicate regions showing reduced expression of *lws2* due to T3 treatment. D, dorsal; V, ventral; ONL, outer nuclear layer; dpf, days postfertilization. Scale bar (in C, applies to C,D) = 50 μm .

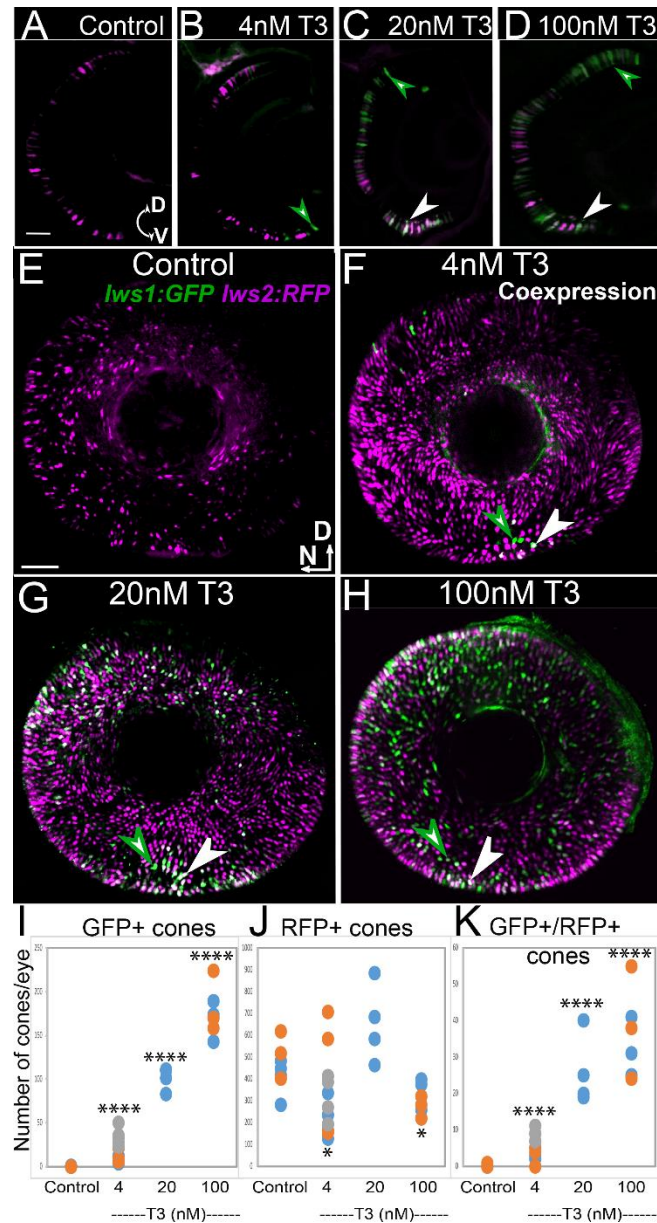


Figure 2. 2. *Lws* reporter transgenic indicates a switch from *lws2* to *lws1* in response to thyroid hormone (T3). (A-D). Cryosections from 4dpf *lws:PAC(H)* eyes treated with DMSO (control; A), 4nM T3 (B), 20nM T3 (C), 100nM T3 (D). (E-H). Whole mounted *lws:PAC(H)* eyes visualized by confocal microscopy of DMSO (control) (E), 4nM T3 (F), 20nM T3 (G), 100nM T3 (H). Green arrowheads indicate GFP+ cones, white arrowheads indicate colabeled cones. RFP is pseudocolored magenta. D, dorsal; V, ventral; N, nasal; dpf, days postfertilization. Scale bars (in A, applies to A-D; in E, applies to E-H) = 50 μ m. (I-K). GFP+ cone numbers, 4nM T3 p=1.28e-07, 20nM T3 p=2.47e-10, 100nM T3 p=4.46e-14 (I). RFP+ cones 4nM T3 p=0.022, 20nM T3 p=0.25, 100nM T3 p=0.03(J) and (K) GFP+/RFP+ cone numbers, 4nM T3 p=2.3e-05, 20nM T3 p=9.8e-09, 100nM T3 p=4.0e-11

from three Z projected images from whole mounts of each condition show a dose-dependent increase in GFP-expressing (*lws1*⁺) cones. Colors of dots correspond to separate experiments. Each dot represents a biological replicate (an individual larva). p-values were calculated by comparing the number of GFP⁺ or GFP⁺RFP⁺ cones for treated vs control from each experiment using the Kruskal-Wallis Test and the Conover post-hoc test further adjusted by the Benjamini-Hochberg False Discovery Rate method. Statistical notation: * p<0.05, **** p<0.0001.

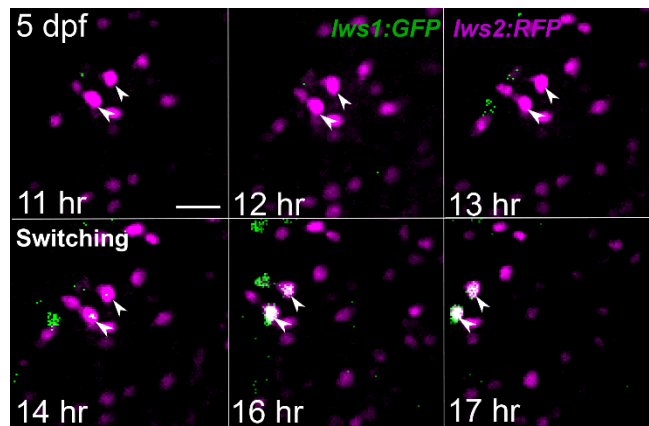


Figure 2.3. Live imaging of 5dpf *lws:PAC(H)* *lws* reporter transgenic confirms a switch from *lws2* to *lws1* in individual cones in response to thyroid hormone (T3). Imaging was conducted for 9 hours starting 8 hours after treatment with 100nM T3 began. Time stamps indicate hours from start of imaging. Arrowheads show two RFP⁺ (*lws2*⁺) cones switching to express GFP (*lws1*) over the time of imaging. Cells move to the left of the region of interest due to growth of the larva. Scale bar = 10 μ m.

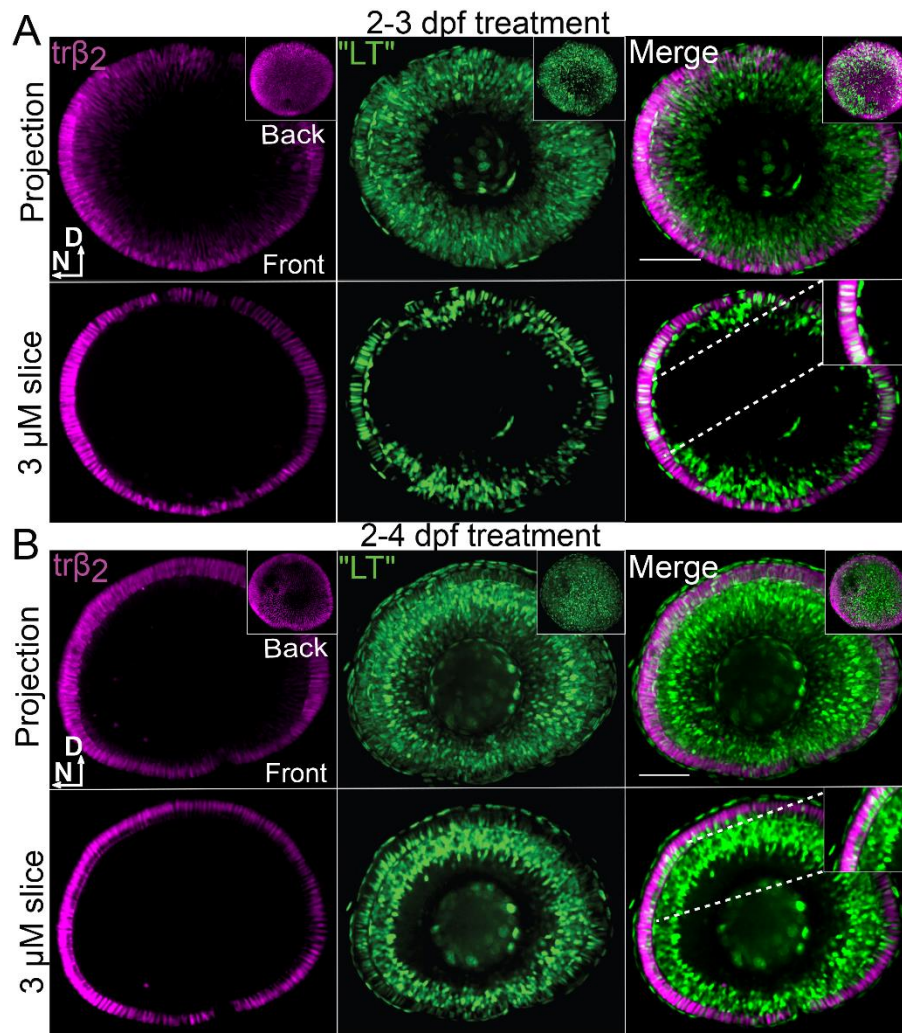


Figure 2.4. Thyroid hormone “Ligand Trap” reporter transgenic and *thyroid receptor β2* reporter transgenic indicate accumulation of thyroid hormone (T3) in *lws+* (TRβ2+) cones after T3 treatment. All panels include visualization of T3 accumulation (ligand trap, GFP+), *trβ2+* cones (tdTomato+), and merge (colabeled cells are white) of whole mounted eyes visualized by confocal microscopy, from larvae treated with 100nM T3 from 2-3dpf (**A**) or 2-4dpf (**B**). D, dorsal; N, nasal; dpf, days postfertilization. Insets in top rows of A and B show views of the back of the eye; insets in bottom rows of A and B show higher magnification of a single 3μm Z slice to visualize coexpressing cones. Scale bar = 50 μm for both A and B.

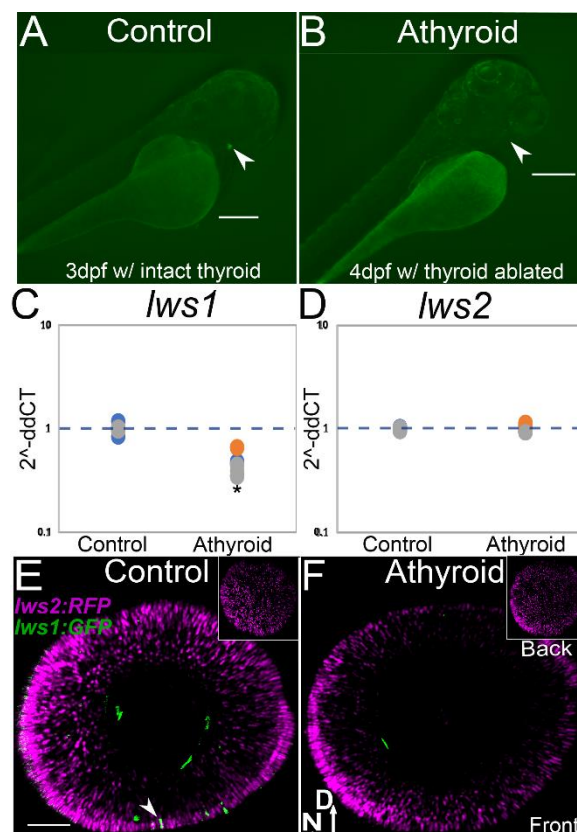


Figure 2.5. Thyroid hormone (TH) loss of function by thyroid ablation suppresses *lws1* expression at time of native onset of expression. (A,B). Transgenic (*Tg(tg:nVenus-2a-nfnB)^{wp.r18}*; that allows for thyroid ablation mediated by metronidazole treatment and nitroreductase expressing thyroglobulin cells) with intact thyroid, indicated by Venus (YFP) expression in embryo (A, arrowhead) and thyroid ablation, indicated by absence of Venus (YFP) (arrowhead shows normal location of thyroid gland) after 24 hour treatment with metronidazole (B). (C,D). Quantitative PCR abundance of *lws1* (C) and *lws2* (D) transcripts (fold change, $2^{-\Delta\Delta\text{CT}}$) in 6dpf DMSO (control) and athyroid larvae. In comparison to control (n=3) samples, *lws1* is reduced in athyroid larvae (n=3) $p=0.04$. (C), and *lws2* is not changed in athyroid larvae (n=3) $p=0.32$. (D). p-values were calculated by comparing the ddCT values for the thyroid ablated groups vs controls from each experiment using a Wilcoxon Mann-Whitney U test. Statistical notation: * $p<0.05$. (E,F). *lws:PAC(H) lws* reporter transgenic, whole mounted eyes visualized by confocal microscopy of 6dpf DMSO (control) (E) and athyroid larvae (F). Insets show views of the back of the eye; arrowhead in E indicates an *lws1* (GFP+) –expressing cone, D, dorsal; N, nasal; dpf, days postfertilization. Scale bar (in E, applies to E,F) = 50 μm .

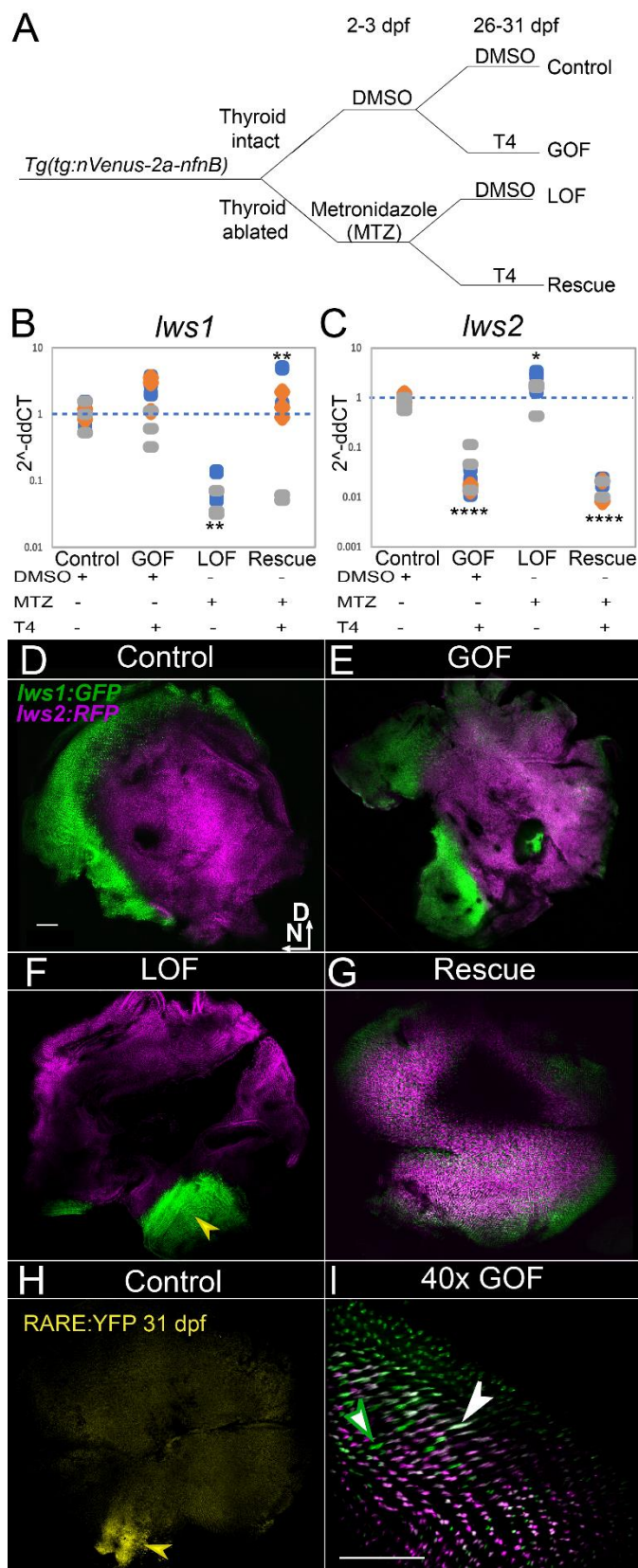


Figure 2.6. Plasticity of *lws* differential expression by thyroid hormone (T4) in normal and athyroid juveniles. (A). Schematic of experimental workflow including thyroid ablation at 2dpf followed by T4 treatment starting at 26dpf for 5 days, of half the athyroid group and half of the controls. GOF, gain-of-function; LOF, loss-of-function. (B, C). Quantitative PCR of *lws1* (A) and *lws2* (B) transcript abundance. Scatter plots indicate fold change abundance ($2^{\Delta\Delta\text{CT}}$) of the indicated transcripts. Colors of dots correspond to separate experiments. Each dot represents a biological replicate (two retinas from an individual fish). *lws1* abundance (B) in DMSO (control) (n=9), is unchanged by T4 GOF (n=9) $p=0.21$ compared to control, decreased in athyroid (LOF) (n=6) $p=0.006$ compared to control, and increased in Rescue (LOF + T4) (n=7) $p=0.006$ compared to LOF. *lws2* abundance (C) in control (n=9), is decreased by T4 GOF (n=9) $p=2.66\text{e-}06$ compared to control, increased in LOF (n=6) $p=4.38\text{e-}02$ compared to control, and decreased in Rescue (n=7) $p=3.61\text{e-}08$ compared to LOF. $\Delta\Delta\text{CT}$ values were calculated by subtracting the ΔCT value for each fish from the average ΔCT values from the control fish in each experiment. p-values were calculated by comparing the $\Delta\Delta\text{CT}$ values for each fish from each condition using the Kruskal- Wallis Test and the Conover post- hoc test further adjusted by the Benjamini-Hochberg False Discovery Rate method. Statistical notation: ** $p<0.01$, **** $p<0.0001$. (D-G). *lws:PAC(H)* whole mounted retinas visualized by confocal microscopy of 31 dpf DMSO (control) (D), T4 (GOF) (E), athyroid (LOF) (F), and Rescue (LOF + T4) (G) juveniles. D, dorsal; N, nasal. Arrowhead in F indicates restricted ventral expression domain of *lws1* in athyroid juvenile retina. (H). Whole mounted retina of an age-matched *RARE:eYFP* juvenile showing domain of retinoic acid signaling restricted to ventral retina (arrow), and matching the domain of GFP (*lws1*) expression in athyroid retinas (arrow in F) of juvenile fish. (I). High magnification view of *lws:PAC(H)* retina showing GFP/RFP colabeling (opsin switching) in T4 treated juveniles [not the same retina pictured in (E)]. Green arrowhead indicates a GFP+ cone. White arrowhead indicates a colabeled (GFP+/RFP+) cone. Scale bar in D (applies to D-H) = 100 μm . Scale bar in I = 50 μm .

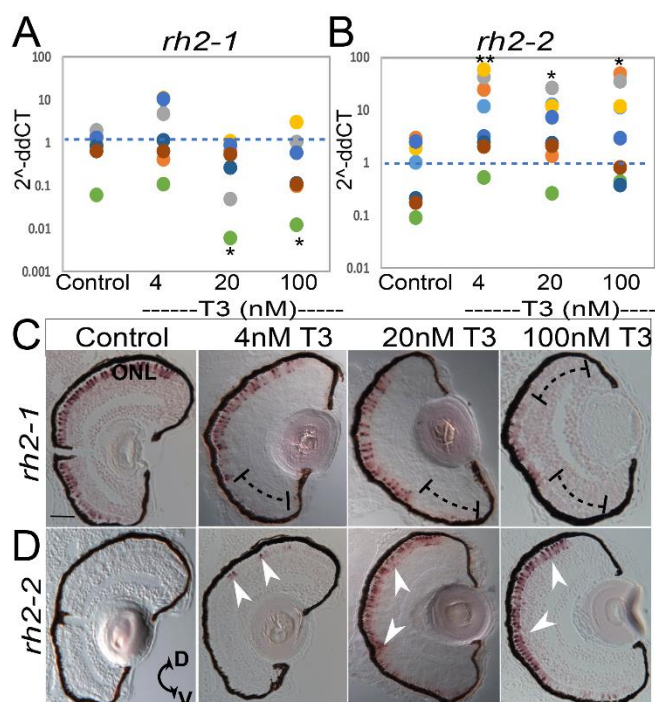


Figure 2.7. Quantitative PCR and in situ hybridization for *rh2-1* and *rh2-2* gene expression reveals differential regulation after thyroid hormone (T3) treatment from 2-4dpf. (A,B). Scatter plots indicate fold change abundance ($2^{-\Delta\Delta CT}$) of the indicated transcripts. Colors of dots correspond to separate experiments. Each dot represents one biological replicate (pooled RNA from ~ five larvae). *rh2-1* abundance (A) in DMSO control (n=7), is unchanged by 4nM T3 (n=7) p=0.53, decreased by 20nM T3 (n=7) p=0.0186, and decreased by 100nM T3 (n=7) p=0.0259. *rh2-2* abundance (B) in control (n=7), is increased by 4nM T3 (n=7) p=0.0043, increased by 20nM T3 (n=7) p=0.037 and increased by 100nM T3 (n=7) p=0.026. p-values were calculated by comparing the ddCT values for treated vs control from each experiment using the Kruskal- Wallis Test and the Conover post- hoc test further adjusted by the Benjamini-Hochberg False Discovery Rate method. Statistical notation: * p<0.05, ** p<0.01. (C,D). In situ hybridization of cryosectioned eyes using gene specific probes for *rh2-1* (C) and *rh2-2* (D) from larvae treated 2-4dpf with DMSO (control) or T3. Brackets in C indicate regions showing reduced expression domain of *rh2-1* due to T3 treatment; arrowheads in D indicate regions showing induced and expanded expression domain of *rh2-2* due to T3 treatment. D, dorsal; V, ventral; dpf, days postfertilization. Scale bar = 50 μ m.

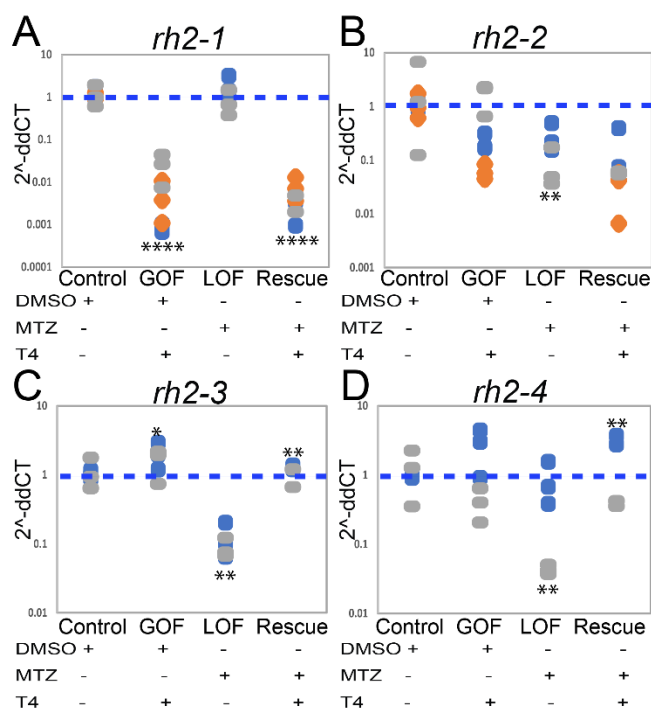


Figure 2.8. Plasticity of *rh2* differential expression by thyroid hormone (T4) in normal and athyroid juveniles. All panels show qPCR measuring *rh2* abundance. Scatter plots indicate fold change in abundance ($2^{-\text{ddCT}}$) of the indicated transcripts. Colors indicate separate experiments. Each marker represents an individual fish. **(A)**. *rh2-1* abundance in DMSO (control) (n=9), is reduced by T4 (GOF) (n=9) p=0.000002, not changed in metronidazole (athyroid; LOF) (n=6) p=0.88 and reduced in Rescue (LOF +T4) (n=7) in comparison to LOF p=0.000003. **(B)** *rh2-2* abundance in control (n=9), is unchanged by T4 GOF (n=9) p=0.052 compared to control, reduced in LOF (n=6) p=0.0098 compared to control, and unchanged in Rescue (n=7) p=0.28 compared to LOF. **(C)**. *rh2-3* in control (n=6), is increased by T4 GOF (n=6) p=0.022, decreased in LOF (n=6) p=0.0023 in comparison with control, and increased in Rescue (n=4) p=0.0015 compared to LOF. **(D)**. *rh2-4* in control (n=6), is not changed by T4 GOF (n=6) p=0.799 compared to control, decreased in LOF (n=4) p=0.0035 compared to control, and increased in Rescue (n=4) p=0.0055 compared to LOF. ddCT values were calculated by subtracting the dCT value for each fish from the average dCT values from the control fish in each experiment. p-values were calculated by comparing the ddCT values for each fish from each condition using the Kruskal- Wallis Test and the Conover post- hoc test further adjusted by the Benjamini-Hochberg False Discovery Rate method. Statistical notation: * p<0.05, ** p<0.01, **** p<0.0001.

Supplementary Figures

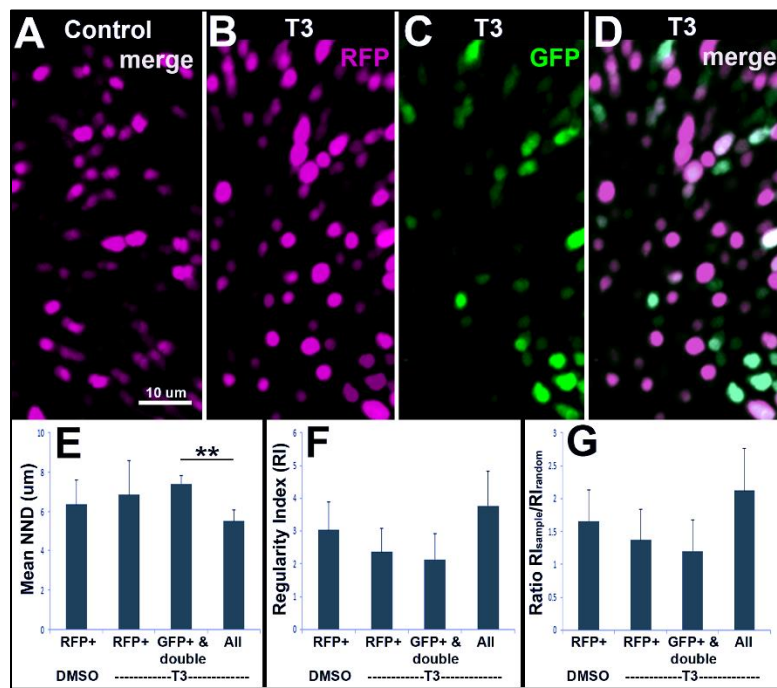


Figure S2.1. Local pattern analysis (two-dimensional nearest-neighbor distance; NND) of LWS cones in *lws:PAC(H)* embryos exposed to 100 nM thyroid hormone (T3): T3-induced GFP+ (*lwsI+*) cones do not disrupt the LWS cone mosaic. (A-D). Selected regions from confocal images at 40X magnification obtained from whole mounted *lws:PAC(H)* eyes of embryos treated with DMSO (A) or 100nM T3 (B-D), 2-4dpf, were used for pattern analysis. Retinal regions from DMSO treated embryos showed *lws2*:RFP+ cones only (magenta) (A), while retinal regions from T3 treated embryos contained RFP+ (B), *lwsI*:GFP+ (green) (C), and RFP+/GFP+ (white) cones (D). (E). Column graphs of mean NNDs of LWS cones show no significant differences between *lws2+* (RFP+) cones in DMSO or T3 treated embryos, but a significant difference between *lwsI+* (GFP+) cones and the entire population of LWS cones in T3 treated embryos (Kruskal-Wallis and Conover's post-hoc test; **p=0.0055), suggesting that the *lwsI+* (GFP+) cones constitute a fraction of a total population. (F). Column graphs of the regularity index (RI, mean NND/s.d.) reveal no significant differences among groups (Kruskal-Wallis), suggesting that the inclusion of GFP+ cones in T3-treated samples does not disrupt the regular cone mosaic. (G). The ratios of the RI_{sample} to RI_{random} are also not significantly different among groups (Kruskal-Wallis), consistent with GFP+ cones not disrupting the cone mosaic. Error bars represent standard deviation (n=5 for DMSO; n=6 for T3).

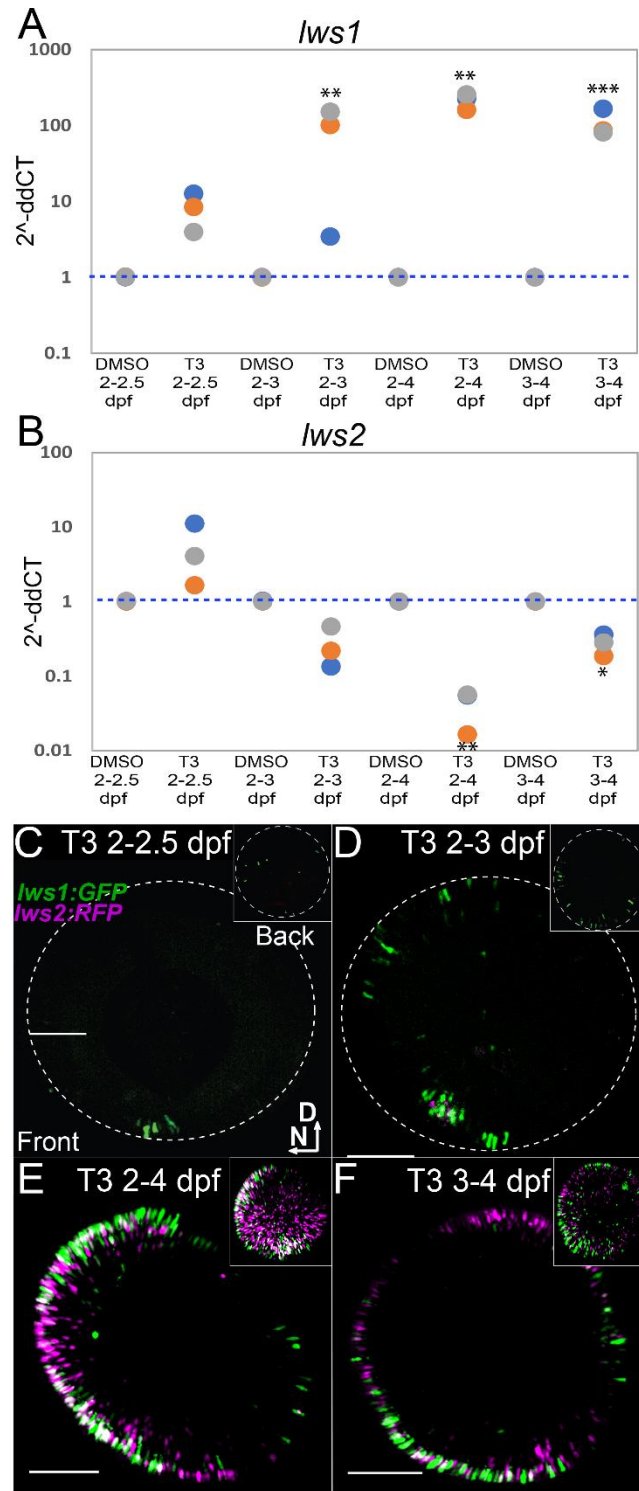


Figure S2.2. Thyroid hormone (T3) treatment time-course reveals kinetics of changes in *lws* regulation in larvae. (A,B). Scatter plots indicate fold change (2^{-ddCT}) abundance of the indicated transcripts. Colors of dots correspond to separate experiments. Each dot represents one biological replicate (pooled RNA from ~five larvae). Quantitative PCR of *lws1* (A) and *lws2* (B) abundance in

larvae treated with DMSO (control) or 100nM T3 at 12 hours treatment (ht) from 2- 2.5dpf, 24 ht from 2-3dpf and 3-4dpf, and 48 ht from 2-4dpf. In 2- 2.5dpf T3 treated (n=3), *lws1* and *lws2* are not changed. In 2-3dpf T3 treated, *lws1* is increased $p=0.0027$, and *lws2* is unchanged. In 3-4 dpf T3 treated, *lws1* is increased $p=0.0008$, and *lws2* is decreased $p=0.012$. In 2-4dpf T3 treated, *lws1* is increased $p=0.001$, and *lws2* is decreased $p=0.001$. p-values were calculated by comparing the ddCT values for treated vs control from each experiment using a Wilcoxon Mann-Whitney U test. **** = $p \leq 0.0001$. (C-E). Whole mounted eyes from *lws:PAC(H)* larvae visualized by confocal microscopy at 12 ht (C), at 24 ht from 2-3dpf (D), at 24 ht from 3-4dpf (E), and 48 ht from 2-4dpf (F). Dashed circles indicate the perimeter of the retina, D, dorsal; N, Nasal; dpf, days postfertilization. Scale bars = 50 μm .

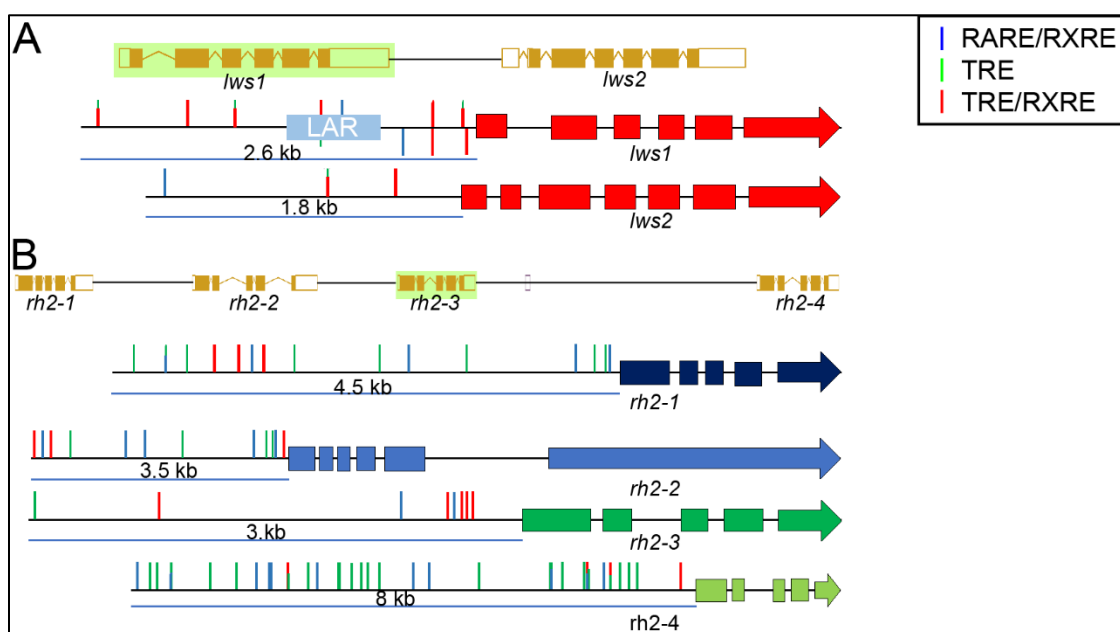


Figure S2.3. Response element analysis of the *lws* and *rh2* proximal upstream regulatory regions. (A) **Top:** Exon-intron structure of the protein coding and intergenic regions of the *lws* gene locus. **Bottom:** Positions of predicted TREs, RAREs, and RXREs upstream of each protein coding region. LAR, *lws* activating region. (B) **Top:** Exon-intron structure of the protein coding and intergenic regions of the *rh2* gene locus. **Bottom:** Positions of predicted TREs, RAREs, and RXREs upstream of each protein coding region. Blue bars = retinoic acid/retinoid X response element (RARE/RXRE), Green bars = thyroid hormone response element (TRE), red bars = TRE/RXRE. Analysis was performed using MatInspector and PROMO.

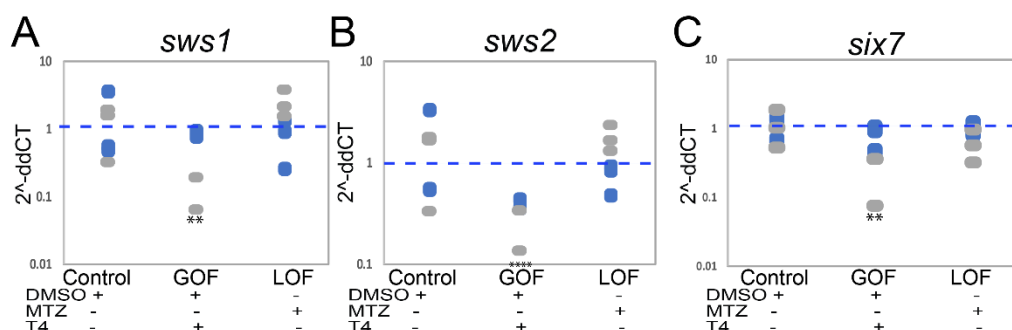


Figure S2.4. Plasticity of *sws1/sws2* opsins and *six7* transcript abundance by thyroid hormone (T4) in control, T4 treated, and athyroid juveniles. (A-C). Quantitative PCR of *sws1*, *sws2*, and *six7* transcript abundance. Scatter plots indicate fold change abundance of the indicated transcripts. Colors of dots correspond to separate experiments. Each dot represents a biological replicate (two retinas of an individual fish). *sws1* abundance (A) in DMSO (control) (n=9), is decreased by T4 (GOF) (n=4) $p=0.0065$ compared to control but is not statistically different in athyroid (LOF) (n=6) $p=0.71$ compared to control. *sws2* abundance (B) in DMSO (control) (n=9), is decreased by T4 (n=4) $p=7.0 \times 10^{-6}$, and not changed in athyroid (LOF) (n=6) $p=0.71$. *six7* abundance (C) in DMSO (control) (n=9), is decreased by T4 (n=6) $p=0.001428$ compared to control, but not statistically different in athyroid (LOF) (n=6) $p=0.077$ compared to control. p-values were calculated using the Kruskal-Wallis Test using the Conover post-hoc test further adjusted by the Benjamini-Hochberg False Discovery Rate method * = $p \leq 0.05$, ** = $p \leq 0.01$, *** = $p \leq 0.001$, **** = $p \leq 0.0001$.

Table S2.1. Quantitative PCR indicates T4 increases abundance of *cyp27c1* transcript in juvenile zebrafish.

Treatment	Experiment	Biological Replicate	CT ^a		dCT ^a
			<i>β-actin</i>	<i>cyp27c1</i>	vs. <i>β-actin</i>
Control (DMSO)	1	1	26.6	NTD ^b	NP ^c
		2	27.6	NTD	NP
	2	1	18.5	28.3	9.80
		2	19.9	28.6	8.72
GOF (DMSO + T4)	1	1	26.4	29.1	2.7
		2	27.7	30.5	2.7
	2	1	17.4	21.8	4.35
		2	17.2	22.7	5.55

^a Higher CT values correspond with the presence of less transcript.

^b NTD, No transcript detected = cycle threshold was “UND” (undetermined) by the instrument, and dCT calculations were not possible. Therefore, ddCT calculations and the presentation of 2^{-ddCT} values in a graph were also not appropriate for this dataset ⁵⁶.

^c NP, dCT calculations not possible.

Table S2.2. Primer pairs used for qPCR.

Gene	Primers
<i>opn1lw1 (lws1)</i>	Forward: CCC-ACA-CTG-CAT-CTC-GAC-AA
	Reverse: AAG-GTA-TTC-CCC-ATC-ACT-CCA-A
<i>opn1lw2 (lws2)</i>	Forward: AGA-GGG-AAG-AAC-TGG-ACT-TTC-AGA
	Reverse: TTC-AGA-GGA-GTT-TTG-CCT-ACA-TAT-GT
<i>opn1sws1 (sws1)</i>	Forward: ATG-GTCCTT-GGC-TGT-TCT-GG
	Reverse: CCT-CGG-GAA-TGT-ATC-TGC-TCC
<i>opn1sws2 (sws2)</i>	Forward: GGG-CAC-CAA-TTA-CAA-GCA-AG
	Reverse: AGG-TTA-CAT-GAG-AAC-TGT-GT
<i>opn1mw1 (rh2-1)</i>	Forward: CAG-CCC-AGC-ACA-AGA-AAC-TC
	Reverse: AGA-GCA-ACC-TGA-CCT-CCA-AGT
<i>opn1mw2 (rh2-2)</i>	Forward: TTT-TTG-GCT-GGT-CCC-GAT-ACA
	Reverse: CAG-GAA-CGC-AGA-AAT-GAC-AGC
<i>opn1mw3 (rh2-3)</i>	Forward: TGC-TTT-CGC-TGG-GAT-TGG-ATT
	Reverse: CCC-TCT-GGA-ATA-TAC-CTT-GAC-CA
<i>opn1mw4 (rh2-4)</i>	Forward: CAC-GCT-TTC-GCA-GGA-TGC
	Reverse: CGG-AAT-ATA-CCT-GGG-CCA-AC
<i>six7</i>	Forward: TTG-CTT-ATC-TTT-CCT-TTA-AT
	Reverse: ACA-TCT-AGC-CTC-TGT-TTC-CAA-C
<i>cyp27c1</i>	Forward: CAT-GAT-GAT-CTG-ATC-GTT-GGA
	Reverse: CGG-GGG-AAG-TTC-TCC-TCAT
<i>18s</i>	Forward: GAA-CGC-CAC-TTGTCCTCTA
	Reverse: GTT-GGT-GGA-GCG-ATT-TGT-CT
<i>β-actin</i>	Forward: GTA-CCA-CCA-GAC-AAT-ACA-GT
	Reverse: CTT-CTT-GGG-TAT-GGA-ATC-TTG-C

Chapter 3: Cis-Regulatory Sequences Required for Differential Regulation of Long Wavelength Sensitive Visual Opsins by Thyroid Hormone

Abstract

Aquatic environments are composed of a complex assortment of visual stimuli. Gene duplication and subsequent neofunctionalization/subfunctionalization has resulted in genomes with tandemly replicated gene arrays composed of members that contribute to the expansion of the types of functions the original gene conferred. In zebrafish, two different gene arrays (*lws1/lws2* and *rh2*) that encode for specialized light sensitive proteins called visual opsins have been tandemly duplicated and quadruplicated, respectively. This allows for the detection and differentiation of different wavelengths of light by the cone photoreceptor subtypes of the retina that are categorized by which opsin subtype that they express. Recently we demonstrated that thyroid hormone (TH) is an endogenous regulator of the differential expression of both arrays. Here we utilize transient transgenesis of reporter constructs for *lws1* and *lws2* to identify the regions of the *lws* locus that are required for the differential regulation of *lws1* vs *lws2* in response to TH.

Introduction

Throughout evolution gene duplication has provided the raw material upon which selection acts to result in the acquirement of new gene functions (neofunctionalization) and diversification of gene functions between the two daughter genes (subfunctionization)^{1,2}. Color vision is an excellent example for how duplication has been harnessed to select for a suite of spectrally sensitive visual opsin proteins, expanding the repertoire of photopigments to meet the visual demands of the innumerable environments across the planet. In vertebrates, color vision is accomplished by the expression of differentially spectrally sensitive opsin proteins in separate populations of cone photoreceptors of the retina. Cone subtypes are categorized by the type of opsin they express. These include: SWS1 (short wavelength-sensitive type 1, UV), SWS2 (short wavelength sensitive type 2, blue), RH2 (medium wavelength sensitive, green), and MWS/LWS (medium to long wavelength sensitive, green/red)³. The numbers of cone subtypes and their spectral sensitivities vary significantly among vertebrates.

Aquatic environments provide an incredibly complex assortment of visual stimuli to sample, filter, and process⁴. The variety of cone opsin subtypes found in the zebrafish retina is an example of how diversification of visual opsin subtypes can be selected for to detect and relay the information in

visually complex environments. For example, zebrafish have a total of eight different cone subtypes including SWS1 (UV), SWS2 (blue), RH2-1/2/3/4 (green), and LWS1/LWS2 (red)^{5,6}. In contrast, mice only have two subtypes including SWS1 (UV) and MWS (green)⁷. Humans have three cone subtypes S (blue), M (green), and L (red)⁸. The human *LWS* and *MWS* opsin gene locus as well as the orthologous *lws1/lws2* array in zebrafish are two striking examples of visual opsin gene duplication. In both arrays the two members are arranged in a tail to head manner on the X chromosome in humans, and on chromosome 11 in zebrafish^{6,9}. The downstream member in both arrays encodes an opsin with a shorter wavelength-shifted sensitivity than the first member and each are expressed in separate cone populations^{6,9}. Both arrays have an upstream regulatory region that contains a regulatory element, called a Locus Control Region (LCR) in humans and *lws* Activating Region (LAR) in zebrafish^{10,11} (Fig. 2.1A). These elements are required for proper expression of each array¹¹. The mechanisms involved that regulate this expression are not fully understood. The widely accepted model for how the human array is regulated involves the preferential association of either the *LWS* or *MWS* promoter with the LCR¹⁰. This association is thought to be permanent and mutually exclusive to prevent expression of both *LWS* and *MWS* opsin in the same cone¹⁰.

Differential expression of zebrafish *lws1* and *lws2* is dynamic across the zebrafish lifespan. *lws2* expression is initiated around 48 hours post fertilization (hpf)¹². *Lws1* expression does not occur until approximately 6 days post fertilization (dpf)¹². The fish eye grows by continuously adding cells to the periphery so that the earlier expression of *lws2* is reflected by the higher ratio of *LWS2* cones in the central retina in adults and *LWS1* in the periphery, mainly in the ventral and dorsal domains¹¹. The difference in ratio between *lws1* and *lws2* as a function of retinal eccentricity is similar to the difference in ratio between *LWS* cones and *MWS* cones in the adult human retina¹³. The mechanisms involved in accomplishing this differential patterning have not been fully elucidated. Recently we reported that retinoic acid (RA) and thyroid hormone (TH) are endogenous regulators of the differential expression of the zebrafish *lws* array^{14,15}. Larvae immersed in TH or RA from 2-4 dpf showed increased expression of *lws1* and decreased expression of *lws2*. Disrupting RA signaling suppressed *lws1* expression but had no effect on *lws2*¹⁴. Disrupting TH signaling increased *lws2* expression and completely abolished *lws1* expression save for an area in the ventral retina that coincides with a domain of RA signaling¹⁵. We demonstrated that TH loss of function effects could be rescued with exogenous TH, and that *lws* expression was neither permanent nor mutually exclusive but remains plastic throughout development and juvenile stages¹⁵.

Thyroid hormone is a nuclear signaling molecule that influences gene transcription by binding to one of the TH receptors (TRs) which interact with *cis*-regulatory sequences in the genome

called thyroid response elements (TREs). Once bound the liganded receptor forms a complex with transcriptional activators to promote transcription¹⁶. There is evidence that when the receptor is unliganded it can still bind with TREs and form a complex with transcriptional repressors that suppresses transcription¹⁷. The TREs are usually composed of a pair of hexameric halfsites, each having the sequence AGGTCA or slight variations of this classical sequence¹⁸. The halfsites can be a direct repeat, an inverted repeat, or an everted repeat¹⁹. The number of base pairs between the halfsites is thought to determine which receptor dimers can bind and whether transcription is promoted or suppressed¹⁹.

An earlier study focused upon the identification of elements of the zebrafish *lws* locus required for *lws* transcript expression within LWS cones, and elements that enhanced expression within these cones¹¹. A strategy was employed that involved microinjection of transient expression constructs containing regulatory regions of the *lws* array and fluorescent reporters for *lws1* and/or *lws2*. When a construct containing the 1.8kb intergenic region upstream of *lws2* driving expression of GFP was injected, there was no expression of GFP in cones at 7 dpf¹¹. However, when the 1.3kb region upstream from *lws1* was included in the construct, there was GFP expression in LWS cones, suggesting that the region upstream of *lws1* contains elements needed for expression of *lws2*. GFP expression became nearly absent when only 0.6kb upstream from *lws1* was included in the construct¹¹. The region between 1.3kb and 0.6kb upstream from *lws1* was therefore designated the *lws* activating region or LAR. Interestingly, when the LAR and the 1.8kb region upstream from *lws2* were used to drive GFP expression (*LAR:lws2up1.8kb:GFP*), GFP expression went from non-existent without the LAR (*lws2up1.8kb:GFP*) to GFP expression in all LWS cones throughout the retina¹¹. This is in stark contrast to a double reporter that contains 2.6kb up from *lws1* driving GFP expression followed by 1.8kb up from *lws2* driving RFP expression (*lws1up2.6kb:GFP-lws2up1.8kb:RFP*) in which the pattern for RFP recapitulated the central retina expression of endogenous *lws2*¹¹. This implies that the 1.8kb upstream from *lws2* does not contain the necessary elements for *lws2* expression but requires the LAR to promote *lws2*. Furthermore, the LAR appears to act as an enhancer but not a regulator of differential expression in the characteristic spatiotemporal pattern. These findings predict there must be an element(s) in the upstream region of *lws1* (which is not the LAR) that restricts *lws2* expression to the central retina and allows for *lws1* expression.

For this study we wished to identify the regions of the *lws* locus that are required for the differential regulation of *lws1* vs *lws2*, specifically in response to TH. We utilized a strategy similar to the transient expression method described above, which was used to identify the LAR. We demonstrate that the 1.8kb region upstream from *lws2* does not contain the necessary sequences to

downregulate *lws2* expression in response to TH treatment. We demonstrate that the 2.6kb region upstream from *lws1* does contain the elements necessary for the upregulation of *lws1* in response to TH. We also show that the 1.3kb region upstream from *lws1* that contains the LAR is sufficient for *lws2* expression, the normal onset of *lws1* expression, and the upregulation of *lws1* in response to TH. Furthermore, we identify two putative, palindromic TREs (ppTREs) in the 0.6kb region between the LAR and *lws1* that are required for proper differential expression of the two members of the *lws* array. The first element is required for *lws2* expression, is required for *lws1* suppression in early development, and is also required for the upregulation of *lws1* in response to TH. The second is also required for *lws1* suppression in early development, and for the upregulation of *lws1* in response to TH. The discovery of these cis-regulatory regions greatly increases our understanding of mechanisms underlying differential expression of tandemly-replicated opsin genes.

Methods and Materials

Animals

Zebrafish were maintained in monitored aquatic housing units on recirculating system water at 28.5°C. Embryos were collected according to²⁰, with light onset considered to be zero hours postfertilization (hpf) and embryonic age timed accordingly thereafter, with 24hpf considered 1 day postfertilization (dpf), 48hpf considered 2dpf, etc. Embryos used for whole mount analyses were kept transparent by incubating them in system water containing 0.003% phenylthiourea (PTU) to inhibit melanin synthesis. All experiments using animals were approved by the University of Idaho's Animal Care and Use Committee. Wild-type embryos were of an in-house outbred strain originally obtained from Scientific Hatcheries (now Aquatica Tropicals, Plant City, FL) and are referred to as "wildtype". The two stable transgenic lines Tg(*lws1up2.6kb*:GFP)#1509 Tg(LAR:*lws2up1.8kb*:GFP)#1499 were acquired from the RIKEN Brain Science Institute¹¹.

Transient transgenic constructs

The (*lws1up2.6kb*:GFP-*lws2up1.8kb*:RFP), (*lws1up1.3kb*:GFP), (*lws1up2.6kb*-0.6kb:GFP) and (Δ ppTRE1-LWS1:GFP-*lws2up1.8kb*:RFP) constructs in the pT2GFP-TKPA¹¹ vector were created within the laboratory of project collaborator Dr. Shoji Kawamura.

The (Δ ppTRE2-LWS1:GFP-*lws2up1.8kb*:RFP) construct was created by inverse PCR using primers in Table 1 to remove the 25bp ppTRE2 element from *lws1up2.6kb*:GFP-*lws2up1.8kb*:RFP. The amplicon was digested with EcoNI to make compatible ends and ligated back together using T4 ligase.

To create the *lws1up1.3kb:GFP- lws2up1.8kb:RFP* , *lws1up2.6kb-0.6kb:GFP- lws2up1.8kb:RFP* constructs, the sv40 polyA-*lws2up1.8kb:RFP* was cut from the *lws1up2.6kb:GFP- lws2up1.8kb:RFP* construct using NOTI and inserted into the *lws1up1.3kb:GFP* and *lws1up2.6kb-0.6kb:GFP* constructs at the NOTI site 5' of the HSV-TK polyA. Correct orientation was confirmed by restriction digest.

To facilitate the screening process of identifying transient transgenics the *cmcl2:GFP* transgenic heart marker was inserted into the *lws1up2.6kb-0.6kb:GFP- lws2up1.8kb:RFP*, (Δ ppTRE1-LWS1:GFP-*lws2up1.8kb:RFP*), and (Δ ppTRE2-LWS1:GFP-*lws2up1.8kb:RFP*) constructs by PCR amplifying the *cgl2:GFP-SV40* element from the pDestTol2CG2 (Tol2 kit #395) vector using the primer set in Table 1 and inserting it between the XHOI and BstBI sites in the multiple cloning site of the pT2GFP-TKPA¹¹ vector using the NEBuilder HIFI DNA assembly kit.

Microinjection

WT embryos were injected at the one cell stage using 30ng/ μ l of transgenesis construct and 25ng/ μ l transposase mRNA. The transposase mRNA was invitro transcribed from pCS2FA-transposase (TOL2 kit #396) using the mMESSAGING mMACHINE kit (Thermofisher).

Tri-iodothyronine (T3) treatments

Stock solutions of T3 were prepared in dimethylsulfoxide (DMSO; Sigma) and stored in the dark at -20°C. Prior to treatment, embryos/larvae were manually dechorionated, and then 1000X stock solution was added to the water to result 100nM final concentration (DMSO was at a final concentration of 0.1%).

Confocal photography and quantification: transgenic embryos

Transgenic embryos were maintained in system water with PTU starting at 12 hpf. At 2dpf, embryos were treated with T3 or DMSO through 4dpf, and then fixed in 4% paraformaldehyde in phosphate-buffered (pH=7.4) 5% sucrose solution for 1 hour, washed once in phosphate-buffered sucrose solution for 30 minutes followed by three washes in phosphate buffered saline (PBS). Following fixation and washing, embryos were incubated in PBS at 4°C in the dark for no longer than 24 hours. Embryos displaying bright, consistent expression of the heart marker were also screened for transgene expression in the eye using a Nikon epifluorescence stereomicroscope (SMZ 1500). Immediately prior to confocal imaging, whole eyes were removed from fixed embryos, the sclera teased away by microdissection, and eyes were then coverslipped in glycerol. Imaging was performed with a 20X dry lens using a Nikon Andor spinning disk confocal microscope equipped with a Zyla

sCMOS camera running Nikon Elements software. A z-series covering the entire globe of the eye was obtained with 3-micron step sizes. FIJI (ImageJ) was used to flatten z stacks via max projection and adjust brightness/contrast. FIJI (ImageJ) cell counter was used to count cells positive for the reporter. Graphing and statistics were performed using Excel. p-values were calculated using a Wilcoxon Mann-Whitney U test.

Results

Cis-regulatory elements required for endogenous patterns of *lws1* vs. *lws2*, and the response to TH, reside in the 2.6kb immediately upstream of *lws1*

To test the hypothesis that the cis-regulatory elements needed for TH-mediated regulation of zebrafish *lws1* vs. *lws2* opsins are the same as those needed for the establishment of their endogenous spatiotemporal expression patterns, we utilized two stable transgenic lines. The first line, *lws1up2.6kb*:GFP (Fig. 3.1B), reports *lws1* with GFP, and displays a pattern of GFP expression in adult retina that is consistent with the endogenous pattern of expression of native *lws1*¹¹. These prior results suggest that the proximal 2.6kb region upstream of *lws1* contains elements necessary to establish the normal expression of *lws1* in the retinal periphery. We treated *lws1up2.6kb*:GFP embryos at 2dpf (48hpf) with 100nM T3, a treatment that is known to increase *lws1* at the expense of *lws2*¹⁵, and visualized GFP expression at 4dpf in comparison to DMSO-treated controls. Treated larvae displayed robust expression of the GFP reporter (Fig. 3.1D,E), in a pattern matching that of T3-induced native *lws1* transcript expression¹⁵. Numbers of GFP+ cones observed in T3-treated *lws1up2.6kb*:GFP larvae were significantly increased in comparison with controls (Fig. 3.1H), and matched those observed within T3-treated larvae of the *lws*:PAC(H) line¹⁵, which faithfully reports *lws1* and *lws2* with fluorescent proteins¹¹. Together these findings indicate that the proximal 2.6kb region upstream of *lws1* contains elements necessary for TH-mediated regulation of *lws1*.

The second transgenic line, *LAR:lws2up1.8kb*:GFP (Fig. 3.1C), reports *lws2* with GFP, such that GFP is expressed within all LWS cones of adult retina¹¹. This finding suggests that the LAR and the 1.8kb intergenic region together do not contain the elements necessary to restrict expression of *lws2* to central retina. *LAR:lws2up1.8kb*:GFP larvae treated 2-4dpf with 100nM T3 did not show the expected reduction of GFP+ cones in comparison with controls¹⁵ but rather an increase (Fig. 3.1I). The LAR and 1.8kb intergenic region therefore together do not contain the elements necessary to reduce *lws2* expression in response to T3 but do contain an element that serves to promote expression of *lws2* in response to T3, at least in the absence of the elements missing on the transgenic construct,.

Collectively the findings from the two stable transgenic lines support the hypothesis that elements needed for differential expression of *lws1* and *lws2* in response to TH, are likely the same as those needed for establishment of their endogenous spatiotemporal expression patterns. Further, these results suggest that the cis-regulatory elements of interest likely reside within the 2.6kb region immediately upstream of *lws1*.

Cis-regulatory elements required for endogenous patterns of *lws1* vs. *lws2*, and the response to TH, likely reside in the 0.6kb immediately upstream of *lws1*

We wished to more specifically localize the regulatory elements residing within the 2.6kb upstream of *lws1*, and so we generated constructs in which *lws1* was reported by GFP, and *lws2* was reported by RFP. In the first of these constructs, *lws1up1.3kb*:GFP:*lws2up1.8kb*:RFP, the 1.3kb residing between the *sws2* locus and the LAR, was deleted (Fig. 3.2A). The remaining 1.3kb region upstream from *lws1* contains the LAR and several predicted TREs and RXREs^{14,15}. Given that ligands for TRs and for RXRs can increase *lws1* at the expense of *lws2*^{14,15}, we reasoned that this region could be considered a candidate for containing the elements of interest. We employed transient transgenesis assays by microinjecting a cassette containing the *lws1up1.3kb*:GFP:*lws2up1.8kb*:RFP, using the Tol2 transgenesis strategy^{11,21}. Injected embryos subjected to control conditions (DMSO, 2-4dpf) expressed only RFP within the retina, in patterns suggesting mosaic incorporation of the construct (Fig. 3.2B). Injected embryos treated with 100nM T3 (2-4dpf), however, expressed both RFP and GFP, again in patterns suggesting mosaic expression, but also with GFP appearing predominantly in the periphery (Fig. 3.2C), consistent with previously-reported T3-mediated induction of *lws1*¹⁵. Interestingly, quantification of numbers of GFP and RFP positive cones confirmed that the T3 treatment increased the GFP+ (reporting *lws1*) cones (Fig. 3.2D) but did not correspondingly decrease the RFP+ (reporting *lws2*) cones (Fig. 3.2E). Together with the findings using stable transgenic lines, these results suggest that the cis-regulatory elements needed for both normal spatial patterns of expression of *lws1* and *lws2*, and for regulation of *lws1* by T3, do not reside within the 1.3kb between *sws2* and the LAR, but instead likely reside within the proximal 1.3kb immediately upstream of *lws1*. These results however, do not resolve where the element for downregulation of *lws2* in response to T3 is located. Our quantification of RFP+ cones showed no significant difference between treated and untreated larvae. It is possible that the element does not reside in the 1.3kb region upstream from *lws1*.

To test the hypothesis that differential expression of *lws1* vs. *lws2* requires elements within the 0.6kb immediately upstream of *lws1*, we generated an additional reporter construct in which this region was deleted and the region from the last exon of *sws2* continuing through to include the LAR,

was used to drive *lws1*:GFP expression: *lws1up2.6-0.6kb*:GFP:*lws2up1.8kb*:RFP (Fig. 3.3A). Injected embryos treated with DMSO 2-4dpf, interestingly, displayed faint GFP and RFP signal that frequently colocalized within very few cells in the retina (Fig. 3.3B), suggesting that the deleted region of the construct contains elements needed for the suppression of *lws1* and for the activation of *lws2* during the embryonic/early larval period. Injected embryos treated with 100nM T3 2-4dpf displayed sporadic expression of GFP and RFP positive cells (Fig. 3.3C). Quantification of GFP positive cells revealed no significant difference compared to controls. Interestingly there were significantly more RFP positive cells in the T3 treated group compared to controls (Fig. 3.3D,E). Collectively these results suggest that the necessary elements for proper spatiotemporal expression of *lws1* and *lws2* and response to T3 do not reside in the 1.3kb region upstream from the LAR and therefore must reside in the 0.6kb region immediately upstream of *lws1*. Furthermore, the increase in *lws2*:RFP positive cells in the T3 treated group is a similar outcome as the T3 treated LAR:*lws2up1.8kb*:GFP (Fig. 3.11). Taken together these results suggest that the LAR may contain an element(s) that serve to promote *lws2* expression in response to T3 when the 0.6kb region immediately upstream from *lws1* is not present.

Two, ~25bp elements containing predicted palindromic TREs are important for regulation of endogenous patterns of *lws1* vs. *lws2*, and the response to TH

We further focused upon selected, smaller elements within the 0.6kb region immediately upstream of *lws1*. Our prior analyses for predicted TREs and RXREs, using MatInspector²² and Promo^{23,24}, found two predicted palindromic TREs (ppTREs) approximately 0.5 kb upstream (ppTRE1), and 0.2kb upstream (ppTRE2) of *lws1*^{14,15}(Figs. 4A; 5A). These ppTREs do not precisely conform to the classical “DR4” TRE consisting of a pair of halvesites: AGGTCA-4bp spacer-AGGTCA^{18,19}, but were identified as candidate TREs. We generated a construct in which a 21bp region encompassing ppTRE1 was deleted (*AppTRE1-lws1up2.6kb*:GFP-*lws2up1.8kb*:RFP; Fig. 3.4A), and examined expression of GFP and RFP in the retinas of injected larvae treated with DMSO vs. 100nM T3. Control *AppTRE1-lws1up2.6kb*:GFP-*lws2up1.8kb*:RFP larvae displayed sporadic GFP expression and no RFP expression (Fig. 3.4B,D,E), while T3-treated *AppTRE1-lws1up2.6kb*:GFP-*lws2up1.8kb*:RFP larvae showed no increase in GFP-expressing cones, and also no RFP expression (Fig. 3.4C, D,E). The 21bp region therefore contains elements important for suppressing *lws1* and critical for activating *lws2* during the embryonic and early larval period, and for activating *lws1* in response to T3. Given that TREs interacting with unliganded receptors can act as suppressors while liganded receptors can act as activators^{16,17}, it is tempting to speculate that the ppTRE1 interacts with

a nuclear hormone receptor(s) that suppresses *lws1* in unliganded form, and activates *lws1* when ligand (T3) is present.

We next generated a construct in which a 25bp region encompassing ppTRE2 was deleted (*AppTRE2-lws1up2.6kb:GFP-lws2up1.8kb:RFP*; Fig. 3.5A), and examined expression of GFP and RFP in the retinas of injected larvae treated with DMSO vs. 100nM T3. Control *AppTRE2-lws1up2.6kb:GFP-lws2up1.8kb:RFP* larvae displayed sporadic GFP expression and also sporadic RFP expression (Fig. 3.5B,D,E), while T3-treated *AppTRE2-lws1up2.6kb:GFP-lws2up1.8kb:RFP* larvae showed GFP and RFP expression very similar to that of controls (Fig. 3.5C, D,E). This 25bp region (ppTRE2) therefore contains elements needed to suppress *lws1* during the embryonic and early larval period, and to activate *lws1* in response to T3. The ppTRE2 may therefore also interact with a nuclear hormone receptor(s) that suppresses *lws1* in unliganded form, and activates *lws1* when ligand (T3) is present. The 25bp region also may contain elements that suppress *lws2* expression in response to T3, since in its absence, *lws2* expression was not significantly different compared to controls (Fig. 3.5E). These outcomes are more challenging to explain in light of the conventional understanding of regulatory functions of TREs and their corresponding receptors. The roles of the 21bp region containing ppTRE1 are nearly, but not absolutely identical to the roles determined for the 25bp region containing ppTRE2, indicating that each region alone is not sufficient for carrying out these regulatory functions. Rather, both ~25bp regions are needed for endogenous control of spatiotemporal differential expression of *lws1* vs. *lws2*, and for the regulation of the *lws* array by T3.

Discussion

We previously demonstrated that the nuclear signaling molecule TH is an endogenous regulator of the differential expression of the tandemly replicated *lws1/lws2* array in zebrafish. Here we significantly expand our knowledge of this regulatory mechanism by identifying the *cis*-regulatory components necessary for the response to TH. We first demonstrated that the 2.6kb region upstream from *lws1* is sufficient for normal suppression of *lws1* at 4 dpf as well as the promotion of *lws1* in response to TH. We then demonstrated that the 1.8kb region upstream from *lws2* does not contain the necessary elements to restrict *lws2* expression to its endogenous expression domain or the necessary elements for suppression of *lws2* in response to TH. We further dissect the minimal components necessary for the response to TH by identifying the 1.3kb region encompassing the LAR and the 0.6kb immediately upstream from *lws1* as having the necessary sequences for suppression of *lws1* at 4dpf, the promotion of *lws1* by TH, but not the suppression of *lws2* by TH. Interestingly, when the 0.6kb region was deleted suppression of *lws1* was lost, as well as the promotion of *lws1* in response to

TH, and instead of suppression of *lws2* in response to TH *lws2* expression increased. Collectively, the only conditions in which *lws2* expression was suppressed in response to TH was when the entire 2.6kb upstream from *lws1* and the 1.8kb upstream from *lws2* was intact. The only condition in which *lws2* was not promoted by TH was when the 0.6kb region upstream from *lws1* was present.

To our great surprise we identified two potential response elements in this 0.6kb region that are critical for the differential regulation of both *lws1* and *lws2* in response to TH. When the ppTRE1 element was deleted, the suppression of *lws1* was abolished, as well as the promotion of *lws1* in response to TH, and retinas completely lacked expression of *lws2*. When the ppTRE2 element was deleted the suppression of *lws1* was also abolished, and the promotion of *lws1* in response to TH, and *lws2* was promoted in response to TH not suppressed. Taken together these findings suggest that both elements are required for suppression of *lws1*, promotion of *lws1* in response to TH, and for the case of ppTRE1 expression of *lws2*, and that of ppTRE2 suppression of *lws2* in response to TH. Interestingly when the 0.6kb region was present but the 1.3kb upstream from LAR was deleted *lws2* was also promoted in response to TH. These two results suggest that an interaction between ppTRE2 and an element in the 1.3kb upstream from the LAR is required for suppression of *lws2* in response to TH. A summary of known roles of cis-regulatory regions of the zebrafish *lws* locus identified here and by (Tsumimura et al., 2010) is provided as Fig. 3.6.

These findings illuminate the intricate complexities involved in regulation of tandemly replicated gene arrays. We previously reported that TH is involved in the differential regulation of the tandemly quadruplicated *rh2* array in zebrafish¹⁵. Our results suggest that TH functions to promote the members of a tandem array that are more red-shifted (*rh2-2*, *rh2-3*, *rh2-4*) and suppress the shorter wavelength sensitive member (*rh2-1*)¹⁵. Interestingly, in contrast to the *rh2* array the more red-shifted member of the *lws* array (*lws1*) is the first member. Taken together, these results suggest that the distance to the upstream regulatory regions from each member is not the deciding factor in the response to TH. The promotion of the more red-shifted members appears to be more related to the spatial domain of expression. The opsins with the more red-shifted sensitivity (*lws1*, *rh2-2*, *rh2-3*, *rh2-4*) are expressed in the periphery of the adult retina and the blue-shifted opsins are in central retina¹². The spatial domain of expression of all the visual opsins in the zebrafish retina is quite dynamic throughout the life history of the developing fish¹². Spatiotemporal regulation of TH signaling provides the means to orchestrate these dynamic changes in expression from both tandemly replicated visual opsin arrays.

Previous reports documenting the involvement of different regions of the *rh2* array in regulating expression of the *rh2* opsins identified a Locus Control Region (LCR) analogous to the

LCR in the human *LWS/MWS* locus²⁵. Much like the human *LWS/MWS* array in which LWS opsin is more abundant than MWS, the transcripts that are more proximal to the LCR are expressed in higher amounts than the distal members²⁵. However, it was demonstrated by inserting the LCR just downstream of *rh2-3* that the relative distance to the LCR not the absolute distance affected expression levels of each member²⁵. Interestingly, *rh2-4* expression remained low and was not affected by the change in distance²⁵. Suggesting that regions proximal to each gene may have elements that suppress expression. Further investigation of the distance effect in concert with the proximal regions of each *rh2* gene revealed that the proximal region of each *rh2* gene except for *rh2-3* contained elements that determined spatial expression patterns²⁶. These findings are in line with the results of the current study that suggests that proximal regions of tandemly replicated arrays contain elements that influence regulation of the expression of each member of the array.

In summary our findings indicate that multiple *cis*-regulatory elements in the zebrafish *lws* array are required for proper differential spatiotemporal expression, and for the response to thyroid hormone treatment. A logical next step is to identify what the *trans*-acting factors that interact with these *cis* elements could be. We have demonstrated that both TH and RA are involved in this regulatory mechanism^{14,15}. These findings imply that a number of potential nuclear hormone receptors and receptor homo/hetero dimer combinations could be involved. Thyroid hormone receptor subtypes include TR α A, TR α B, TR β 1, and TR β 2. LWS cones fail to differentiate in zebrafish lacking TR β 2²⁷⁻²⁹. This makes TR β 2 a likely candidate for a *trans*-acting factor involved in the differential regulation of the *lws* locus. However, our results suggest that more than one response element may be involved. Findings from our previous study describing the role of RA in this regulatory mechanism suggested the effects of RA were mediated by RXR γ ¹⁴. RXR γ is known to heterodimerize with TR β 2. Further studies are required to determine which receptors may be involved in this regulatory mechanism. Additional regulatory features to be unraveled include potential roles for changes in chromatin accessibility, and changes in chromosomal looping created by two or more interacting elements.

Literature Cited

- 1 Zhang, J. Evolution by gene duplication: an update. *Trends in Ecology & Evolution* **18**, 292-298, doi:[https://doi.org/10.1016/S0169-5347\(03\)00033-8](https://doi.org/10.1016/S0169-5347(03)00033-8) (2003).
- 2 Gu, Z., Nicolae, D., Lu, H. H. & Li, W. H. Rapid divergence in expression between duplicate genes inferred from microarray data. *Trends in genetics : TIG* **18**, 609-613, doi:10.1016/s0168-9525(02)02837-8 (2002).

- 3 Yokoyama, S. Molecular evolution of vertebrate visual pigments. *Progress in Retinal and Eye Research* **19**, 385-419, doi:[https://doi.org/10.1016/S1350-9462\(00\)00002-1](https://doi.org/10.1016/S1350-9462(00)00002-1) (2000).
- 4 Carleton, K. L., Escobar-Camacho, D., Stieb, S. M., Cortesi, F. & Marshall, N. J. Seeing the rainbow: mechanisms underlying spectral sensitivity in teleost fishes. *J Exp Biol* **223**, doi:10.1242/jeb.193334 (2020).
- 5 Raymond, P. A., Barthel, L. K., Rounsifer, M. E., Sullivan, S. A. & Knight, J. K. Expression of rod and cone visual pigments in goldfish and zebrafish: A rhodopsin-like gene is expressed in cones. *Neuron* **10**, 1161-1174, doi:[https://doi.org/10.1016/0896-6273\(93\)90064-X](https://doi.org/10.1016/0896-6273(93)90064-X) (1993).
- 6 Chinen, A., Hamaoka, T., Yamada, Y. & Kawamura, S. Gene duplication and spectral diversification of cone visual pigments of zebrafish. *Genetics* **163**, 663-675 (2003).
- 7 Applebury, M. L. *et al.* The Murine Cone Photoreceptor: A Single Cone Type Expresses Both S and M Opsins with Retinal Spatial Patterning. *Neuron* **27**, 513-523, doi:[https://doi.org/10.1016/S0896-6273\(00\)00062-3](https://doi.org/10.1016/S0896-6273(00)00062-3) (2000).
- 8 Nathans, J., Thomas, D. & Hogness, D. S. Molecular genetics of human color vision: the genes encoding blue, green, and red pigments. *Science* **232**, 193-202 (1986).
- 9 Vollrath, D., Nathans, J. & Davis, R. Tandem array of human visual pigment genes at Xq28. *Science* **240**, 1669-1672, doi:10.1126/science.2837827 (1988).
- 10 Wang, Y. *et al.* Mutually exclusive expression of human red and green visual pigment-reporter transgenes occurs at high frequency in murine cone photoreceptors. *Proceedings of the National Academy of Sciences of the United States of America* **96**, 5251-5256 (1999).
- 11 Tsujimura, T., Hosoya, T. & Kawamura, S. A single enhancer regulating the differential expression of duplicated red-sensitive opsin genes in zebrafish. *PLoS Genet* **6**, e1001245, doi:10.1371/journal.pgen.1001245 (2010).
- 12 Takechi, M. & Kawamura, S. Temporal and spatial changes in the expression pattern of multiple red and green subtype opsin genes during zebrafish development. *J Exp Biol* **208**, 1337-1345, doi:10.1242/jeb.01532 (2005).
- 13 Kuchenbecker, J. A., Sahay, M., Tait, D. M., Neitz, M. & Neitz, J. Topography of the long- to middle-wavelength sensitive cone ratio in the human retina assessed with a wide-field color multifocal electroretinogram. *Vis Neurosci* **25**, 301-306, doi:10.1017/S0952523808080474 (2008).
- 14 Mitchell, D. M. *et al.* Retinoic Acid Signaling Regulates Differential Expression of the Tandemly-Duplicated Long Wavelength-Sensitive Cone Opsin Genes in Zebrafish. *PLoS Genet* **11**, e1005483, doi:10.1371/journal.pgen.1005483 (2015).
- 15 Mackin, R. D. *et al.* Endocrine regulation of multichromatic color vision. *Proceedings of the National Academy of Sciences*, 201904783, doi:10.1073/pnas.1904783116 (2019).

- 16 Brent, G. A. Mechanisms of thyroid hormone action. *J Clin Invest* **122**, 3035-3043, doi:10.1172/JCI60047 (2012).
- 17 Shibusawa, N., Hollenberg, A. N. & Wondisford, F. E. Thyroid hormone receptor DNA binding is required for both positive and negative gene regulation. *J Biol Chem* **278**, 732-738, doi:10.1074/jbc.M207264200 (2003).
- 18 Wu, Y., Xu, B. & Koenig, R. J. Thyroid hormone response element sequence and the recruitment of retinoid X receptors for thyroid hormone responsiveness. *J Biol Chem* **276**, 3929-3936, doi:10.1074/jbc.M006743200 (2001).
- 19 Paquette, M. A., Atlas, E., Wade, M. G. & Yauk, C. L. Thyroid hormone response element half-site organization and its effect on thyroid hormone mediated transcription. *PLoS One* **9**, e101155, doi:10.1371/journal.pone.0101155 (2014).
- 20 Westerfield, M. *The Zebrafish Book. A Guide for The Laboratory Use of Zebrafish (Danio rerio)*. Vol. 385 (2000).
- 21 Urasaki, A., Morvan, G. & Kawakami, K. Functional dissection of the Tol2 transposable element identified the minimal cis-sequence and a highly repetitive sequence in the subterminal region essential for transposition. *Genetics* **174**, 639-649, doi:10.1534/genetics.106.060244 (2006).
- 22 Cartharius, K. *et al.* MatInspector and beyond: promoter analysis based on transcription factor binding sites. *Bioinformatics (Oxford, England)* **21**, 2933-2942, doi:10.1093/bioinformatics/bti473 (2005).
- 23 Messeguer, X. *et al.* PROMO: detection of known transcription regulatory elements using species-tailored searches. *Bioinformatics (Oxford, England)* **18**, 333-334 (2002).
- 24 Farré, D. *et al.* Identification of patterns in biological sequences at the ALGGEN server: PROMO and MALGEN. *Nucleic acids research* **31**, 3651-3653 (2003).
- 25 Tsujimura, T., Chinen, A. & Kawamura, S. Identification of a locus control region for quadruplicated green-sensitive opsin genes in zebrafish. *Proceedings of the National Academy of Sciences of the United States of America* **104**, 12813-12818, doi:10.1073/pnas.0704061104 (2007).
- 26 Tsujimura, T., Masuda, R., Ashino, R. & Kawamura, S. Spatially differentiated expression of quadruplicated green-sensitive RH2 opsin genes in zebrafish is determined by proximal regulatory regions and gene order to the locus control region. *BMC Genet* **16**, 130, doi:10.1186/s12863-015-0288-7 (2015).
- 27 Suzuki, S. C. *et al.* Cone photoreceptor types in zebrafish are generated by symmetric terminal divisions of dedicated precursors. *Proc Natl Acad Sci U S A* **110**, 15109-15114, doi:10.1073/pnas.1303551110 (2013).

- 28 Volkov, L. I. *et al.* Thyroid hormone receptors mediate two distinct mechanisms of long-wavelength vision. *Proc Natl Acad Sci U S A* **117**, 15262-15269, doi:10.1073/pnas.1920086117 (2020).
- 29 Deveau, C. *et al.* Thyroid hormone receptor beta mutations alter photoreceptor development and function in *Danio rerio* (zebrafish). *PLoS Genet* **16**, e1008869, doi:10.1371/journal.pgen.1008869 (2020).

Figures

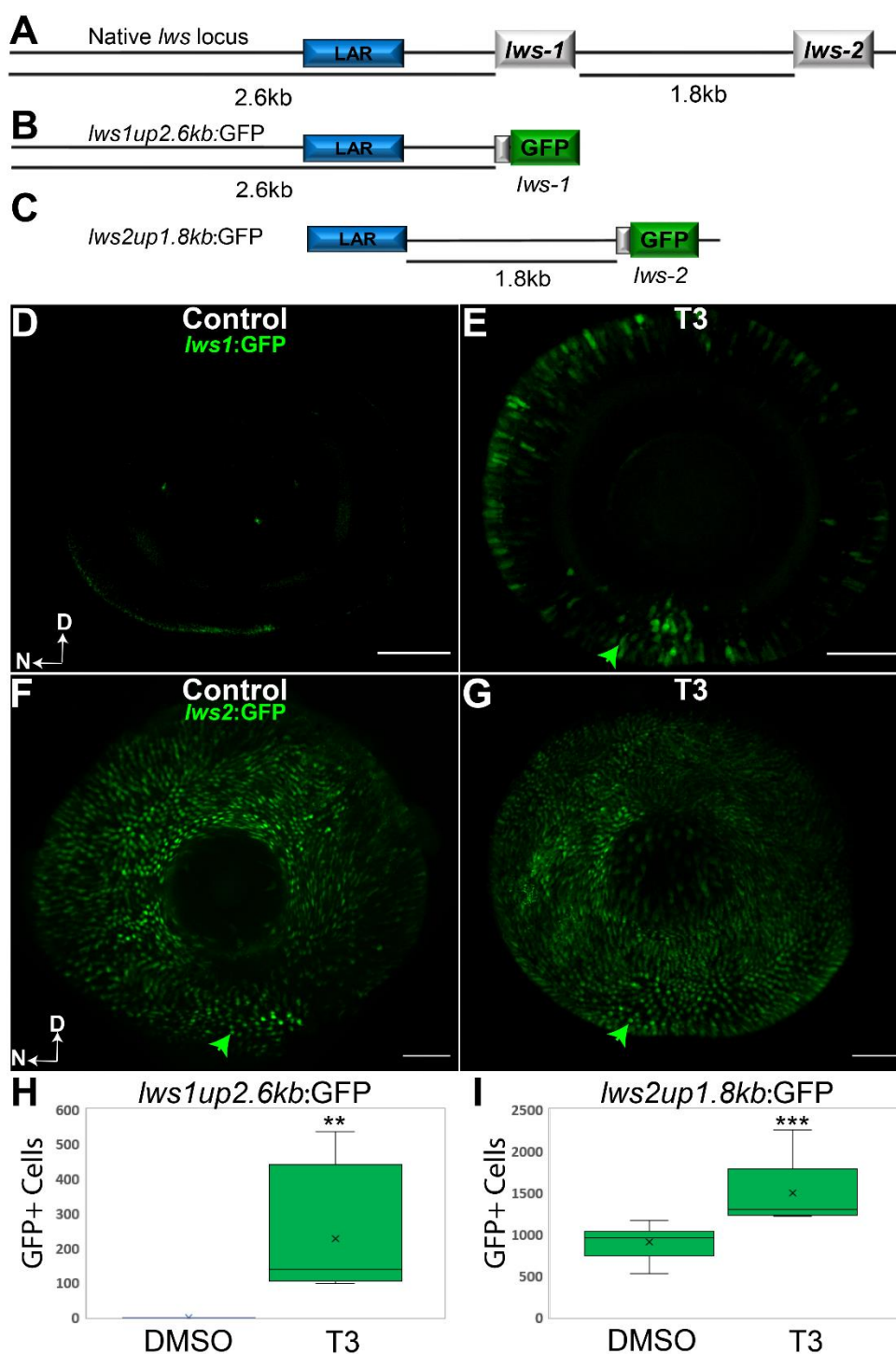


Fig 3.1. The element required for upregulation of *lws1* in response to TH (T3) resides in the 2.6kb region upstream from *lws1* but the element required for the downregulation of *lws2* in response to T3 is not in the 1.8kb region upstream from *lws2*. (A-C) Schematic representations of

(A) the native *lws* locus which contains the *lws* activating region (LAR) and the tandemly replicated *lws1* and *lws2*. (B) The *lws1up2.6kb*:GFP reporter construct (C) the *LAR:lws2up1.8kb*:GFP reporter construct. (D, E) Whole-mounted 4dpf *lws1up2.6kb*:GFP eyes visualized by confocal microscopy of (D) DMSO-treated (control) or (E) T3-treated. (F, G) Whole mount 4dpf *LAR:lws2up1.8kb*:GFP eyes treated with (F) DMSO-treated or (G) T3-treated. Green arrowheads indicate GFP+ cones. D, dorsal; N, nasal. Scale bars = 50 μ m (H, I) Numbers of GFP+ cones for (H) DMSO vs T3 treated *lws1up2.6kb*:GFP P = 0.00512, and numbers of GFP+ cones for (I) DMSO vs T3 treated *LAR:lws2up1.8kb*:GFP P = 0.00094. N = six z-stack images for each condition from *lws1up2.6kb*:GFP eyes and eight z-stack images for each condition from *LAR:lws2up1.8kb*:GFP eyes. P values were calculated by comparing GFP+ cones from the treated vs control group using the Mann-Whitney U test. Statistical notation: **P \leq 0.001, ***P \leq 0.0001.

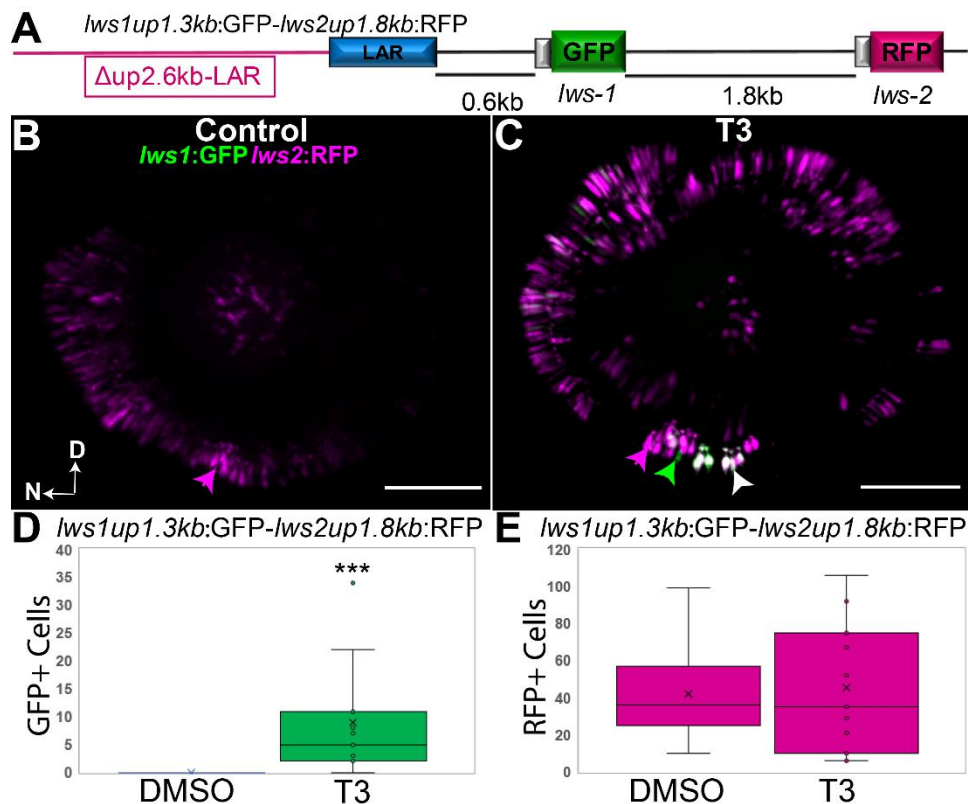


Fig 3.2. The 1.3kb region upstream from *lws1* that includes the LAR and 0.6kb immediately upstream from *lws1* is sufficient for normal *lws* expression at 4 days, the upregulation of *lws1* in response to T3 but not the downregulation of *lws2* in response to T3. (A) Schematic representations of the *lws1up1.3kb*:GFP-*lws2up1.8kb*:RFP reporter construct. Deleted region

indicated by red line. (B, C) Whole-mounted 4dpf *lws1up1.3kb:GFP-lws2up1.8kb:RFP* eyes visualized by confocal microscopy of (B) DMSO- treated (control) or T3- treated (C). RFP has been pseudo-colored magenta. Green arrowheads indicate GFP+ cones, magenta arrowheads indicate RFP+ cones, and white arrowheads indicate co-labeled cones. D, dorsal; N, nasal. Scale bars = 50 μ m (D, E) Numbers of GFP+ cones for (D) DMSO vs T3 treated *lws1up1.3kb:GFP-lws2up1.8kb:RFP* P = 0.00034, and numbers of RFP+ cones for (I) DMSO vs T3 treated *lws1up1.3kb:GFP-lws2up1.8kb:RFP* P = 0.92. N = fifteen z-stack images for each condition from *lws1up1.3kb:GFP-lws2up1.8kb:RFP* eyes. P values were calculated by comparing GFP+ and RFP+ cones from the treated vs control group using the Mann-Whitney U test. Statistical notation: ***P \leq 0.0001.

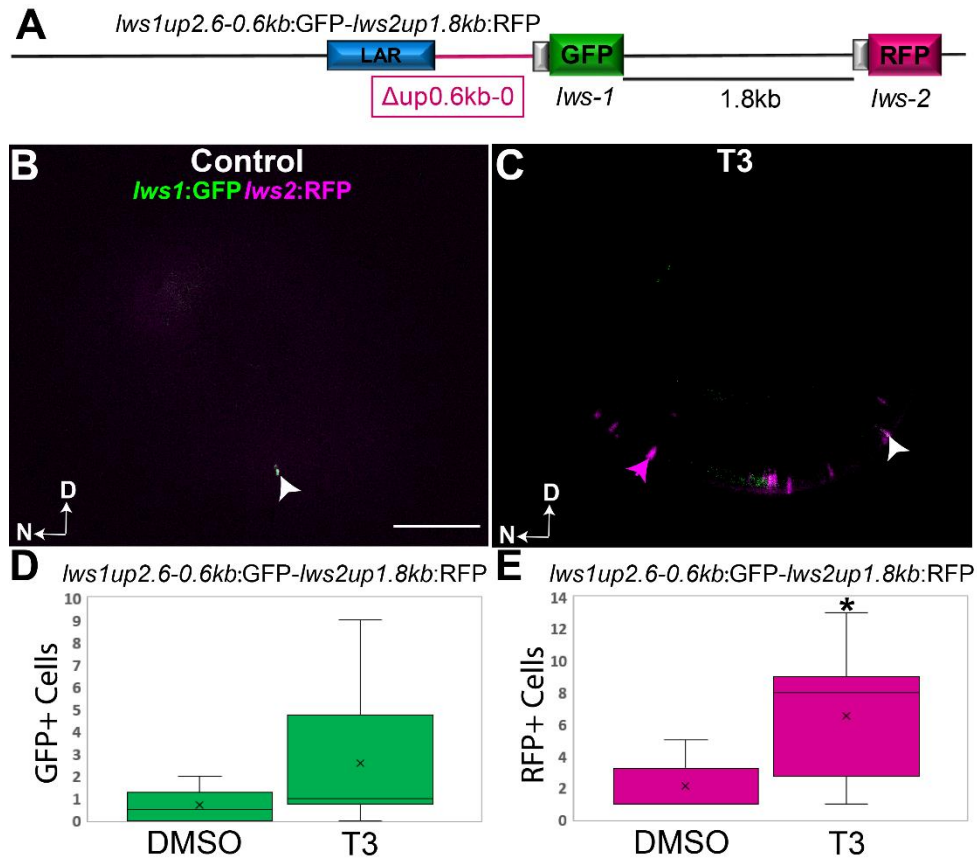


Fig 3.3. The 2.6kb-0.6kb region upstream is not sufficient for normal expression of the *lws* array at 4dpf or the upregulation of *lws1* in response to T3. The numbers of *lws2* positive cones increased in response to T3 instead of decreased with the intact locus. (A) Schematic representations of the *lws1up2.6kb-0.6kb:GFP-lws2up1.8kb:RFP* reporter construct. Deleted region is

indicated by the red line. (B, C) Whole-mounted 4dpf *lws1up2.6kb-0.6kb:GFP-lws2up1.8kb:RFP* eyes visualized by confocal microscopy of (B) DMSO- treated (control) or (C) T3-treated. RFP has been pseudo-colored magenta. magenta arrowheads indicate RFP+ cones, and white arrowheads indicate co-labeled cones. D, dorsal; N, nasal. Scale bar in B applies to B and C. Scale bar = 50 μ m (D, E) Numbers of GFP+ cones for (D) DMSO vs T3 treated *lws1up2.6kb-0.6kb:GFP-lws2up1.8kb:RFP* P = 0.16, and RFP+ cone numbers for (E) DMSO vs T3 treated *lws1up2.6kb-0.6kb:GFP-lws2up1.8kb:RFP* P = 0.028. N = ten z-stack images for each condition from *lws1up2.6kb-0.6kb:GFP-lws2up1.8kb:RFP* eyes. P values were calculated by comparing GFP+ and RFP+ cones from the treated vs control group using the Mann-Whitney U test. Statistical notation: *P \leq 0.05.

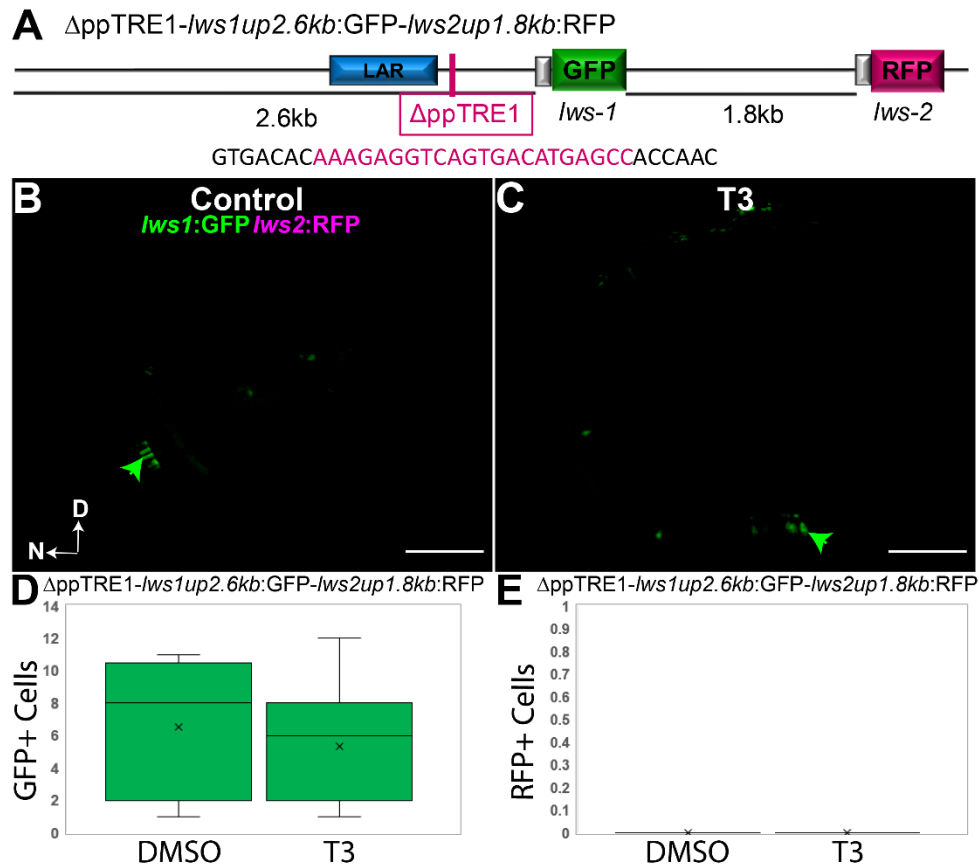


Fig 3.4. The ppTRE1 element is required for suppression of *lws1* at 4dpf, expression of *lws2* at 4dpf, and upregulation of *lws1* in response to T3. (A) Schematic representations of the Δ ppTRE1-*lws1up2.6kb:GFP-lws2up1.8kb:RFP* reporter construct. Nucleotide sequence of the deleted region is shown, with the ppTRE1 sequence highlighted in red font. (B,C) Whole-mounted 4dpf Δ ppTRE1-

lws1up2.6kb:GFP-lws2up1.8kb:RFP eyes visualized by confocal microscopy of (B) DMSO-treated (control) or (C) T3-treated. RFP has been pseudo-colored magenta. Green arrowheads indicate GFP+ cones. D, dorsal; N, nasal. Scale bar = 50 μ m (D,E) Numbers of GFP+ cones for (D) DMSO vs T3 treated Δ ppTRE1-*lws1up2.6kb:GFP-lws2up1.8kb:RFP* P=0.53, and numbers of RFP+ cones for (E) DMSO vs T3 treated Δ ppTRE1-*lws1up2.6kb:GFP-lws2up1.8kb:RFP* P=1. N = nine z-stack images for each condition from Δ ppTRE1-*lws1up2.6kb:GFP-lws2up1.8kb:RFP* eyes. P values were calculated by comparing GFP+ and RFP+ cones from the treated vs control group using the Mann-Whitney U test.

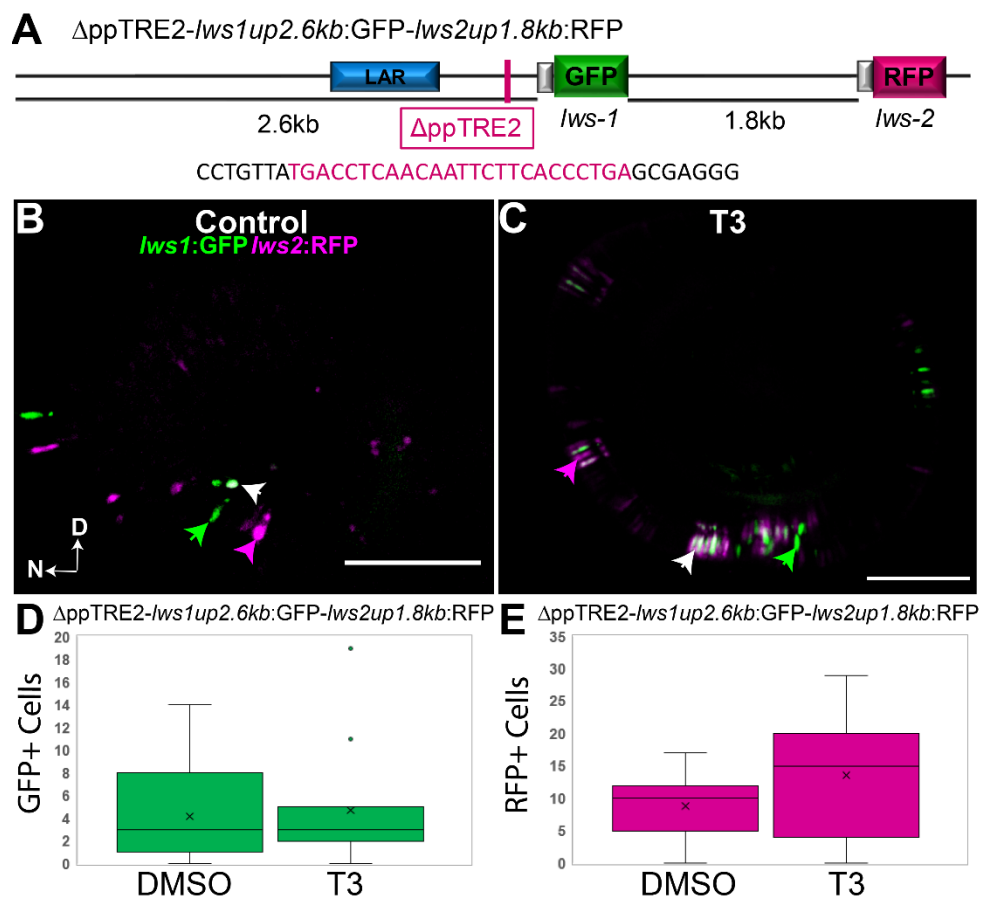


Fig 3.5. The ppTRE2 element is required for *lws1* suppression at 4dpf, the upregulation of *lws1* in response to T3, and the downregulation of *lws2* in response to T3. (A) Schematic representations of the Δ ppTRE2-*lws1up2.6kb:GFP-lws2up1.8kb:RFP* reporter construct. Nucleotide sequence of the deleted region is shown, with the ppTRE2 sequence highlighted in red font. (B,C) Whole-mounted 4dpf Δ ppTRE2-*lws1up2.6kb:GFP-lws2up1.8kb:RFP* eyes visualized by confocal

microscopy of (B) DMSO-treated (control) or (C) T3-treated. RFP has been pseudo-colored magenta. Green arrowheads indicate GFP+ cones, magenta arrowheads indicate RFP+ cones, and white arrowheads indicate co-labeled cones. D, dorsal; N, nasal. Scale bar = 50 μ m (D,E) Numbers of GFP+ cones for (D) DMSO vs T3 treated Δ ppTRE2-*lws1up2.6kb*:GFP-*lws2up1.8kb*:RFP P=0.60, and numbers of RFP+ cones for (E) DMSO vs T3 treated Δ ppTRE2-*lws1up2.6kb*:GFP-*lws2up1.8kb*:RFP P=0.13. N = fifteen z-stack images for each condition from Δ ppTRE2-*lws1up2.6kb*:GFP-*lws2up1.8kb*:RFP eyes. P values were calculated by comparing GFP+ and RFP+ cones from the treated vs control group using the Mann-Whitney U test.

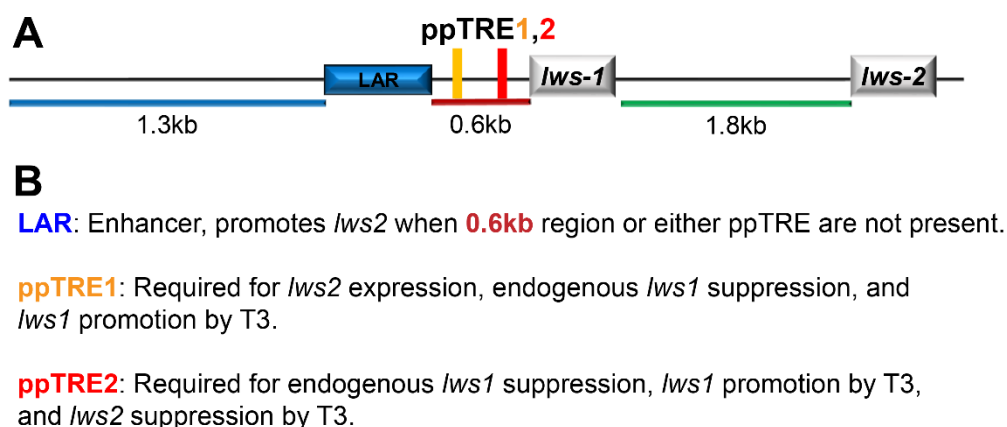


Fig 3.6. The *lws* locus contains more than one element that contributes to proper endogenous regulation and response to T3. (A, B) Schematic of the *lws* locus with the (A) cis-regulatory components labeled and the (B) known functions of each element.

Supplementary Table S3.1. Primers for modification of reporter constructs

	Forward Primer	Reverse Primer
PT2GFP TKPA- pDEST cmcl2:GFP	ggagatcacttggccccggctgcacagcaccttgacctg	tgtgtgtcgactgcagaatttgataattcactggccgtcg

Chapter 4: Nuclear Signaling Molecule Regulation of Visual Opsin Expression in Human iPSC Derived 3D Retinal Organoids.

Abstract

The understanding of extrinsic factors involved in the development of the human retina is a prerequisite for the advancement of novel therapeutics for the treatment of visual disorders. Age related macular degeneration is just one example of a visual disorder that extracts a significant toll from more than 11 million people in the United States alone. The development of three-dimensional retinal organoids or Retina Cups (RCs) derived from human induced pluripotent stem cells offer both a model to test which factors are necessary for proper development and differentiation of retinal cellular subtypes but also a potential tool that could be harnessed for modern medical interventions such as cell transplantation of healthy cells into a diseased retina. We describe here that the nuclear signaling molecules retinoic acid (RA) and thyroid hormone (TH) are extrinsic factors that can be supplied exogenously to culture mediums used in the differentiation of the RCs to either promote or suppress expression of all four human visual opsins. Most noteworthy is that exogenous TH can promote the long wavelength sensitive (*LWS*) opsin transcript at the expense of the middle wavelength sensitive (*MWS*) opsin transcript from the tandemly-replicated *LWS/MWS* gene array. This finding stands to greatly alter the widely accepted “stochastic” model for regulation of this array.

Introduction

Visual disorders pose a significant health burden to the global populace. Age related macular degeneration (AMD) and retinitis pigmentosa (RP) are characterized by the degradation and death of the photoreceptors of the retina, which leads to vision loss and eventual complete loss of sight. There are an estimated 11 million people in the US with AMD ¹. With 200,000 new cases added a year the total is projected to double by 2050 ¹. There is currently no cure. Significant time and resources have been devoted to the development of novel therapeutics to combat these disorders. There is intense interest in emerging strategies such as regenerative medicine and cell replacement therapies that aim to replace damaged photoreceptors from endogenous sources or replace them with new cells from cultured sources. One promising approach involves the differentiation of three dimensional (3D) retinal organoids or retina cups (RCs) derived from human induced pluripotent stem cells (hiPSCs) ^{2,3}. RCs are not only promising tools for the development of replacement therapies for photoreceptor disorders but are excellent models for studying the fundamental processes and mechanisms that determine photoreceptor fate, identity, and survival ^{4 3}.

Tremendous progress has been made in determining protocols for differentiating hiPSCs into a fully laminated retinal structure that contains functioning photoreceptors as well as all other retinal cell types in the correct arrangement in the appropriate layer⁵. These efforts have demonstrated that select lines of hiPSCs can differentiate into apparently self-organized RCs under the appropriate conditions⁵. Establishment of these simple and efficient protocols has allowed for the use of RC systems to test hypotheses concerning mechanisms that determine cell fate and identity. For example, recent progress has been made elucidating mechanisms that specify cone photoreceptor subtypes⁴. Humans have three cone subtypes that are maximally sensitive to red, green, and blue wavelengths⁶. The cone subtype is determined by which visual pigment opsin gene is expressed and the spectral sensitivity the encoded opsin possesses. Human cone opsin subtypes include long wavelength sensitive (LWS; red), medium wavelength sensitive (MWS; green), and short wavelength sensitive (SWS; blue)⁶.

Cone photoreceptors are critical for color contrast sensitivity and high acuity vision. A specialized area of the human retina called the fovea is composed of densely packed LWS and MWS cones⁷. SWS cones are completely absent in the central fovea⁸. In fetal retina SWS cones are specified first, followed by LWS/MWS cones a few weeks later⁹. It was recently demonstrated in RCs that deletion of the DNA binding domain of both isoforms of the thyroid hormone receptor TR β gene resulted in all cones expressing SWS opsin and having an SWS cone morphology as well as a complete absence of LWS/MWS cones⁴. The same study demonstrated that when RCs were supplemented with thyroid hormone (TH) over the course of cone differentiation the RCs showed an increased number of LWS/MWS cones and fewer SWS cones⁴, suggesting that TH signaling via the TR β receptor regulates human cone specification. The order in which human LWS vs. MWS cones are specified during human fetal development is not known. Currently there are no antibodies or in situ probes that can selectively detect these opsin proteins or their corresponding transcripts, due to their high sequence similarity. Rod photoreceptors, also excluded from the central fovea¹⁰, function for vision in very dim lighting (scotopic) conditions, as they are exquisitely sensitive¹¹. Rods express rhodopsin (RHO), and RHO-expressing photoreceptors appear in human fetal retina shortly after the LWS/MWS cones appear¹².

The human *OPN1LW* (LWS) and *OPN1MW* (MWS) genes that encode LWS opsin and MWS opsin, respectively, are the result of a tandem duplication and reside in a tail to head orientation on the X chromosome¹³. The widely-accepted model for how each are regulated involves preferential association of either the *LWS* or *MWS* promoter with an upstream regulatory element called the Locus Control Region (LCR)¹⁴. This association is thought to be permanent and mutually exclusive to

ensure that LWS and MWS opsin are expressed in separate cone populations¹⁴. The mechanism that determines the association of either *LWS* or *MWS* promoter with the LCR is believed to be stochastic¹⁴. However, the ratio of LWS cones to MWS cones increases as a function of distance from the central retina¹⁵. This topographic pattern of LWS and MWS cones in the retina suggests that there may be more to the model for differential regulation of LWS vs MWS than strictly a stochastic mechanism can predict, such as a gradient of a developmental signal. For example, the striking topographic pattern of MWS opsin-expressing vs. SWS opsin-expressing cones in mouse is likely due to higher levels of TH in dorsal vs. ventral retina¹⁶.

We recently demonstrated that TH and retinoic acid (RA) are endogenous regulators of the differential expression of the tandemly duplicated *lws* opsin array in zebrafish^{17 18}. This zebrafish array is orthologous to the human *LWS/MWS* array^{19,20}, although the replications were independent events in primates vs. cyprinid fishes.. When zebrafish larvae were treated with exogenous TH during photoreceptor differentiation, there was increased expression of the first member of the array (*lws1*) at the expense of the second member (*lws2*)¹⁷. These changes in expression (“opsin switching”) were directly observed to occur within individual cones, which indicates that in response to TH there is a molecular mechanism that shifts promotion of expression of the second member of the duplicated array to suppression while initiating promotion of expression of the first member¹⁷.

Here we test the hypothesis that TH and RA supplementation can regulate the differential expression of *LWS* vs *MWS* opsin transcripts in human iPSC derived RCs. We utilized quantitative PCR with gene specific primers that differentiate between the *OPNILW* (*LWS*) and *OPNIMW* (*MWS*) transcripts. We demonstrate that TH supplementation initially promotes both *LWS* and *MWS* opsin expression when sampled at 90 days, but by 150 days *LWS* opsin continues to have higher expression compared to controls, while *MWS* opsin transcript abundance is significantly decreased compared to controls. These results suggest that much like in zebrafish, TH switches promotion of expression from the more blue shifted member of this tandemly replicated array to the member with the longer wavelength sensitivity. These findings suggest the potential for regulation of *LWS* and *MWS* opsin by TH in developing human retina, rather than stochastic regulation as the endogenous mechanism. Further, these findings now offer a possible experimental strategy for controlling cone ratios in human RCs for photoreceptor cell replacement therapies that result in the restoration of high acuity, color vision.

Methods and Materials

Differentiation of three-dimensional retinal organoids and treatment conditions

The protocol for differentiation of three-dimensional retinal organoids was performed as described previously⁵. The control (CT) condition did not include any exposure to RA or T3, other than the small amounts present in serum and supplements, but did include treatment with 0.1% DMSO, the vehicle used for other conditions, from 63d until termination of experiments. The RA condition involved exposure to 1 μ M RA 63-90d, and then 0.5 μ M RA from 90d until termination of experiments⁵. The T3 condition involved exposure to 500nM T3 from 63d until termination of experiments. We collected the organoids at 90d, 120d, 150d, and 180d, and measured levels of cone opsin transcripts using qPCR. Primer sequences are provided within Table 1.

Quantitative reverse transcriptase polymerase chain reaction analysis

Total RNA from each treatment group of pooled (3) whole retina cups was extracted using the Machery-Nagel kit, and was used to synthesize cDNA template using the High Capacity cDNA Reverse Transcription kit with random primers (Applied Biosystems, Inc. [ABI], Foster City, CA). Gene-specific primer pairs are listed in Supplemental Table 2. Amplification to measure abundance of specific transcripts was performed on a model 7900HT Fast Real-Time PCR System using SYBR-Green PCR Master Mix (ABI). Relative quantitation of gene expression using the ddCT method (Applied Biosystems-Guide to Performing Relative Quantitation of Gene Expression Using Real-Time Quantitative PCR) between control and experimental treatments was determined using the *Hypoxanthine-guanine phosphoribosyltransferase (HPRT)* and *Glyceraldehyde 3-phosphate dehydrogenase (GAPDH)* transcripts as the endogenous references. Primer sequences are provided within Table 1. Graphing and statistics were performed using Excel. p-values were calculated using a Wilcoxon Mann-Whitney U test.

Results

Thyroid hormone treatment of human 3D retinal organoids dynamically increases the abundance of LWS opsin transcripts and decreases MWS transcripts

To test the hypothesis that the endocrine signal and nuclear hormone receptor ligand thyroid hormone (TH) can regulate differential expression of human LWS vs. MWS opsins, we utilized a well-established protocol for the differentiation of 3D retinal organoids from human induced pluripotent stem cells (iPSCs)⁵. This protocol promotes the differentiation of a laminated retinal structure, with RHO+ rod photoreceptors and SWS+ cone photoreceptors appearing by 17 weeks (119d), and MWS/LWS+ cone photoreceptors by 21 weeks (147d). This protocol includes a four-

week window of exposure to 1 μ M all-trans retinoic acid (RA), 70-98d, primarily for the purposes of promoting rod development and maturation when assessed for RHO at week 21 (app. 150 days)⁵, as observed in animal models²¹.

Both thyroid hormone (tri-iodothyronine; T3) and to a lesser degree RA, regulate differential expression of the zebrafish orthologue of the human *LWS/MWS* array, *lws1/lws2*^{17,18}. To test the hypothesis that one or both of these regulatory strategies may be conserved in humans, we established conditions in which levels of RA or T3 were modified during 3D retinal organoid differentiation. The control (CT) condition did not include any exposure to RA or T3, other than the small amounts present in serum and supplements, but did include treatment with 0.1% DMSO, the vehicle used for other conditions, from 63d until termination of experiments. The RA condition involved exposure to 1 μ M RA 63-90d, and then 0.5 μ M RA from 90d until termination of experiments⁵. The T3 condition involved exposure to 500nM T3 from 63d until termination of experiments. We collected the organoids at 90d, 120d, 150d, and 180d, and measured levels of cone opsin transcripts using qPCR. Because human *LWS* and *MWS* are ~97% identical at the nucleotide level⁶, we specifically targeted regions where several mismatches reside (Supplemental Fig. 4.1 ; Table 1), and sequence-validated the resulting amplicons derived from postmortem adult human retina samples, and from the 3D retinal organoids (Supplemental Fig. 4.1).

In 90d organoids, the RA condition resulted in undetectable levels of *LWS*, and interestingly, a 5-fold decrease in *MWS* in comparison with controls (Fig. 4.1A,B). The RA condition resulted in no difference in *SWS* or *RHO* transcripts compared to controls (Fig. 4.1C, D). The T3 condition, in contrast, resulted in increased levels of both *LWS* (50-fold) and *MWS* (153-fold) in comparison with controls (Fig. 4.1A, B). These findings for T3 are consistent with those of Liu et al. (2007)²², in which supplemental T3 augmented levels of both *LWS* and *MWS* opsin transcripts in a human-derived retinoblastoma cell line. These findings are also consistent with those of Eldred et al. (2018)⁴, in which human ESC-derived retinal organoids exposed to T3 from 20-200d, showed increased numbers of *LWS/MWS*+ cones, and decreased numbers of *SWS* cones. In contrast to previous studies,⁴ the T3 condition resulted in an increase in levels of *SWS* transcript (2.5-fold) compared to controls (Fig. 4.1C). There was no significant difference in *RHO* transcript levels in the T3 condition compared to controls (Fig. 4.1D). It is noteworthy that, at 90d, the CT condition generated levels of *LWS* transcript that were just within in the detectable range (CT values of 35-39), suggesting that the T3 condition may be necessary to initially promote the production of *LWS* transcript, at least at this early developmental time in RCs.

In 120d organoids, the RA condition resulted in no difference in levels of *LWS* transcripts in comparison with controls, but further decreased *MWS* levels (160-fold) (Fig. 4.2A,B). The RA condition resulted in no difference in *SWS* transcripts in comparison with controls but significantly decreased *RHO* (5.8-fold) (Fig. 4.2C, D). The T3 condition at 120d continued to increase levels of *LWS* transcript (49-fold), and interestingly, slightly but significantly decreased levels of *MWS* (1.5-fold) (Fig. 4.2A, B). These findings hint that T3 may act to initially promote expression of both *LWS* (and of *MWS*), but then with longer exposures begins to act as a “toggle” to promote *LWS* and suppress *MWS*. The T3 condition resulted in decreased levels of *SWS* transcripts (1.7-fold) in comparison with controls and significantly decreased *RHO* (1.7-fold) (Fig. 4.2C, D) The decrease in *SWS* in the T3 condition is consistent with the findings from Eldred et al. (2018)⁴ but the decrease in *RHO* is another completely novel finding. There have been no findings to date that indicate a role for T3 in regulating *RHO* expression.

At 150d, organoids subjected to the RA condition continued to show a decrease in abundance of both *LWS* (2.7-fold) and *MWS* (4.5-fold) opsin transcripts (Fig. 4.3A,B). This finding appears distinctive to our previous studies in zebrafish, in which all-trans RA increased the first member of the orthologous, *lws1/lws2* locus, at the expense of the second member¹⁸. Surprisingly, the RA condition resulted in increased levels of *SWS* (5-fold) transcripts in comparison with controls but no difference in *RHO* (Fig. 4.3C, D). This is an unexpected outcome because it has been demonstrated that suppression of *SWS* homologues in mice is mediated by the retinoid x receptor (*RXR* γ)²³ and is downregulated in zebrafish exposed to all-trans RA²⁴. Further, the RA condition has been shown to increase numbers of *RHO*+ rods by 150d⁵, and so the outcome of no difference in transcript levels of *RHO* due to RA was also unexpected. The T3 condition continued to promote higher levels of *LWS* transcripts (4-fold), and more strongly suppressed *MWS* transcript abundance (2-fold), in comparison with the CT condition (Fig. 4.3A, B). The T3 condition resulted in decreased levels of *SWS* transcripts (3.3-fold) in comparison with controls and continued to decreased *RHO* (6.2-fold) (Fig. 4.3C, D).

At 180d, organoids subjected to the RA condition still show a decrease in abundance of both *LWS* (1.9-fold) and *MWS* (2.4-fold) opsin transcripts (Fig. 4.4A,B). The RA condition resulted in a continued increase of *SWS* (4.5-fold) transcripts in comparison with controls and in contrast to earlier timepoints, an increase in *RHO* (3.3-fold) (Fig. 4.4C, D). Since at 120 days RA had no effect on *SWS* but significantly decreased *RHO* transcript levels when compared to controls, but retina cups at 180 days exposed to RA show increased levels of *SWS* and *RHO* this suggests a function for RA that is temporally dependent, and perhaps manifests at the level of transcript abundance, differently than at

the level of number of RHO+ rods. The T3 condition continued to promote higher levels of *LWS* transcripts (5.7-fold), and suppressed *MWS* transcript abundance (1.6-fold), in comparison with the CT condition (Fig. 4.4A, B). The T3 condition still resulted in decreased levels of *SWS* transcripts (3.7-fold) in comparison with controls and continued to decreased *RHO* (2.7-fold) (Fig. 4.4C, D). Collectively, it is clear that the magnitude of the changes in the T3 treated RCs compared to controls were more pronounced in the earlier timepoints but appear to have reached more of a steady state in which *LWS* is promoted and *MWS*, *SWS*, and *RHO* are suppressed. Summaries of the effects of each treatment condition vs. controls, over time in culture, are provided as Tables 1 and 2.

Discussion

The generation of cell culture sources for treating visual disorders involving degeneration of the photoreceptors as well as understanding the factors that determine photoreceptor fate and identity have been two intensely investigated areas of vision research. The present study contributes significantly to the realization of both of these goals. Our findings have revealed functions for thyroid hormone signaling in regulating differential expression of the tandemly-replicated *LWS/MWS* visual opsin genes in 3D retinal organoids derived from human iPSCs. Our previous findings in zebrafish demonstrated that TH is an endogenous regulator of the tandemly replicated *lws1/lws2* array and functions by promoting the first member (*lws1*) at the expense of the second member (*lws2*)¹⁷. The current study demonstrates a conserved mechanism for TH in the regulation of the human *LWS/MWS* array by promotion of the first member (*LWS*) and suppression of the second (*MWS*). Our previous studies of retinoic acid signaling also demonstrated that RA was an endogenous regulator of the *lws1/lws2* array in zebrafish¹⁸. However, the current study does not support a conserved mechanism for RA signaling in the differential regulation of the *LWS/MWS* array in humans.

In general, the initial promotion of both *LWS* and *MWS* transcripts by TH, followed by the toggling effect of promoting *LWS* while suppressing *MWS*, strikingly resembles the time-course of TH effects upon zebrafish *lws1/lws2* differential expression¹⁷, consistent with the hypothesis that the role of TH signaling may be conserved for the regulation of these tandemly-replicated cone opsins. These findings provide evidence that the widely-accepted model for “stochastic” regulation of human *LWS* vs. *MWS* opsin may not strictly apply, at least in the context of human 3D retinal organoids. Collectively, it is also clear that the magnitude of the changes in the TH treated RCs compared to controls were more pronounced in samples collected at the earlier timepoints but appear to have reached more of a steady state in which *LWS* is promoted and *MWS*, *SWS*, and *RHO* are suppressed. It is tempting to speculate that early in the development of the retina thyroid hormone signaling could

provide the necessary cues to establish an area of *LWS/MWS* cones while simultaneously excluding *SWS* and *RHO* expressing photoreceptors. Therefore, TH may provide the means to meet some of the necessary requirements for establishing the fovea of the human retina.

These findings significantly extend previous studies that demonstrated TH supplementation in human RC differentiation protocols resulted in decreased numbers of *SWS* cones and increased numbers of *LWS/MWS* cones⁴. However, the methods used⁴ could not distinguish between *LWS* and *MWS* cone subtypes. It is of great interest that the initial choice between the *SWS* fate and the *LWS/MWS* fate is TH dependent as well as, according to our findings, the final decision between the *LWS* and *MWS* fate. The TH signaling system may have been evolutionarily co-opted for regulating *LWS* vs. *MWS* as these genes were replicated and became functionally divergent. Also of interest, RCs deficient in *TRβ* the gene that codes for the TH receptor *TRβ1/TRβ2* isoforms, completely lack *LWS* and *MWS* cones and show an increased number of *SWS* cones. Therefore, *TRβ* appears to be the likely candidate that mediates *LWS* vs *MWS* expression in response to TH. The suppression of *MWS* by RA suggests that *TRβ* likely heterodimerizes with either an RAR or RXR possibly at a distinct response element from that which is involved with promoting *LWS*.

The initial promotion of *SWS* by TH was not expected. The suppression of *SWS* by prolonged exposure to TH was in agreement with prior work⁴. It is of note that TH treatment at day 90 resulted in an increase in all cone transcripts suggesting a role for TH in differentiation in cones in general. Promotion of human *SWS* transcription by RA is also a novel finding. Our data suggests that initially RA has no effect on *SWS* transcription but after prolonged treatment *SWS* transcription is promoted by RA, suggesting a temporal requirement for RA signaling. In zebrafish, prolonged treatment with RA results in promotion of rod and *lws1* expressing cones and inhibition of *sws1* and *sws2* expressing cones²¹. Previous studies in mice have demonstrated that disrupting the retinoid X receptor (*RXRγ*) resulted in increased *SWS* positive cones which suggests a suppressive role for *RXRγ*²³. Retinoic acid is a known ligand of *RXRγ*. However, RA also can bind to many other receptors including *RXRs* and *RARs*. Our findings suggest novel roles for RA signaling in regulation of human *SWS*.

The suppression of *RHO* transcription by TH is also something that has not been documented and to my knowledge is the first evidence that suggests TH can suppress rod specific transcripts. These findings lay the groundwork for future studies investigating the role for TH in regulation of *RHO*. Our findings for the suppression of *RHO* by RA at least until day 120, is somewhat in conflict with previous studies demonstrating an increased number of rods using the RA supplementation regime included in the present study compared to the same control conditions⁵. The previous study utilized immunohistochemistry in order to label and quantify the number of rhodopsin positive cells.

Our data does not include a quantification of cells but rather a quantification of the abundance of *RHO* transcript. This could be explained by more rhodopsin positive cells that express lower levels of *RHO* transcript in the RA condition. Further studies are required to address these discrepancies. Our data does support the finding that RA can promote the expression of rhodopsin in day 180 RCs treated with RA compared to controls (Fig. 4.4). Other studies in rat retina and zebrafish embryos have also demonstrated a role for RA in promotion of rod differentiation^{21,25}.

We have demonstrated that TH initially promotes both *LWS* and *MWS* expression before switching to a toggle that is biased towards promoting *LWS* expression. In addition, TH suppresses both *SWS* and *RHO* transcription. Collectively, these findings suggest that TH may be involved in the formation of the highly specialized area of the human retina, the fovea, which consists of densely packed *LWS* and *MWS* cones and no rods or *SWS* cones. Previous studies in RCs demonstrated that thyroid hormone signaling components are expressed sequentially in order to maintain low levels of TH signaling early in development and increased levels as development progresses⁴. The same changes in thyroid hormone signaling have been demonstrated in the developing human retina²⁶. These findings highlight the complex overlap of extrinsic factor signaling that occurs during 3D retina cup differentiation and possibly fetal retinal development *in vivo* to specify cone subtypes. These findings also reveal new roles for both TH and RA in photoreceptor identity determination in human retinal cells that bring the field of vision science one step closer to a complete model for photoreceptor development.

Literature Cited

- 1 Rein, D. B. *et al.* Forecasting Age-Related Macular Degeneration Through the Year 2050: The Potential Impact of New Treatments. *Archives of Ophthalmology* **127**, 533-540, doi:10.1001/archophthalmol.2009.58 (2009).
- 2 Artero Castro, A., Rodríguez Jimenez, F. J., Jendelova, P. & Erceg, S. Deciphering retinal diseases through the generation of three dimensional stem cell-derived organoids: Concise Review. *STEM CELLS* **37**, 1496-1504, doi:10.1002/stem.3089 (2019).
- 3 Brooks, M. J. *et al.* Improved Retinal Organoid Differentiation by Modulating Signaling Pathways Revealed by Comparative Transcriptome Analyses with Development In Vivo. *Stem Cell Reports* **13**, 891-905, doi:10.1016/j.stemcr.2019.09.009 (2019).
- 4 Eldred, K. C. *et al.* Thyroid hormone signaling specifies cone subtypes in human retinal organoids. *Science* **362**, doi:10.1126/science.aau6348 (2018).
- 5 Zhong, X. *et al.* Generation of three-dimensional retinal tissue with functional photoreceptors from human iPSCs. *Nat Commun* **5**, 4047, doi:10.1038/ncomms5047 (2014).

- 6 Nathans, J., Thomas, D. & Hogness, D. S. Molecular genetics of human color vision: the genes encoding blue, green, and red pigments. *Science* **232**, 193-202 (1986).
- 7 Hendrickson, A. A morphological comparison of foveal development in man and monkey. *Eye (London, England)* **6 (Pt 2)**, 136-144, doi:10.1038/eye.1992.29 (1992).
- 8 Cornish, E. E., Hendrickson, A. E. & Provis, J. M. Distribution of short-wavelength-sensitive cones in human fetal and postnatal retina: early development of spatial order and density profiles. *Vision Res* **44**, 2019-2026, doi:10.1016/j.visres.2004.03.030 (2004).
- 9 Xiao, M. & Hendrickson, A. Spatial and temporal expression of short, long/medium, or both opsins in human fetal cones. *Journal of Comparative Neurology* **425**, 545-559, doi:10.1002/1096-9861(20001002)425:4<545::Aid-cne6>3.0.Co;2-3 (2000).
- 10 Curcio, C. A., Sloan, K. R., Kalina, R. E. & Hendrickson, A. E. Human photoreceptor topography. *J Comp Neurol* **292**, 497-523, doi:10.1002/cne.902920402 (1990).
- 11 Stabell, B. RODS AS COLOR RECEPTORS IN SCOTOPIC VISION. *Scandinavian Journal of Psychology* **8**, 132-138, doi:10.1111/j.1467-9450.1967.tb01385.x (1967).
- 12 O'Brien, K. M., Schulte, D. & Hendrickson, A. E. Expression of photoreceptor-associated molecules during human fetal eye development. *Molecular vision* **9**, 401-409 (2003).
- 13 Vollrath, D., Nathans, J. & Davis, R. Tandem array of human visual pigment genes at Xq28. *Science* **240**, 1669-1672, doi:10.1126/science.2837827 (1988).
- 14 Wang, Y. *et al.* Mutually exclusive expression of human red and green visual pigment-reporter transgenes occurs at high frequency in murine cone photoreceptors. *Proceedings of the National Academy of Sciences of the United States of America* **96**, 5251-5256 (1999).
- 15 Kuchenbecker, J. A., Sahay, M., Tait, D. M., Neitz, M. & Neitz, J. Topography of the long- to middle-wavelength sensitive cone ratio in the human retina assessed with a wide-field color multifocal electroretinogram. *Vis Neurosci* **25**, 301-306, doi:10.1017/S0952523808080474 (2008).
- 16 Roberts, M. R., Srinivas, M., Forrest, D., Morreale de Escobar, G. & Reh, T. A. Making the gradient: Thyroid hormone regulates cone opsin expression in the developing mouse retina. *Proceedings of the National Academy of Sciences of the United States of America* **103**, 6218-6223, doi:10.1073/pnas.0509981103 (2006).
- 17 Mackin, R. D. *et al.* Endocrine regulation of multichromatic color vision. *Proceedings of the National Academy of Sciences*, 201904783, doi:10.1073/pnas.1904783116 (2019).
- 18 Mitchell, D. M. *et al.* Retinoic Acid Signaling Regulates Differential Expression of the Tandemly-Duplicated Long Wavelength-Sensitive Cone Opsin Genes in Zebrafish. *PLoS Genet* **11**, e1005483, doi:10.1371/journal.pgen.1005483 (2015).

- 19 Hofmann, C. M. & Carleton, K. L. Gene duplication and differential gene expression play an important role in the diversification of visual pigments in fish. *Integr Comp Biol* **49**, 630-643, doi:10.1093/icb/icp079 (2009).
- 20 Chinen, A., Hamaoka, T., Yamada, Y. & Kawamura, S. Gene duplication and spectral diversification of cone visual pigments of zebrafish. *Genetics* **163**, 663-675 (2003).
- 21 Stevens, C. B., Cameron, D. A. & Stenkamp, D. L. Plasticity of photoreceptor-generating retinal progenitors revealed by prolonged retinoic acid exposure. *BMC Dev Biol* **11**, 51, doi:10.1186/1471-213X-11-51 (2011).
- 22 Liu, Y., Fu, L., Chen, D. G. & Deeb, S. S. Identification of novel retinal target genes of thyroid hormone in the human WERI cells by expression microarray analysis. *Vision Res* **47**, 2314-2326, doi:10.1016/j.visres.2007.04.023 (2007).
- 23 Roberts, M. R., Hendrickson, A., McGuire, C. R. & Reh, T. A. Retinoid X receptor (gamma) is necessary to establish the S-opsin gradient in cone photoreceptors of the developing mouse retina. *Invest Ophthalmol Vis Sci* **46**, 2897-2904, doi:10.1167/iovs.05-0093 (2005).
- 24 Prabhudesai, S. N., Cameron, D. A. & Stenkamp, D. L. Targeted effects of retinoic acid signaling upon photoreceptor development in zebrafish. *Dev Biol* **287**, 157-167, doi:10.1016/j.ydbio.2005.08.045 (2005).
- 25 Kelley, M. W., Williams, R. C., Turner, J. K., Creech-Kraft, J. M. & Reh, T. A. Retinoic acid promotes rod photoreceptor differentiation in rat retina in vivo. *NeuroReport* **10**, 2389-2394 (1999).
- 26 Hoshino, A. *et al.* Molecular Anatomy of the Developing Human Retina. *Dev Cell* **43**, 763-779 e764, doi:10.1016/j.devcel.2017.10.029 (2017).

Figures

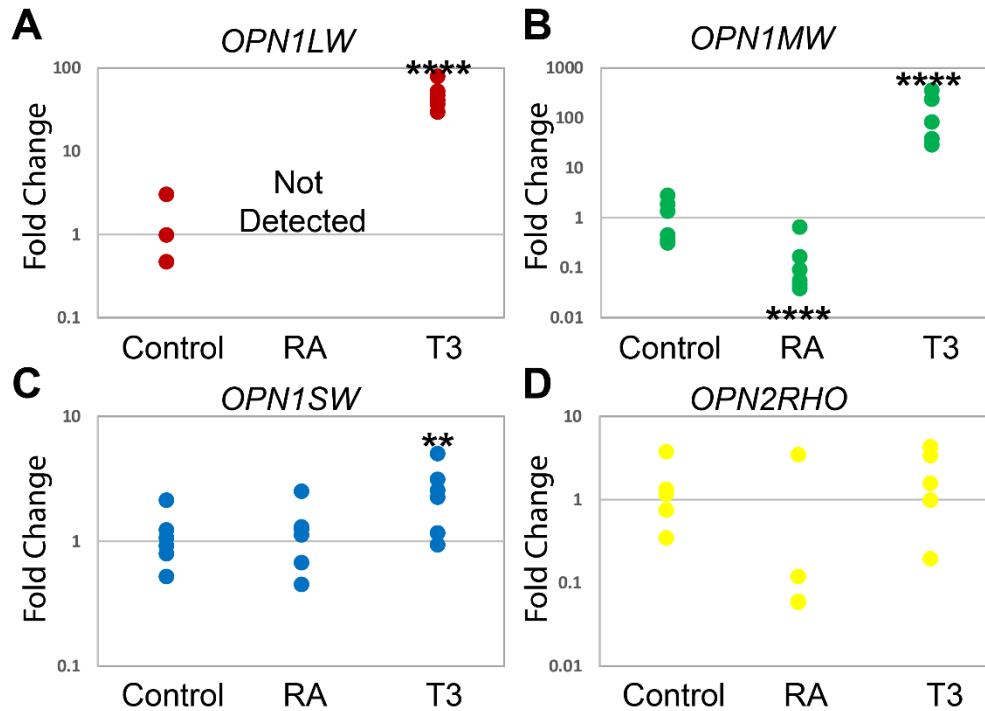


Fig 4.1. Quantitative PCR for *OPN1LW*, *OPN1MW*, *OPN1SW*, *OPN2RHO* transcript abundance reveals a decrease in abundance for *OPN1LW* and *OPN1MW* transcripts in the retinoic acid (RA) treated retina cups (RCs) and an increase in abundance for all transcripts save *OPN2RHO* in the thyroid hormone (T3) treated RCs at 90 days. (A-D) Scatter plots indicate fold change (2^{-ddCT}) abundance of the indicated transcripts. Each dot represents one biological sample (pooled RNA from ~ three RCs). For each condition $n = 6$ (A). *OPN1LW* abundance in control, not detected in RA treated, increased by T3 $p < 1.0E^{-5}$. (B). *OPN1MW* abundance in control, was decreased by RA $p < 1.0E^{-5}$ but increased by T3 $p < 1.0E^{-5}$. (C). *OPN1SW* abundance in control, no change in RA treated but increase by T3 $p < 0.01$. (D). *OPN2RHO* abundance in control, no change by RA or T3. The p-values were calculated by comparing the ddCT values for treated vs control from each experiment using the Mann-Whitney U test. Statistical notation: ** $p < .01$ **** $p < 0.0001$.

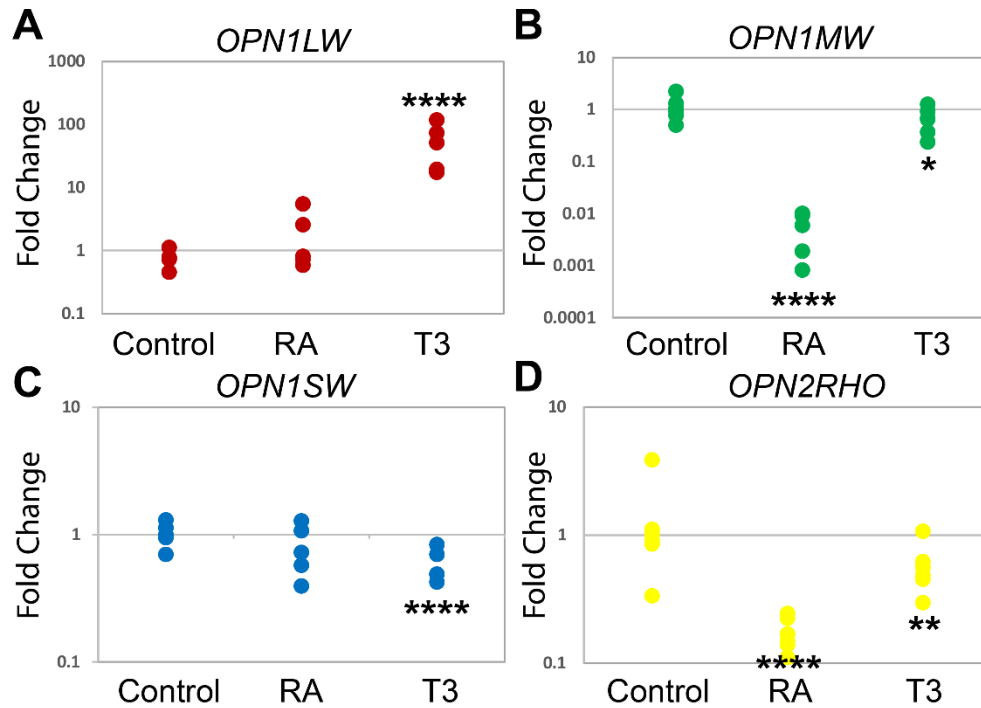


Fig 4.2. Quantitative PCR for *OPN1LW*, *OPN1MW*, *OPN1SW*, *OPN2RHO* transcript abundance reveals a switch in regulation of *OPN1MW* by T3 and new roles for RA and T3 suppressing *OPN2RHO* transcription in treated RCs at 120 days. (A-D) Scatter plots indicate fold change (2^{-ddCT}) abundance of the indicated transcripts. Each dot represents one biological sample (pooled RNA from ~ three RCs). For each condition $n = 6$ (A). *OPN1LW* abundance in control, no change in RA treated, increased by T3 $p < 1.0E^{-5}$. (B). *OPN1MW* abundance in control, was decreased by RA $p < 1.0E^{-5}$ and decreased by T3 $p = 0.0155$. (C) *OPN1SW* abundance in control, no change by RA, but decreased by T3 $p < 1.0E^{-5}$. (D) *OPN2RHO* abundance in control, decrease by RA treated $p < 1.0E^{-5}$, and decrease in T3 treated $p = 0.0056$. The p-values were calculated by comparing the ddCT values for treated vs control from each experiment using the Mann-Whitney U test. Statistical notation: * $p < .05$, ** $p < 0.01$, **** $p < 0.0001$.

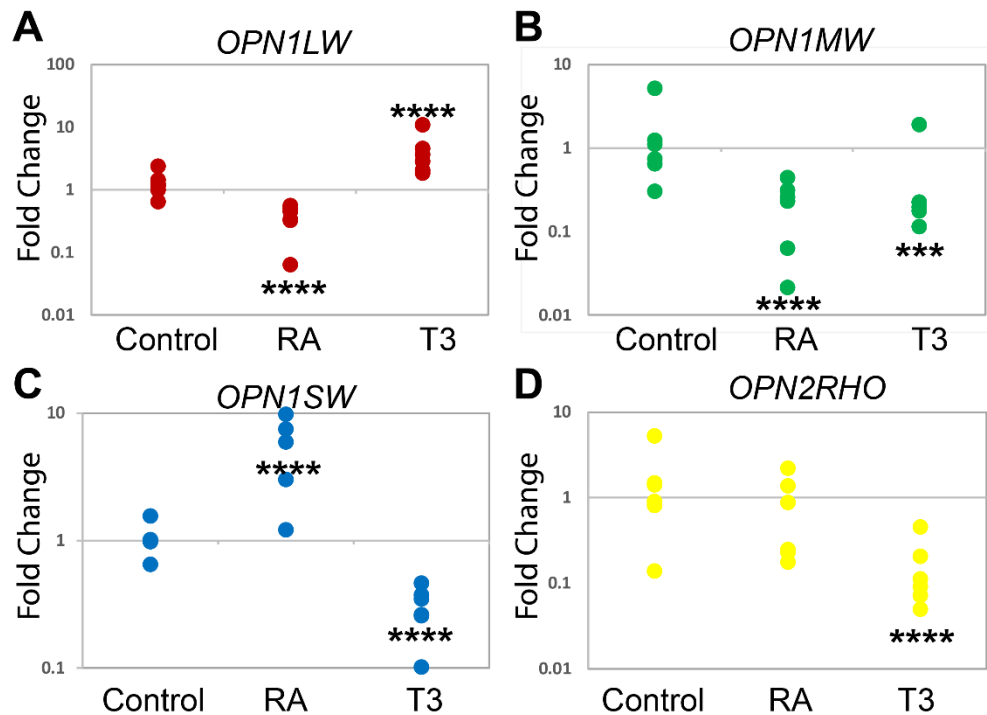


Fig 4.3. Quantitative PCR for *OPN1LW*, *OPN1MW*, *OPN1SW*, *OPN2RHO* transcript abundance reveals differential regulation of *OPN1LW* vs *OPN1MW* by T3 in RCs at 150 days as well as new roles for RA in promoting *OPN1SW* transcription. (A-D) Scatter plots indicate fold change (2^{-ddCT}) abundance of the indicated transcripts. Each dot represents one biological sample (pooled RNA from ~ three RCs). For each condition $n = 6$ (A). *OPN1LW* abundance in control, a decrease by RA $p < 1.0E^{-5}$, increased by T3 $p < 1.0E^{-5}$. (B). *OPN1MW* abundance in control, was decreased by RA $p < 1.0E^{-5}$ and decreased by T3 $p = 0.00026$. (C) *OPN1SW* abundance in control, increased by RA $p < 1.0E^{-5}$, but decreased by T3 $p < 1.0E^{-5}$. (D) *OPN2RHO* abundance in control, no change by RA, and decrease in T3 treated $p < 1.0E^{-5}$. The p-values were calculated by comparing the ddCT values for treated vs control from each experiment using the Mann-Whitney U test. Statistical notation: *** $p < 0.001$, **** $p < 0.0001$.

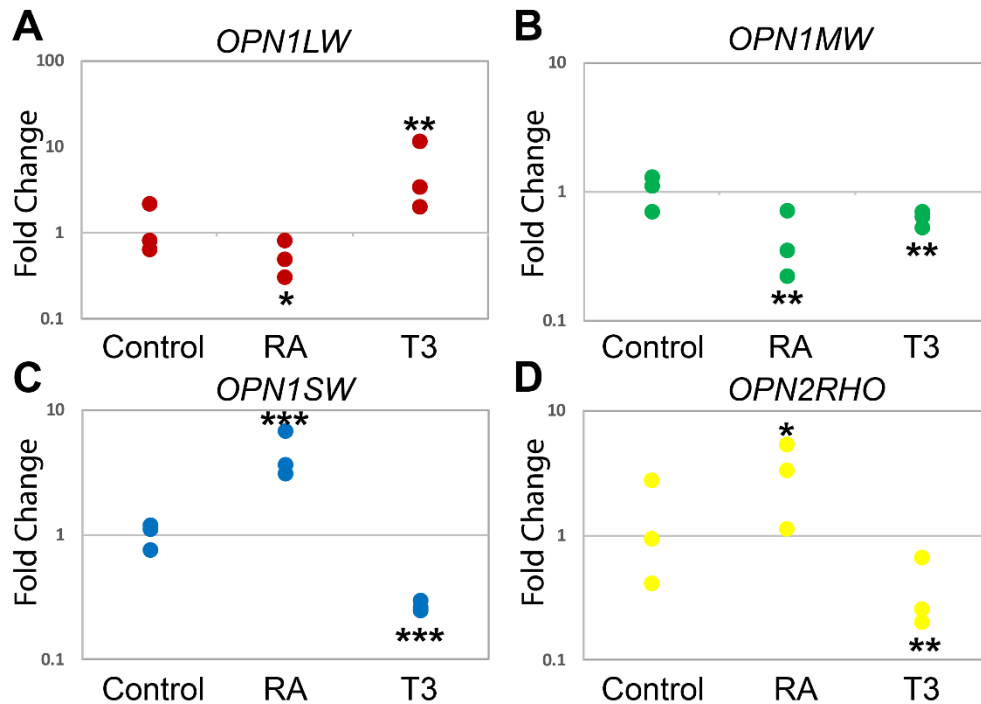
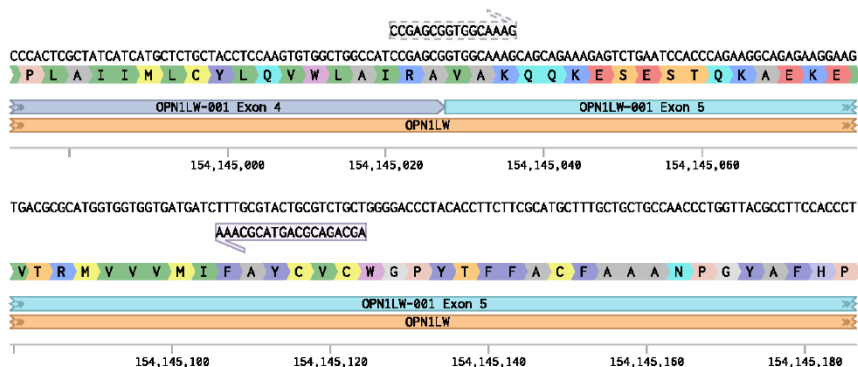
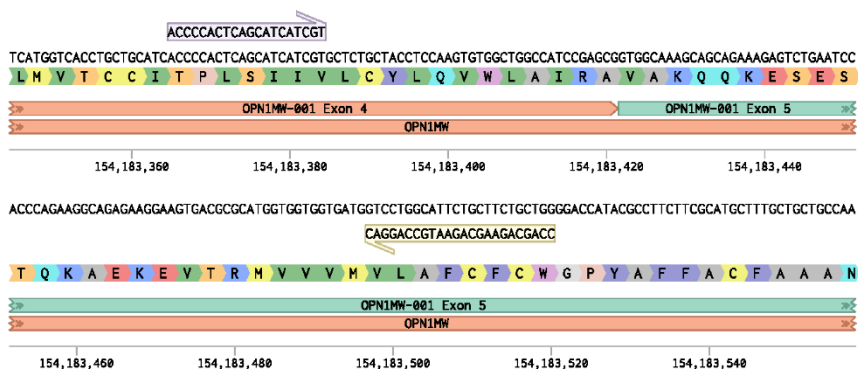


Fig 4.4. Quantitative PCR for *OPN1LW*, *OPN1MW*, *OPN1SW*, *OPN2RHO* transcript abundance reveals continued differential regulation of *OPN1LW* vs *OPN1MW* by T3 in RCs at 180 days as well as a switch from suppression of *OPN2RHO* at 150 days to promotion by RA at 180 days. (A-D) Scatter plots indicate fold change ($2^{-\text{ddCT}}$) abundance of the indicated transcripts. Each dot represents one biological sample (pooled RNA from ~ three RCs). For each condition $n = 3$ (A). *OPN1LW* abundance in control, a decrease by RA $p = 0.02$, increased by T3 $p = 0.0027$. (B). *OPN1MW* abundance in control, was decreased by RA $p = 0.002$ and decreased by T3 $p = 0.0036$. (C) *OPN1SW* abundance in control, increased by RA $p = 0.00042$, but decreased by T3 $p = 0.00042$. (D) *OPN2RHO* abundance in control, an increase by RA $p = 0.02$, and decrease in T3 treated $p = 0.008$. The p-values were calculated by comparing the ddCT values for treated vs control from each experiment using the Mann-Whitney U test. Statistical notation: * $p < .05$, ** $p < 0.01$, *** $p < 0.001$.

A OPN1LW-001 (ENST00000369951, CCDS14742) (1261 bp)



B OPN1MW-001 (ENST00000595290, CCDS14743) (1242 bp)



Supplementary Fig 4.1 (A,B) Sequences of (A) OPN1LW and (B) OPN1MW. Forward and Reverse primers used for qPCR are annotated.

Supplementary Table S4.1 Primer sequences used in qPCR

Gene	Forward Primer	Reverse Primer
OPN1LW	CCGAGCGGTGGCAAAG	AGCAGACGCAGTACGCAA
OPN1MW	ACCCCACTCAGCATCATCGT	CCAGCAGAAGCAGAATGCCAGGAC
OPN1SW	CGCCAGCTGTAACGGATACT	TACCAATGGTCCAGGTAGCC
OPN2RHO	TTTTCTGCTATGGGCAGCTC	CATGAAGATGGGACCGAAGT
HPRT	TGCTGACCTGCTGGATTACAT	TTGCGACCTTGACCATCTTT
GAPDH	CCCACCACACTGAATCTCC	GGTACTTTATTGATGGTACATGACAAG

Future Directions

Through this body of work, I have demonstrated that thyroid hormone (TH) is an endogenous regulator of the differential expression of the tandemly replicated *lws1/lws2* and *rh2* arrays in zebrafish¹ as well as TH's involvement in differentially regulating the *LWS/MWS* array in human iPSC derived 3D retinal organoids. I've demonstrated that specific regions of the *lws* locus contain potential response elements that each contribute to the endogenous control of expression of each member of the array. Interestingly, similar sequences to the ppTREs identified in the zebrafish *lws* locus can be found approximately 7.7kb upstream from the first exon of *LWS* (ppTRE1) and between *LWS* exon 4 and 5 (ppTRE2) in the human *LWS/MWS* array (data not shown) suggesting conservation of response elements regulating the tandemly duplicated human array. Further studies are required to confirm whether these conserved sequences are indeed response elements involved in differential regulation of the array. This can be accomplished by genomic editing using CRISPR-Cas9 to disrupt these elements in order to ascertain the contribution of each element in the regulation of the array and the response to TH treatment.

Another critical component of transcriptional regulatory mechanisms involves *trans*-acting factors that interact with *cis*-regulatory sequences. We have identified retinoic acid (RA)² and TH¹ as ligands that contribute to the regulatory mechanism. Each ligand can bind with several nuclear receptors that act in a *trans*-regulatory manner to control transcription. TR β 2 is required for *LWS* cone differentiation in zebrafish³⁻⁵ and TR β is required for *LWS/MWS* cone differentiation in humans⁶. It is also possible that TR β and the TR β 2 isoform could be potential candidates for regulation of these tandemly replicated arrays in mediating the response to TH. The fact that the cell type of interest fails to differentiate without the receptor poses an interesting problem for elucidating the contribution of the receptor to influencing transcription of genes selective for the cell type. I've designed two separate strategies for solving this dilemma in zebrafish. The first involves microinjection of TR β mRNA into the single cell stage of TR β mutant zebrafish embryos. The goal is to supply a temporary induction of TR β expression in order to promote differentiation of the *LWS* cones. Once the mRNA is degraded and if the continued survival of *LWS* cones is not dependent on continued TR β expression it will be possible to treat the injected larvae to ascertain whether TH can regulate the *lws* array in the absence of TR β . The other strategy leverages cutting edge technology such as CRISPR-Cas9 to disrupt TR β expression. I've created transgenic zebrafish that contain a heat shock inducible Cas9 and two ubiquitous promoters driving two different guide RNAs targeting the TR β gene (Fig. 5.1A). Successful induction of the transient system was confirmed by heat shocking

injected larvae at 3 days post-fertilization (dpf) and GFP expression reporting Cas9 was analyzed by epifluorescence in larvae at 4 dpf (Fig. 5.1C). A proof of principle experiment using this transient expression system was performed on wild-type embryos injected at the one-cell stage, then heat shocked for 60 minutes starting at 1 dpf (before *LWS* cone differentiation), *lws2* expression was analyzed by qPCR in embryos positive for the transgenic heart marker and ubiquitous GFP expression reporting activated Cas9 compared to GFP negative embryos (Fig. 5.1D). Preliminary results indicate a significant decrease in the expression of *lws2* in the GFP positive embryos (Fig. 5.1E). The inducibility of the CRISPR-Cas9 system will allow for normal differentiation of the *LWS* cones. Once differentiation of the *LWS* cones has occurred the disruption of TR β can be induced by a 30-60 minute heat shock of larvae, followed by TH treatment, and quantification of *lws1/lws2* expression. Future studies are planned to investigate the effects of T3 treatment on *lws1/lws2* expression in larvae that have been heat shocked after *LWS* cone differentiation.

Preliminary results for the effects of TH treatment on TR β mutant larvae (germline mutants not inducible as described previously) has revealed that the differential regulation of *rh2-1* vs *rh2-2* by TH is maintained. This suggests that TR β is not required for the regulation of the *rh2* array by TH (Fig 2A). Other receptor mutants that have been tested for their involvement in this regulatory mechanism include the thyroid receptor α B (TR α B) and the retinoid X receptor γ a (RXR γ a). Preliminary results for TH treatment of these receptor knockouts has revealed that the normal promotion of *lws1* (Fig 3A, Fig 4A) and *rh2-2* (Fig 2D, Fig 3D) is maintained but instead of the expected downregulation of *lws2* (Fig 3B, Fig 4B) and *rh2-1* (Fig 3C, Fig 4C) there was a significant increase in both transcripts in response to TH. Our previous results identifying the potential of multiple response elements involved in this regulatory mechanism in concert with the results from TH treatment in receptor mutants suggests that multiple receptors may contribute to the regulation of each member of the array in response to TH.

Future studies involving chromatin immunoprecipitation sequencing (CHIPseq) using antibodies against each receptor and sequencing of the genomic regions of the *lws* locus that each receptor binds will definitively identify exactly which receptor is interacting with which response element in treated vs untreated conditions. Other methods could be employed to identify what the downstream effects of the binding of receptors to response elements are. Including potential roles for changes in chromatin accessibility, and changes in chromosomal looping created by two or more interacting elements.

Future studies involving the differentiation of the human iPSC derived retina cups will focus on the effects of combined TH and RA treatment on opsin expression. The current iPSC line used in our studies was from a human female. Females have two X chromosomes and most males only have one. The *LWS/MWS* array is located on the X chromosome so it is possible that the regulation of the locus in the current studies could affect both copies of the *LWS/MWS* locus. Future studies will evaluate the effects of our differentiation protocols using an iPSC line derived from a male.

This body of work has provided a solid foundation for further efforts to expand upon our understanding of extrinsic and intrinsic factors involved in regulation of tandemly replicated visual opsin genes. The *lws* and *rh2* array in zebrafish and the *LWS/MWS* array in humans provide three different models for how regulation by TH occurs. The differences in response element sequences could provide insight into how certain sequences influence the binding of which receptors and the effect on transcriptional regulation once the interaction with response elements occurs. This insight could be expanded upon to increase our understanding of how TH influences transcriptional regulation of other genes that have been duplicated or contain TH response elements in their regulatory regions.

Literature Cited

- 1 Mackin, R. D. *et al.* Endocrine regulation of multichromatic color vision. *Proceedings of the National Academy of Sciences*, 201904783, doi:10.1073/pnas.1904783116 (2019).
- 2 Mitchell, D. M. *et al.* Retinoic Acid Signaling Regulates Differential Expression of the Tandemly-Duplicated Long Wavelength-Sensitive Cone Opsin Genes in Zebrafish. *PLoS Genet* **11**, e1005483, doi:10.1371/journal.pgen.1005483 (2015).
- 3 Deveau, C. *et al.* Thyroid hormone receptor beta mutations alter photoreceptor development and function in *Danio rerio* (zebrafish). *PLoS Genet* **16**, e1008869, doi:10.1371/journal.pgen.1008869 (2020).
- 4 Volkov, L. I. *et al.* Thyroid hormone receptors mediate two distinct mechanisms of long-wavelength vision. *Proc Natl Acad Sci U S A* **117**, 15262-15269, doi:10.1073/pnas.1920086117 (2020).
- 5 Suzuki, S. C. *et al.* Cone photoreceptor types in zebrafish are generated by symmetric terminal divisions of dedicated precursors. *Proc Natl Acad Sci U S A* **110**, 15109-15114, doi:10.1073/pnas.1303551110 (2013).
- 6 Eldred, K. C. *et al.* Thyroid hormone signaling specifies cone subtypes in human retinal organoids. *Science* **362**, doi:10.1126/science.aau6348 (2018).

Figures

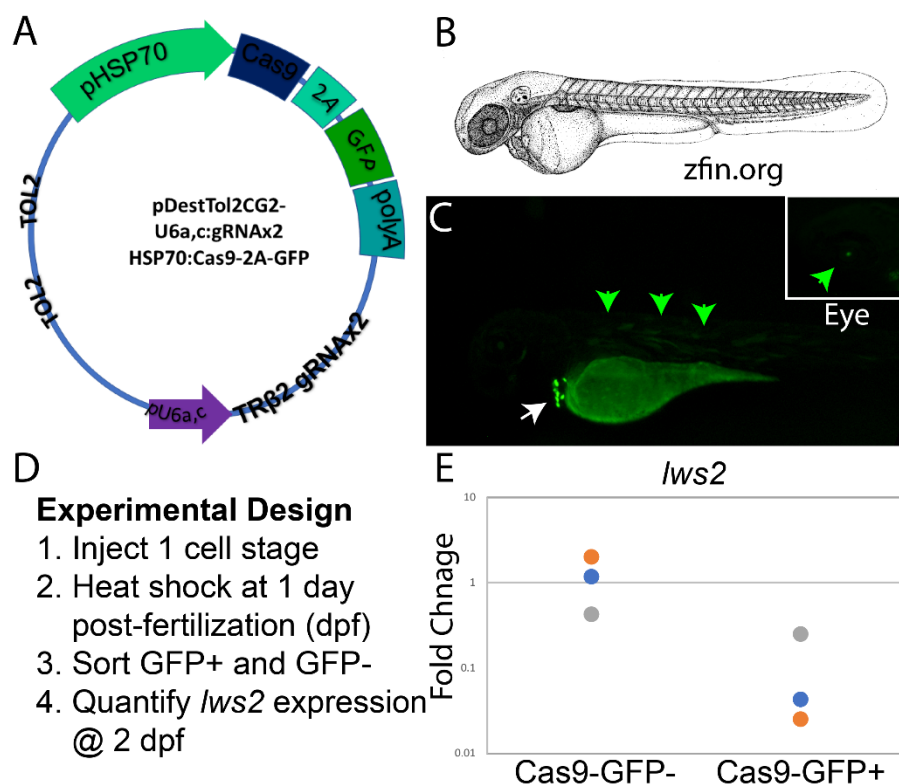


Fig. 5.1. Inducible CRISPR-Cas9 mediated disruption of thyroid hormone receptor TR β . (A). Schematic of transgenesis vector including Tol2 sites for genomic insertion, HSP70 promoter driving Cas9 and GFP, ubiquitous U6a and U6c promoter driving two gRNAs targeting exon 9 of *tr β* . (B) Drawing of zebrafish larvae. (C). Image of GFP expression after 1hr heat shock at 3 days post fertilization (dpf) in transient transgenic larvae at 4dpf. Inset is GFP expression in the eye. (D) Workflow for proof of principle experiment validating effect on *lws2* expression after *tr β* disruption. Green arrows indicate GFP reporting Cas9 expression. White arrows indicate GFP expression from the *cmcl2* transgenic heart marker. (E). Scatter plots indicate fold change ($2^{-\Delta\Delta\text{CT}}$) abundance of the indicated transcript. Each colored dot represents one biological sample (pooled RNA from ~ three larvae). For each condition $n = 3$. *lws2* abundance was decreased in Cas9+ $p < 0.001$ compared to Cas9- controls. The p-values were calculated by comparing the $\Delta\Delta\text{CT}$ values for Cas9+ vs Cas9- controls from each experiment using the Mann-Whitney U test. Statistical notation: *** $p < 0.001$.

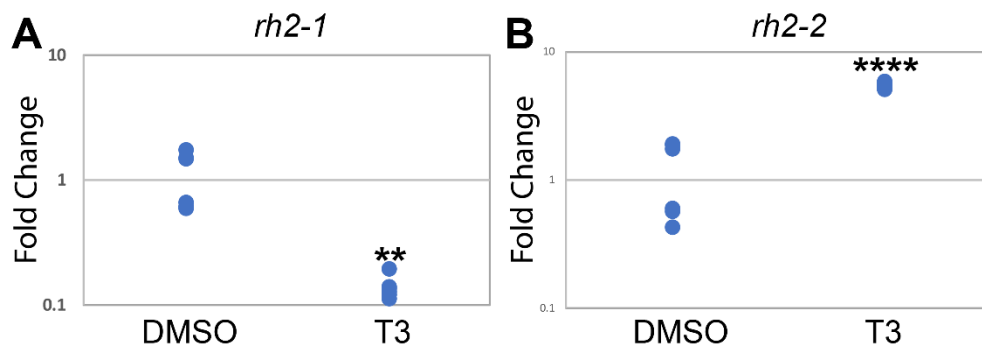


Fig 5.2. The *rh2* thyroid hormone response is still maintained in the absence of TR β 2. (A,B) Scatter plots indicate fold change ($2^{\Delta\Delta\text{CT}}$) abundance of the indicated transcripts. Each dot represents one biological sample (pooled RNA from ~ three larvae). For each condition $n = 6$. (A). *rh2-1* abundance in control was decreased by T3 $p < .01$. (B) *rh2-2* abundance in control was increased by T3 $p < .0001$. The p-values were calculated by comparing the ddCT values for treated vs control from each experiment using the Mann-Whitney U test. Statistical notation: ** $p < 0.01$, **** $p < 0.0001$.

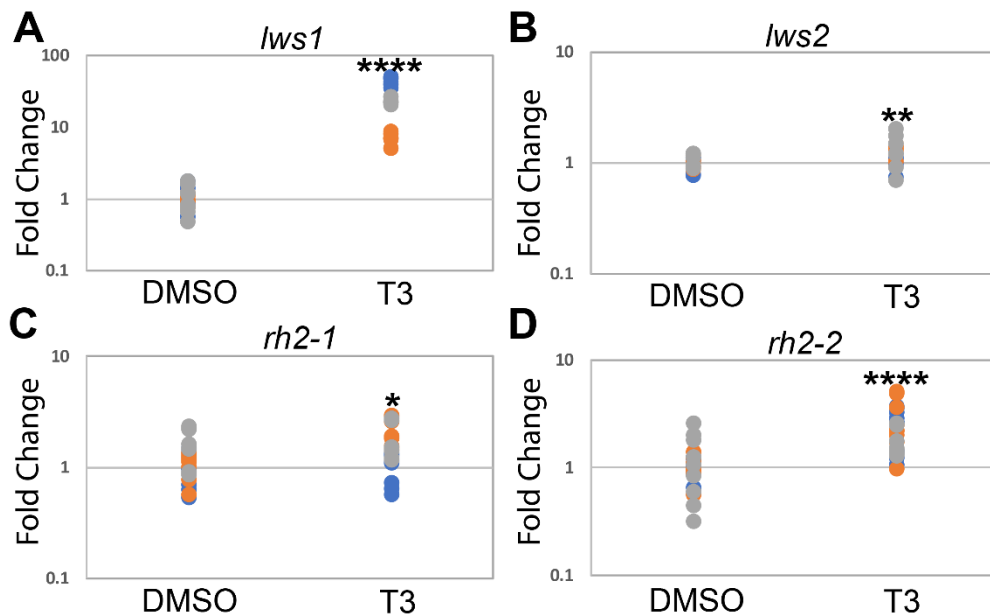
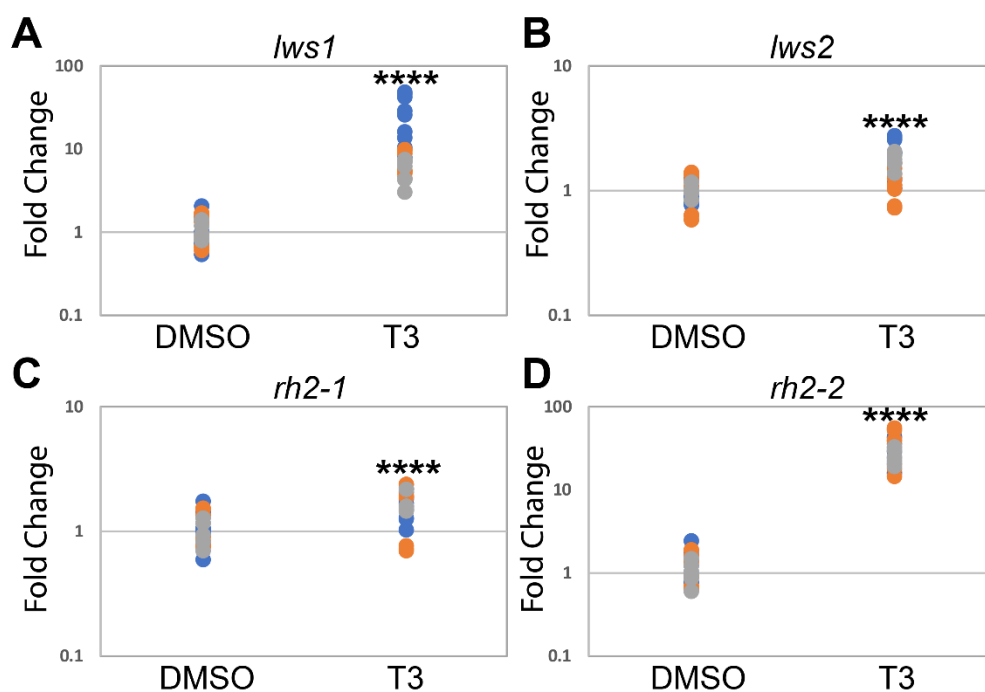


Fig 5.3. Downregulation of *lws2* and *rh2-1* in response to TH is dependent on TR α B. (A-D)

Scatter plots indicate fold change ($2^{\Delta\Delta\text{CT}}$) abundance of the indicated transcripts. Each colored dot represents technical triplicates from one biological sample (pooled RNA from ~ three larvae). For each condition n = 9. (A). *lws1* abundance in controls was increased by T3 p < 0.0001. (B). *lws2* abundance was increased by T3 p < 0.01. (C). *rh2-1* abundance in control was increased by T3 p < 0.01. (D) *rh2-2* abundance in control was increased by T3 p < 0.0001. The p-values were calculated by comparing the ddCT values for treated vs control from each experiment using the Mann-Whitney U test. Statistical notation: *p < 0.05 ** p < 0.01, **** p < 0.0001.

**Fig 5.4. Downregulation of *lws2* and *rh2-1* in response to TH is dependent on RXR γ .** (A-D)

Scatter plots indicate fold change ($2^{\Delta\Delta\text{CT}}$) abundance of the indicated transcripts. Each colored dot represents technical triplicates from one biological sample (pooled RNA from ~ three larvae). For each condition n = 9. (A). *lws1* abundance in controls was increased by T3 p < 0.0001. (B). *lws2* abundance was increased by T3 p < 0.0001. (C). *rh2-1* abundance in control was increased by T3 p < 0.0001. (D) *rh2-2* abundance in control was increased by T3 p < 0.0001. The p-values were

calculated by comparing the ddCT values for treated vs control from each experiment using the Mann-Whitney U test. Statistical notation: * $p < 0.05$ ** $p < 0.01$, **** $p < 0.0001$.